

AD A1000641

LEVEL II

(12)

RADC-TR-80-413  
Final Technical Report  
May 1981



## GROWTH OF PURE SINGLE CRYSTALS OF ALKALI HALIDES AND ALKALINE EARTH FLUORIDES

Oregon State University

Sponsored by  
Defense Advanced Research Projects Agency (DoD)  
ARPA Order No. 3096

DTIC  
ELECTED  
JUN 25 1981  
S E D

APPROVED FOR PUBLIC RELEASE; DISTRIBUTION UNLIMITED

The views and conclusions contained in this document are those of the authors and should not be interpreted as necessarily representing the official policies, either expressed or implied, of the Defense Advanced Research Projects Agency or the U. S. Government.

DTIC FILE COPY

**ROME AIR DEVELOPMENT CENTER  
Air Force Systems Command  
Griffiss Air Force Base, New York 13441**

81 6 25 024

This report has been reviewed by the RADC Public Affairs Office (PA) and is releasable to the National Technical Information Service (NTIS). At NTIS it will be releasable to the general public, including foreign nations.

RADC-TR-80-413 has been reviewed and is approved for publication.

APPROVED:

*Joseph A. Adamski*  
JOSEPH A. ADAMSKI  
Project Engineer

APPROVED:

*Clarence D. Turner*  
CLARENCE D. TURNER  
Acting Director  
Solid State Sciences Division

FOR THE COMMANDER:

*John P. Huss*  
JOHN P. HUSS  
Acting Chief, Plans Office

If your address has changed or if you wish to be removed from the RADC mailing list, or if the addressee is no longer employed by your organization, please notify RADC (ESM) Hanscom AFB MA 01731. This will assist us in maintaining a current mailing list.

Do not return this copy. Retain or destroy.

**GROWTH OF PURE SINGLE CRYSTALS OF ALKALI  
HALIDES AND ALKALINE EARTH FLOURIDES**

**W. J. Fredericks**

**Contractor:** Oregon State University  
**Contract Number:** F19628-76-C-0156  
**Effective Date of Contract:** 1 March 1976  
**Contract Expiration Date:** 30 September 1978  
**Short Title of Work:** Growth of Pure Single  
Crystals of Alkali Halides  
and Alkaline Earth Flourides

**Program Code Number:** 8D10  
**Period of Work Covered:** Mar 76 - Sep 78

**Principal Investigator:** W. J. Fredericks  
**Phone:** (503) 754-2191

**Project Engineer:** Joseph A. Adamski  
**Phone** (617) 861-4841

Approved for public release; distribution unlimited.

This research was supported by the Defense Advanced Research Projects Agency of the Department of Defense and was monitored by Joseph A. Adamski (ESM), Hanscom AFB MA 01731 under Contract F19628-76-C-0156.

Accession For	
NTIS GRA&I	<input checked="" type="checkbox"/>
DTIC TAB	<input type="checkbox"/>
Unannounced	<input type="checkbox"/>
Justification _____	
By _____	
Distribution/ _____	
Availability Codes	
Dist	Avail and/or Special
A	

## UNCLASSIFIED

SECURITY CLASSIFICATION OF THIS PAGE (When Data Entered)

19) REPORT DOCUMENTATION PAGE		READ INSTRUCTIONS BEFORE COMPLETING FORM
1. REPORT NUMBER <b>(18) RADC-TR-80-413</b>	2. GOVT ACCESSION NO. <b>AD-A100641</b>	3. RECIPIENT'S CATALOG NUMBER
4. TITLE (and Subtitle) <b>GROWTH OF PURE SINGLE CRYSTALS OF ALKALI HALIDES AND ALKALINE EARTH FLUORIDES</b>	5. TYPE OF REPORT & PERIOD COVERED <b>Final Technical Report.</b> <b>1 Mar 76 - 30 Sep 78.</b>	
7. AUTHORED <b>(19) W. J. Fredericks</b>	6. PERFORMING O&G. REPORT NUMBER <b>N/A</b>	
9. PERFORMING ORGANIZATION NAME AND ADDRESS <b>Oregon State University Department of Chemistry Corvallis OR 97331</b>	10. PROGRAM ELEMENT, PROJECT, TASK AREA & WORK UNIT NUMBERS <b>(15) 61101E 3096AR20 (16) 17) AR</b>	
11. CONTROLLING OFFICE NAME AND ADDRESS <b>Defense Advanced Research Projects Agency 1400 Wilson Blvd Arlington VA 22209</b>	12. REPORT DATE <b>(11) May 1981</b>	
14. MONITORING AGENCY NAME & ADDRESS (if different from Controlling Office) <b>Deputy for Electronic Technology (RADC/ESM) Hanscom AFB MA 01731</b>	13. NUMBER OF PAGES <b>146 (12) 152</b>	
16. DISTRIBUTION STATEMENT (of this Report)  <b>Approved for public release; distribution unlimited.</b>	15. SECURITY CLASS. (of this report) <b>UNCLASSIFIED</b>	
17. DISTRIBUTION STATEMENT (of the abstract entered in Block 20, if different from Report)  <b>Same</b>	18a. DECLASSIFICATION/DOWNGRADING SCHEDULE <b>N/A</b>	
18. SUPPLEMENTARY NOTES <b>RADC Project Engineer: Joseph A. Adamski (ESM)</b>		
19. KEY WORDS (Continue on reverse side if necessary and identify by block number) <b>Purification Potassium Bromide Ion exchange - reactive gas purification Purification ratio for alkali ions</b>	<b>Strontium Fluoride Barium Fluoride</b>	
20. ABSTRACT (Continue on reverse side if necessary and identify by block number)  <b>The final report covers the design of ion selective filters and development of an ion exchange purification system for potassium bromide. The system consists of an ion selective filter for passage of potassium ions and a bromide anion exchange system for reduction of anionic impurities. Because of the high ionic strength of the solutions used and particularly their ability to hydrolyze amide and ester bonds, limitations are imposed on the materials that can be used for construction of those parts</b>		

272260

JOB

**UNCLASSIFIED**

**SECURITY CLASSIFICATION OF THIS PAGE(When Data Entered)**

of the systems that contact these solutions. Certain addition polymers are more promising for construction of the components of such a system than others, these are discussed in the body of the report. A special group of components have been designed and assembled to provide the fittings, valves, electrode chambers, sampling valves, columns and filters necessary for a closed purification system. The preparation of the resins for use in such a system required that their conversion to the forms required for purification of KBr, require that the reactions for this conversion go almost to completion. The extent of conversion of the resins affect the operational characteristics of the system and are discussed in this report. The product of the initial purification is a strongly acid KBr solution and techniques were developed to minimize external contamination during reduction of the purified salt solution to a solid.

The final purification step made during the growth of the crystal is treatment with a reactive gas. A greaseless reactive gas manifold was constructed and several reactive gas treatments were used in an attempt to purify the KBr. It was observed that KBr from various sources exhibits different characteristics during growth. These depend on the care taken to assure that the potassium bromide is pure. Some of these varying characteristics are discussed in this report.

**UNCLASSIFIED**

**SECURITY CLASSIFICATION OF THIS PAGE(When Data Entered)**

## SUMMARY

Sections I through XI of this report cover the design of an ion selective filter for potassium ions and an ion exchange system for bromide ions.

Sections XIII through XIX discuss the characteristics of ion exchange resins toward alkaline earth ions and the development of ion selective filters for strontium and barium ions.

Because of the high ionic strength of the solutions used in these processes, limitations are imposed on the materials that can be used in these systems. Their ability to hydrolyze amide and ester bonds limit materials of construction of the components which contact the solutions to addition polymers. The residual mold release compounds can contribute a significant amount of impurities to the solutions unless they are chemically removed. Elastomers can not be cleaned and the fittings that require them must be designed such that O-rings are not in the main solution flow.

A group of fittings and components were designed for the closed system chemistry required for ion-exchange, precipitation and reactive gas purification of KBr, SrF<sub>2</sub>, BaF<sub>2</sub>.

Crystals were grown by pulling KBr treated with HBr and HBr-O<sub>2</sub> atmospheres. Strontium Fluoride and Barium Fluoride were treated with HF and a Stockbarger system using a traveling furnace was designed for growth of small crystals.

## CONTENTS

SUMMARY . . . . .	1
LIST OF FIGURES . . . . .	3
LIST OF TABLES. . . . .	6
I INTRODUCTION. . . . .	8
II ION EXCHANGE RESINS AND THEIR CHARACTERISTICS . .	8
III ION EXCHANGE PURIFICATION OF KBr. . . . .	16
IV MATERIALS OF CONSTRUCTION . . . . .	32
V SYSTEM COMPONENTS . . . . .	38
VI RAW MATERIALS AND CHEMICALS . . . . .	56
VII CONVERSION AND REGENERATION OF RESINS . . . . .	60
VIII OPERATION OF PURIFICATION SYSTEM. . . . .	66
IX REACTIVE GAS TREATMENT AND CRYSTAL GROWTH . . . .	75
X RESULTS . . . . .	92
XI DISCUSSION. . . . .	97
XII PURIFICATION OF ALKALINE EARTH FLUORIDES. . . . .	106
XIII ION EXCHANGE RESINS AND THEIR CHARACTERISTICS . .	106
XIV DESIGN OF THE PURIFICATION SYSTEM . . . . .	120
XV CONSTRUCTION OF THE SYSTEM. . . . .	127
XVI MATERIALS . . . . .	135
XVII OPERATION OF ALKALINE EARTH PURIFICATION SYSTEMS.	138
XVIII REACTIVE GAS TREATMENT AND CRYSTAL GROWTH . . . .	141
XIX RESULTS . . . . .	145

## LIST OF FIGURES

Figure 1:	Separation Coefficient Surfaces for Chelex 100 from Acidic KBr Solutions. . . . .	18
Figure 2:	Separation Coefficient Surfaces for Chelex 100 from Neutral KBr Solutions . . . . .	19
Figure 3:	Separation Coefficient Surfaces for Chelex 100 from Basic KBr Solutions . . . . .	20
Figure 4:	Separation Coefficient Surfaces for AG50W-X8 from Acidic KBr Solutions. . . . .	21
Figure 5:	Separation Coefficient Surfaces for AG50W-X8 from Neutral KBr Solutions . . . . .	22
Figure 6:	Separation Coefficient Surfaces for AG50W-X8 from Basic KBr Solutions . . . . .	23
Figure 7:	Exchange of Br <sup>-</sup> for OH <sup>-</sup> on AG2-X8. . . . .	28
Figure 8:	Schematic of KBr Ion Exchange System . . . . .	30
Figure 9:	Basic Valve Assembly . . . . .	40
Figure 10:	Devices Based on Standard Valve. . . . .	42
Figure 11:	Fittings for Ion Exchange System . . . . .	43
Figure 12:	Top Plate for Column . . . . .	44
Figure 13:	Bottom Plate for Column. . . . .	45
Figure 14:	Millipore Filter Case. . . . .	46
Figure 15:	Mixing Column and Filter . . . . .	48
Figure 16:	Solution Collector . . . . .	50
Figure 17:	Ion Exchange System Installed in Laboratory. .	52
Figure 18:	Impedance Matching and Calibration Amplifier .	54

Figure 19: Sampling Technique . . . . .	55
Figure 20: Voltages of pH Electrode During Run 318 for Electrodes 1, 2, 3, 4. . . . .	69
Figure 21: Voltages of pH Electrode During Run 318 for Electrodes 5, 6, 7 . . . . .	70
Figure 22: Voltages of pH Electrode During Run 319 for Electrodes 1, 2, 3, 4. . . . .	71
Figure 23: Voltages of pH Electrode During Run 319 for Electrodes 5, 6, 7 . . . . .	72
Figure 24: Crystal Growing Furnace. . . . .	76
Figure 25: Details of Crystal Growing Furnace . . . . .	77
Figure 26: Three Stage Seal . . . . .	78
Figure 27: Reactive Gas Manifold. . . . .	80
Figure 28: A Portion of a Crystal . . . . .	88
Figure 29: Spectra of Metaborate Ion in Alkali Halides. .	104
Figure 30: Separation Coefficients for $\text{Ca}^{2+}$ , $\text{Sr}^{2+}$ , and $\text{Ni}^{2+}$ on Chelex 100 in the Barium Form. . . . .	110
Figure 31: Separation Coefficients for Calcium and Barium on Bio-Rex 70 in the Strontium Form. . . . .	112
Figure 32: Separation Coefficient for $\text{Ca}^{2+}$ on Bio-Rex 70 from 0.99M $\text{Ba}(\text{Br})_2$ Solution with a pH of 5.08	114
Figure 33: Separation Coefficients for $\text{Ba}^{2+}$ , $\text{Ca}^{2+}$ , and $\text{Ni}^{2+}$ on Bio-Rex 70 in the Strontium Form . . . . .	115
Figure 34: Separation Coefficients for $\text{Ba}^{2+}$ , $\text{Ca}^{2+}$ , and $\text{Ni}^{2+}$ on AG50W-X8 from a 1.05M Solution of $\text{SrBr}_2$ at a pH of 6.06. . . . .	116

Figure 35: Separation Coefficients for $\text{Ba}^{2+}$ , $\text{Ca}^{2+}$ , and $\text{Ni}^{2+}$ on AG50W-X8 from a 1.05M Solution of $\text{SrBr}_2$ at a pH of 6.06. . . . .	117
Figure 36: Separation Coefficients for $\text{Ba}^{2+}$ , $\text{Ca}^{2+}$ , and $\text{Ni}^{2+}$ on Bio-Rex 40 from 1.05M $\text{SrBr}_2$ at a pH of 5.06. . . . .	118
Figure 37: System Schematic for Precipitation of Strontium Carbonate or Barium Carbonate. . . . .	122
Figure 38: Schematic of the Strontium Fluoride Ion Exchange System. . . . .	124
Figure 39: The Monovalent Ion Removal System. . . . .	126
Figure 40: Top Closure for Precipitation Column . . . . .	128
Figure 41: Bottom Closure for Precipitation Column. . . . .	130
Figure 42: Filter for Fluoride Column . . . . .	132
Figure 43: Fluoride Ion Exchange Board Assembly . . . . .	133
Figure 44: Final Assembly Photograph of the Strontium Fluoride System. . . . .	134

LIST OF TABLES

Table 1:	E is a Function of any Factor that Affects the Various Activities . . . . .	9
Table 2:	Application of Resins. . . . .	10
Table 3:	Dilute Solution Selectivities, $E_K^M$ . . . . .	12
Table 4:	Stepwise Formation Constants for Mononuclear Complexes. . . . .	13
Table 5:	Dilute Solution Selectivity Order on AG-1-X2 and AG-2-X8 Anion Exchange Resins. . . . .	25
Table 6:	Trace Elements in Various Materials by INAA. .	33
Table 7:	Levels of Impurities in Mallinckrodt Reagent Grade KBr, Lot #WD6K . . . . .	57
Table 8:	Levels of Impurities in J. T. Baker Chemical Co., Reagent KBr . . . . .	58
Table 9:	Capacities of Resins in Milliequivalents . . .	65
Table 10:	Reactions of Hydrogen Halides with Alkali Metal Salts. . . . .	84
Table 11:	Hydrogen Bromide Reactions with Other Potassium Halides. . . . .	85
Table 12:	Analysis of KBr Crystals by INAA . . . . .	94
Table 13:	Laser Calorimetric Absorption Measurements . .	96
Table 14:	Analysis of Crystals Used for Absorption Measurements . . . . .	98
Table 15:	Absorption Coefficients of Laser Window Material . . . . .	99

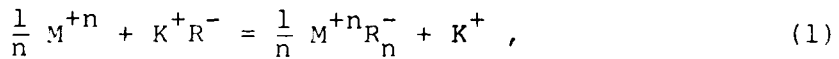
Table 16:	Distribution Coefficients on Dowex 50W-X12 . .	107
Table 17:	Effect of Nitric Acid Concentration on Distribution Coefficients on Dowex 50W-X12 . .	109
Table 18:	Properties of Certain Resins for Purification of Strontium Bromide and Barium Bromide Solutions. . . . .	119
Table 19:	Analysis of Strontium and Barium Compounds . .	136
Table 20:	Gibbs Free Energies (in Kcal) for Alkaline Earth Halides in 1 atm . . . . .	142
Table 21:	Solubilities of Strontium and Barium Halides .	142
Table 22:	Gibbs Free Energies (Kcal) for the Reaction of HF with Alkaline Earth Oxides. . . . .	143

## I. INTRODUCTION

This report discusses the use of ion exchange resins and reactive gas atmospheres for the purification of potassium bromide. The process described is an extension of techniques used earlier for the preparation of pure potassium chloride and sodium chloride. The design of selective ion filters for alkali ions and the use of ion exchange resins for purification of a single ionic species are described. The selection of resins for this purpose and materials for construction of purification systems will be discussed as well as the use of reactive atmospheres for final purification and the reduction of trace impurities by reactive gas atmospheres.

## II. ION EXCHANGE RESINS AND THEIR CHARACTERISTICS

Ion exchange methods are based on the reversible exchange of ions between an external liquid phase and an ionic solid phase. The solid phase consists of a polymeric matrix which is insoluble but permeable, contains fixed charge groups, and mobile counter ions of an opposite charge. These counter ions can be exchanged for other ions in the external liquid phase. The enrichment of one or more of the components can be obtained if selective exchange forces are operative. In using ion exchange resins to separate a mixture of trace ionic impurities from a desired major constituent, one utilizes the property of the resin to bind various ions to itself with binding energies specific to each species. This is illustrated by the equilibrium reaction



where  $M^{+n}$  is an impurity ion of charge +n and  $K^+R^-$  a potassium ion on an exchangeable resin site. The selectivity E is a mass action constant given by

$$E_K^{M/n} = \frac{[a_{M^{+n}}]_R [a_K^+]}{[a_{K^+}]_R [a_{M^{+n}}]}, \quad (2)$$

where a is the activity of the various components, R denotes the resin phase, and other ions are in the solution phase. The selectivity is not constant for a particular ion on a particular resin but is a function of any of the conditions of the resin or solution that affect the activity of the components in either phase. The major factors that control the magnitude of E are given in Table 1.

Table 1

E is a Function of Any Factor that Affects the Various Activities

1. Resin type and structure (energy of sorption)
2. Extent of resin cross linking
3. Resin swelling
4. Ionic charge
5. Total ionic strength of passing solution
6. Relative ionic strength of exchanging ions
7. Extent of hydration of ions (size)
8. Strength of hydration bond
9. pH of the solution
10. Temperature

This property of differential absorption for various ions on the resin can be used in many ways to separate a mixture of such ions. In Table 2, we list the principal ways in which one employs these resins to separate mixtures of ions.

Table 2. Application of Resins

1. Ion exchange chromatography
2. Ion exclusion
3. Ion conversion
4. Frontal analysis
5. Selective ion filters (requires more than one resin)

Selectivity coefficients are determined by equilibrium measurements in which a small quantity of resin is shaken for several hours with a small quantity of solution. Then the solution is removed and the resin is washed to remove the ions it has absorbed, then both solutions are analyzed. However, a more practical measurement is a quantity we call the separation coefficient which is given by equation 3.

$$S_i = \frac{C(i)}{C_o(i)} = f(\text{Resin, } C_j, T, Q, \dots, \text{etc.}), \quad (3)$$

where  $C_o(i)$  is the concentration of impurity  $i$  in a solution whose major component  $j$  is at concentration  $C_j$  and  $C(i)$  is the concentration of impurity  $i$  after this solution has passed over a specific quantity of resin  $R$  at a flow rate  $Q$  at temperature  $T$  at a constant pH. The quantity  $S_i$  is a practical

measure of the effect of the factors given in Table 2 and not a thermodynamic quantity. It can be quickly measured and determine the effect of  $C_j$ , pH, and Q on the separation of trace quantities of i from j.

There are many resins from which to choose in designing selective ion filters or conventional ion exchange systems. For systems that involve ionic solutions, one must choose a polymeric matrix that is not attacked by the solutions in contact with it. In the purification of potassium bromide or other alkali halide this involves concentrated salt solutions, strong acids, and strong bases. Polystyrene forms a reasonably satisfactory matrix in which the reactive groups are distributed. This matrix will leach some organic materials as it ages when in contact with solutions. For cation exchanges there are a rather wide range of possible resins, but for anion exchange the ideal resins have not yet been developed.

Of the five methods given in Table 2, the two most useful in preparation of materials for crystal growth are ion exchange chromatography and selective ion filters. For ion exchange chromatography, the major component and the impurities contained in its solution are absorbed on a resin. Then the various ions are eluted from the resin in a solvent in a sequential order. This process is not particularly efficient when one of the components far exceeds the others in concentration. It is a process of last resort and purification of salt systems for crystal growth because the high concentration sometimes causes overlapping elution bands as the resin becomes saturated. Thus excessively long size columns are required. The preferred method is a selective ion filter. These operate with a combination of resins in which the orders of selectivity for various ions differ between two or more resins. Table 3 lists the selectivities of four cation exchange resins in which the order

monovalent ions differ.

Table 3. Dilute Solution Selectivities,  $E_K^M$ .

Chelex 100	$H >> Li > Na > K > Rb > Cs; Cu^{++}/Na^+ >> 100^*$
AG50W	$Ag > Rb > Cs > K > NH_4^+ > Na > Li$
Bio Rex 40	$Cs > Rb > K > Na > H > Li$
Bio Rex 70	$H > Ag > K > Na > Li$

$$*E_{\frac{Cu^{2+}}{Na^+}}^2$$

The Chelex 100 will absorb hydrogen, lithium, sodium more strongly than potassium while in the other three; in particular AG50W, silver, rubidium, and cesium are absorbed more strongly than potassium and potassium more strongly than ammonia, sodium, and lithium. Thus, if you pass a solution containing a mixture of these ions first through Chelex in potassium form the hydrogen, lithium, and sodium will be removed. Then passing the same solution through AG50W in the potassium form silver, rubidium, and cesium will be removed. The combination passes a solution whose only monovalent cation is potassium.

The other principal cationic impurities in the alkali halides are divalent cations; these may exist as free ions or as complex ions. Table 4 provides an illustration of the formation constants of mononuclear complexes for various ions that might be present as impurities in the alkali halides. Equilibrium constants given in Table 4 were measured at various ionic strengths in sodium perchlorate solutions, a medium that

Table 4. STEPWISE FORMATION CONSTANTS FOR MONONUCLEAR COMPLEXES\*

Ligand	Central Ion	Logarithm of Equilibrium Constant					Medium and Ionic Strength
		$K_1$	$K_2$	$K_3$	$K_4$	$K_5$	$K_6$
Cl <sup>-</sup>	Ag <sup>+</sup>	2.85	1.87	0.32	0.86		0.2 M NaClO <sub>4</sub>
	Cd <sup>++</sup>	1.32	0.90	0.09	-0.45		4.5 M NaClO <sub>4</sub>
	Hg <sup>++</sup>	6.74	6.48	0.85	1.00		0.5 M NaClO <sub>4</sub>
	Pb <sup>+++</sup>	0.88	0.61	-0.40	-0.15		1.0 M KCl
	In <sup>+++</sup>	1.42	0.81	1.00	-0.20		1.0 M NaClO <sub>4</sub>
	Fe <sup>+++</sup>	0.62	0.11	-1.40	-1.92		1.0 M NaClO <sub>4</sub>
	Fe <sup>++</sup>	0.63	0.04				2.0 M NaClO <sub>4</sub>
Br <sup>-</sup>	Ag <sup>+</sup>	4.15	2.96	0.84	0.94		0.1 M NaClO <sub>4</sub>
	Cd <sup>++</sup>	1.56	0.46	0.23	0.41		1.0 M NaClO <sub>4</sub>
	Hg <sup>++</sup>	9.05	8.28	2.41	1.26		0.5 M NaClO <sub>4</sub>
I <sup>-</sup>	Cd <sup>++</sup>	2.08	0.87	2.09	1.59		4.5 M NaClO <sub>4</sub>
	Hg <sup>++</sup>	12.87	10.95	3.78	2.23		0.5 M NaClO <sub>4</sub>
CN <sup>-</sup>	Cd <sup>++</sup>	5.48	6.14	4.56	3.58		3.0 M NaClO <sub>4</sub>
	Hg <sup>++</sup>	18.00	16.70	3.83	2.98		0.1 M NaNO <sub>3</sub>
SCN <sup>-</sup>	Ag <sup>+</sup>	4.59	3.70	1.77	1.20		4.0 M NaClO <sub>4</sub>
	Ni <sup>++</sup>	1.18	0.46	0.17			1.0 M NaClO <sub>4</sub>
	Cr <sup>+++</sup>	3.10	1.70	1.00	0.30	-0.70	0 corr (50°C) <sup>†</sup>
	Fe <sup>+++</sup>	1.96	2.02	-0.41	-0.14	-1.57	1.8 M KNO <sub>3</sub> . Values vary widely with medium.
S <sub>2</sub> O <sub>3</sub> <sup>=</sup>	Ag <sup>+</sup>	8.82	4.64	0.69		0 corr (20°C)	

\*Values from Stability Constants. The ligands are all anions of strong acids except CN<sup>-</sup>. For HCN, pK<sub>a</sub> = 9.32.

<sup>†</sup>"0 corr" means that data taken in dilute ionic media have been extrapolated to zero ionic strength.

(From Butler, N. N. "Ionic Equilibrium," Addison-Wesley, Palo Alto (1964))

does not form complexes. In our case, the bromide ion concentration would be very high and a significant amount of complex ion formation would occur.

The free divalent cations are principally removed on Chelex 100, the Bio-Rad Laboratory\* gives the ratio of copper to sodium selectivities as much greater than 100 and rough Si measurements in this laboratory show this to be typical for divalent ion impurities on this resin. Most of the free divalent ions are collected in the Chelex column. As the free ions are removed, the complexes dissociate to maintain the equilibrium and more of the ion is removed on the Chelex column. This requires that the amount of Chelex be large and the rate of passage be slow enough to allow the process to approach equilibrium. Dowex 50, used here as AG50W, in the potassium form will only remove those divalent ions with a selectivity greater than 2.28 for the 8% divinylbenzene (DVB) resin. The remaining divalent ions represented by the amount contained as a complex in equilibrium with a small amount of free ion are removed on anion exchange resins. In these columns, the polyvalent negatively charged bromide complexes are absorbed on the resin and as that occurs more complex forms from the free ion and the effluent from that column is essentially free of divalent impurities. The amount of divalent impurities remaining in the salt is controlled by the amount of resin, the length of the column, and the rate of the flow through the column.

The removal of anionic impurities cannot be as easily accomplished as that of the cationic impurities. A large number of impurity ions have selectivities lower than that of

---

\*Bio-Rad Laboratory supplied the analytical grade resins used in these studies. They do not manufacture resins but purify them.

bromide on Dowex 1 and Dowex 2. This is typical of all anion exchange resins and at present resins are not available that have reversed orders of selectivities, so that the development of an ion selective filter is impossible. Thus, anion purification is accomplished in two steps: the first ion exchange and the second reactive gas treatment. If the solution contains divalent anions, these are removed. Almost any exchange resin will have a much higher selectivity coefficient for divalent ions than any of the monovalent ions. Ions such as hydroxide, bicarbonate, aminoacetate, bisulphite, bromate, and cyanide can be reduced to vanishingly small concentrations by making the solution strongly acid and removing dissolved gasses by passing oxygen-free nitrogen through the solution at elevated temperatures. Of the remaining ions, chloride and fluoride are the only ones present in any significant quantity. The acetates, formates, and phosphates may be present as their corresponding acid. These are the major impurities in potassium bromide. Selectivity orders given in the literature (1) are for very dilute solutions passed under ideal conditions, and by converting the anion resin to the bromide form these orders of selectivity can be inverted in some cases due to the extremely high bromide concentration on the resin. Both the resins are strongly basic resins ( $E_{Cl}^{OH} = 0.09$  on Dowex 1). If the bromide concentration is made sufficiently great, it is possible to invert the bromide/hydroxide selectivity coefficients, so that considerable control can be exercised over the behavior of the resins by control of the ionic strength of the solutions passing through a column. The principal anionic impurities of an acidic salt solution passing through anion exchange columns should be chloride ion and fluoride ion. The solution should contain exceedingly small amounts of hydroxide, because after passage through a strongly acid cation exchange resin followed by the anion exchange resins in the bromide form, the

solution will be extremely acid. HBr treatment of the salt will remove both chloride and fluoride ions, converting them to bromide. These conversions will be discussed in more detail later in this report.

With this basic introduction to the principles that will be used in the purification of KBr, a discussion of the design of a specific system for purification of KBr and the materials problems associated with purification of ionic salts is given.

### III. ION EXCHANGE PURIFICATION OF POTASSIUM BROMIDE

The data in Table 3 shows Chelex 100 to be the only resin with selectivities in the order  $H \gg Li > Na > K > \dots$ . Therefore, Chelex 100 and one of the other resins listed must be used to obtain the reversed order of selectivities necessary for a selective ion filter. The initial measurements necessary for the design of the selective ion filter are to determine the separation coefficients of the most difficultly separable ions on various resins under conditions that simulate the operation of a purification system. Such measurements were discussed in the first semi-annual technical report. Here we need only outline the method and report all measurements of separation coefficients made for the resins utilized in the purification system.

To a solution of potassium bromide of known concentration, known quantities of various alkali ions are added to produce a solution rich in these impurities. This solution is analyzed to determine the initial concentration of impurities. It is then passed through a measured amount of resin and the effluent collected in polypropylene sample vials. Each sample contains a volume of solution equal to the volume of the resin under

test. These samples were analyzed by atomic absorption for lithium, sodium, cesium, and rubidium and for a particular concentration of potassium bromide solution. To generate a complete separation surface for a resin, these measurements must be made at a variety of salt concentrations and pH's.

Initial measurements on these four resins indicated that Chelex 100 and AG50W-X8 would be effective in purification of potassium ion. Figures 1, 2, and 3 show the separation surfaces for Chelex 100 as a function of volume of solution passed through the column and the concentration of KBr in the test solution. The convolutions that occur in the surfaces as a function of concentration are interesting. However, it is the ion adjacent to potassium on the higher selectivity side, sodium, that determines the best operating conditions for Chelex 100. In Figure 3, the best separation coefficients for sodium and potassium occur at concentrations at 1 mole per liter to about 1.8 mole per liter at pH of 8.5. Quite acceptable values occur at concentrations of 1.5 moles per liter and this provides manageable solution volumes and some latitude for concentration variation. At this pH, cesium, rubidium, and lithium appear to separate well.

It is possible to use Chelex 100 in an acid solution to obtain separation, but the separation coefficients are not as good and in the presence of hydrogen ion the potassium is quickly displaced from the Chelex resin requiring the system to be stopped and regenerated prematurely. A satisfactory pH range for these separations is 7.5 to 9.

Figures 4, 5, and 6 show this laboratory's experimentally measured separation surfaces for AG50W-X8 at pH's 4.8, 7, and 9.2. Here the cesium and rubidium separation surfaces are the critical ones. While separation is available at all pH's, the acidic pH at 4.6 is somewhat better in the concentration range between 1 and 2 moles per liter.

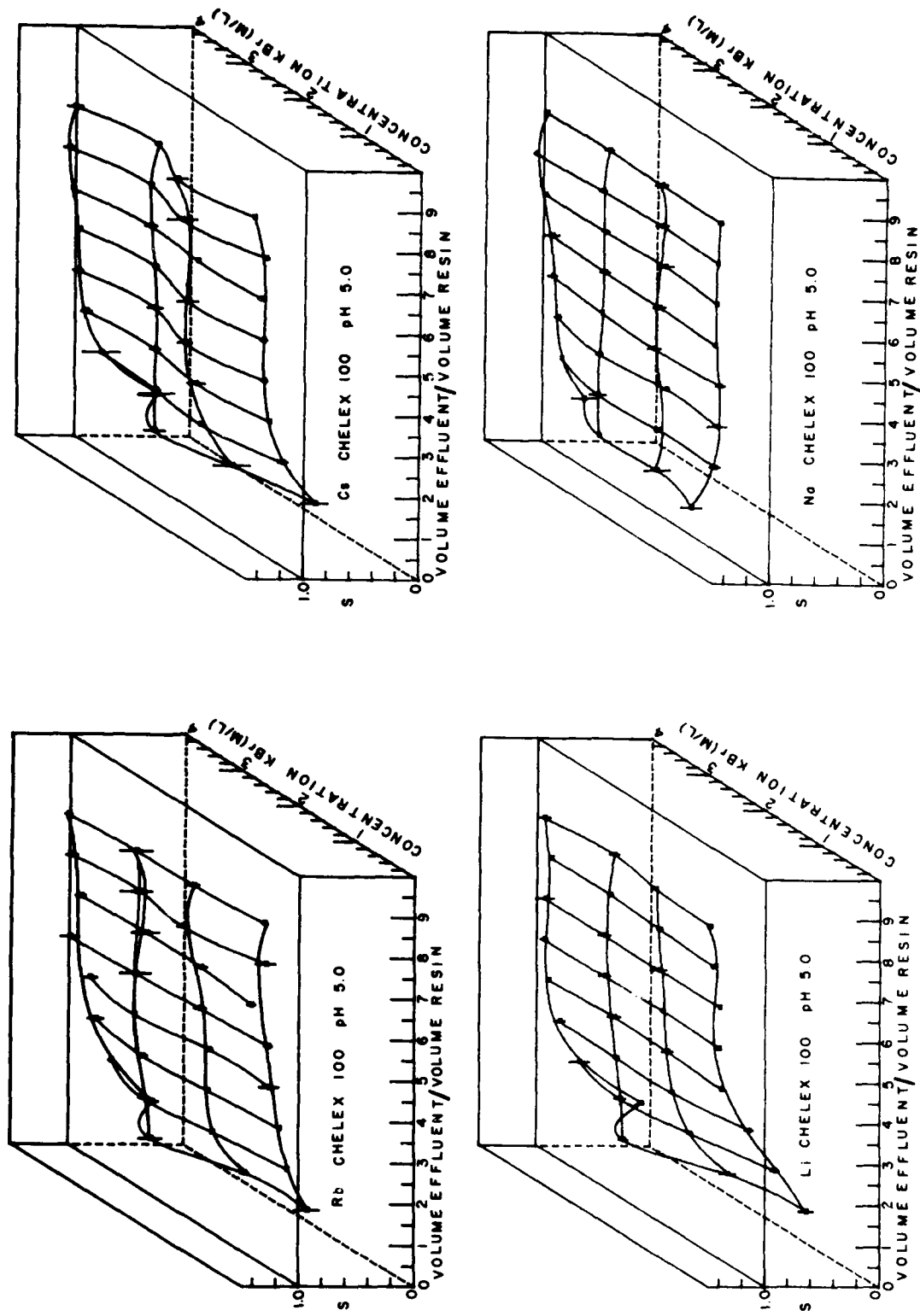


Figure 1: Separation Coefficient Surfaces for Chelex 100 from Acidic KBr Solutions

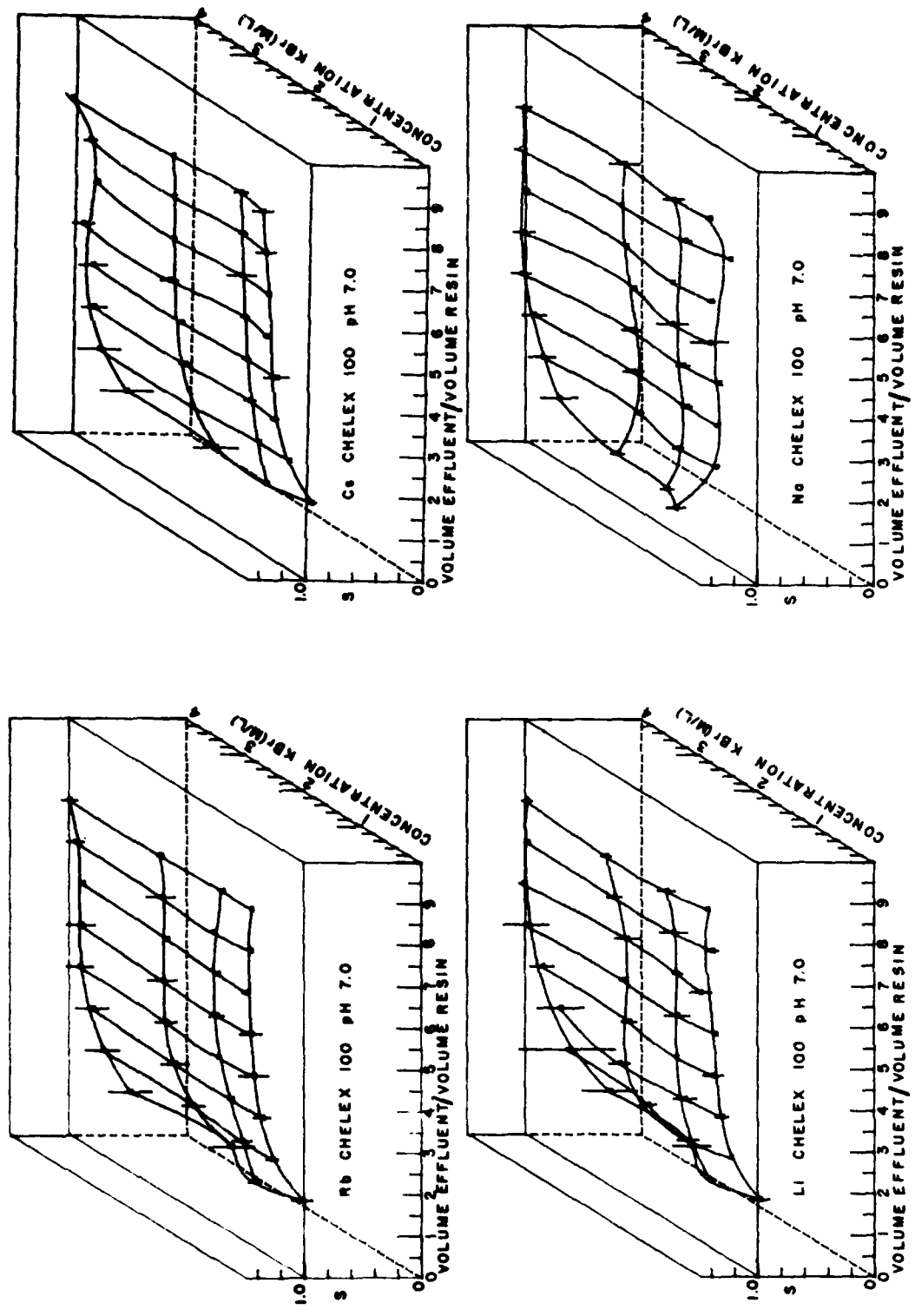


Figure 2: Separation Coefficient Surfaces for Chelex 100 from Neutral KBr Solutions

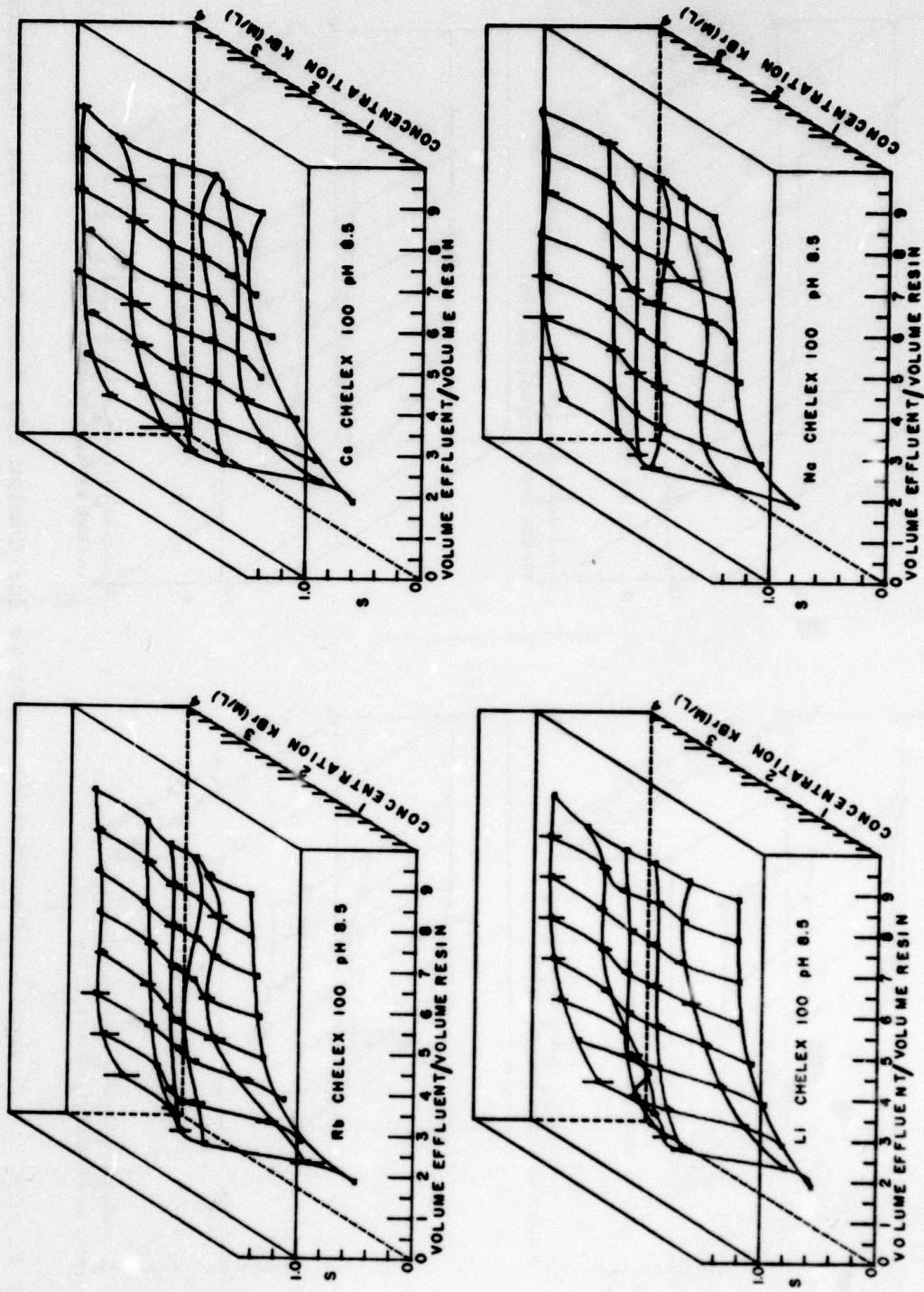


Figure 3: Separation Coefficient Surfaces for Chelex 100 from Basic KBr Solutions

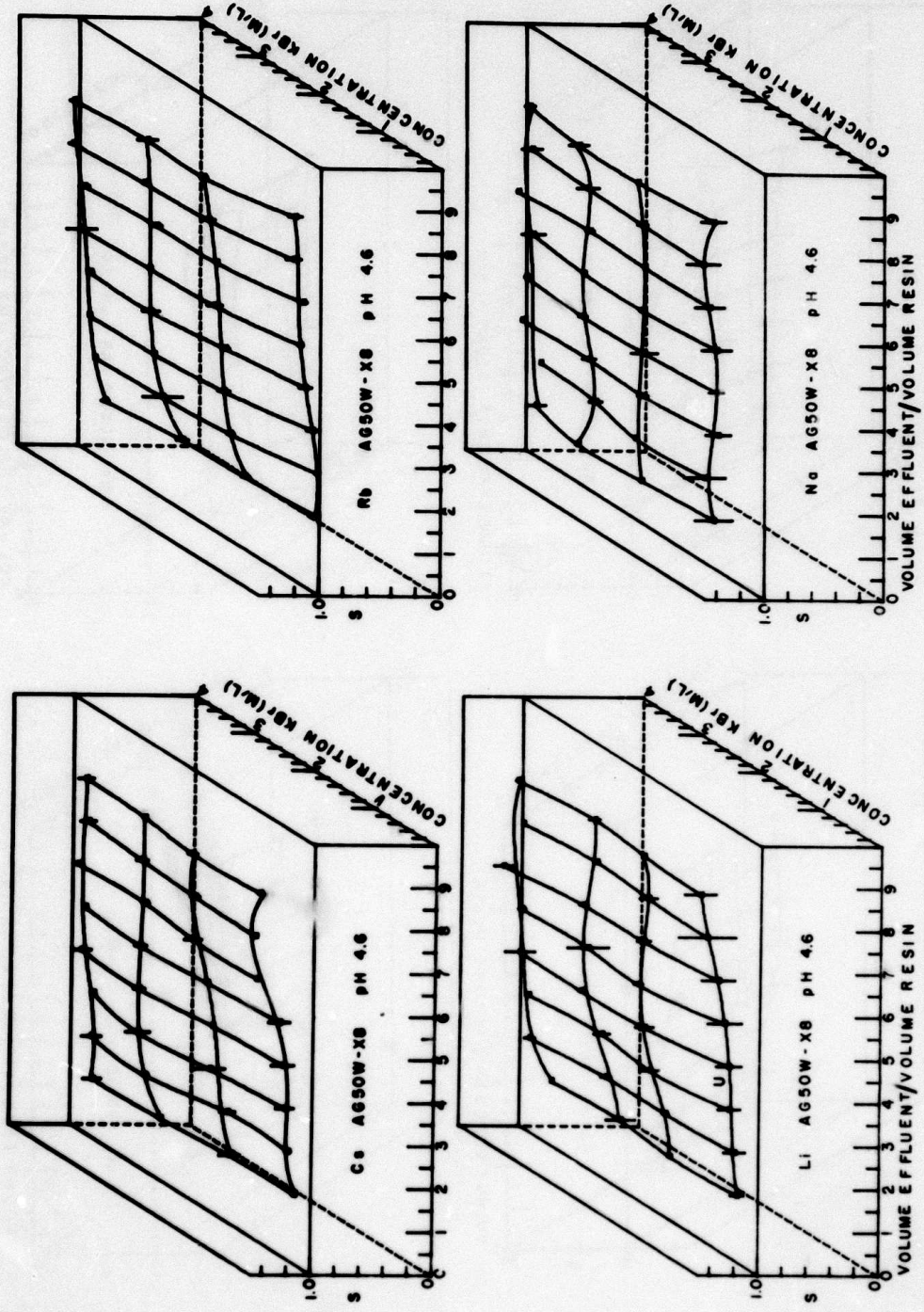


Figure 4: Separation Coefficient Surfaces for AG50W-X8 from Acid KBr Solutions

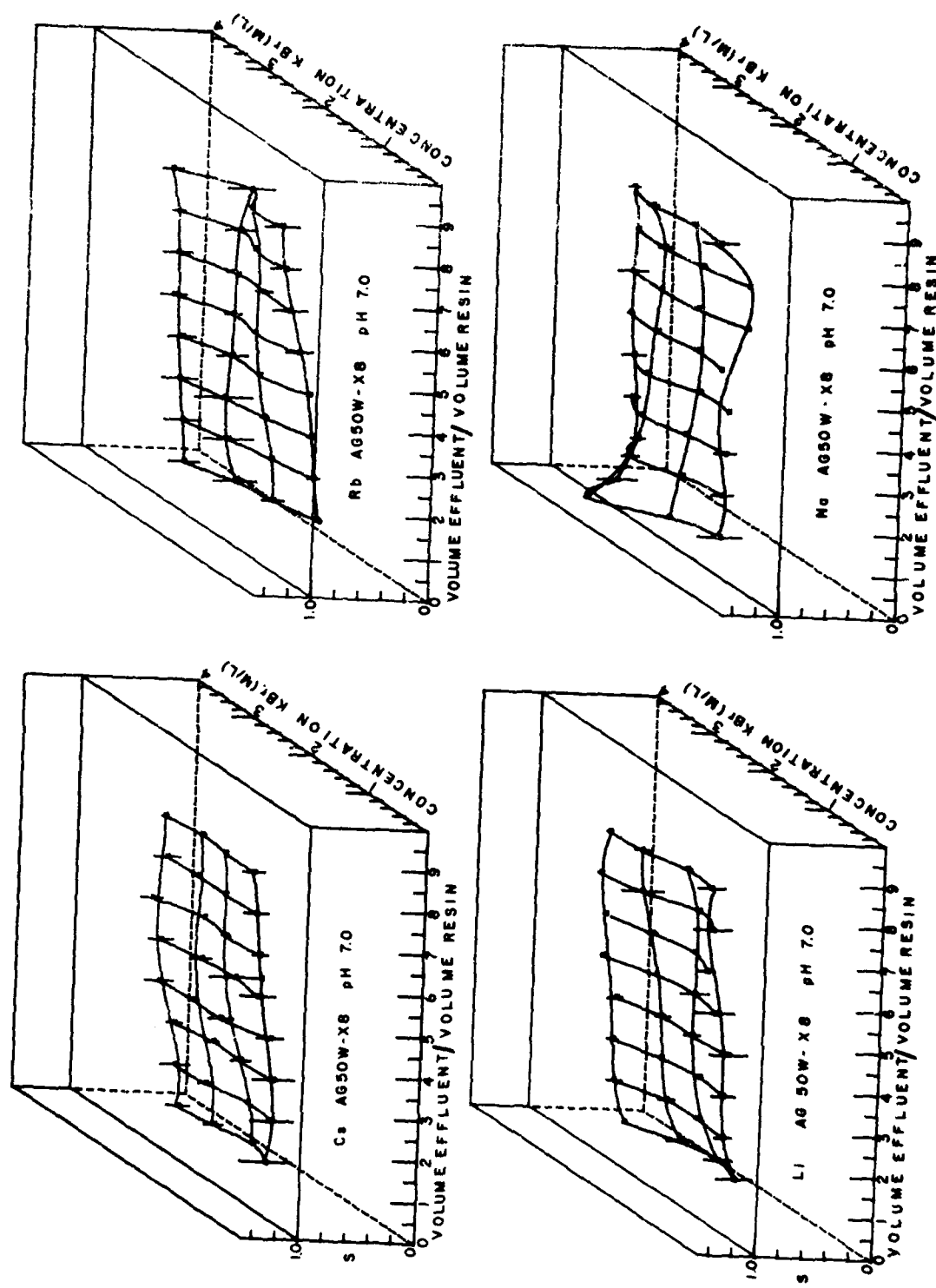


Figure 5: Separation Coefficient Surfaces for AG50W-X8 from Neutral KBr Solutions

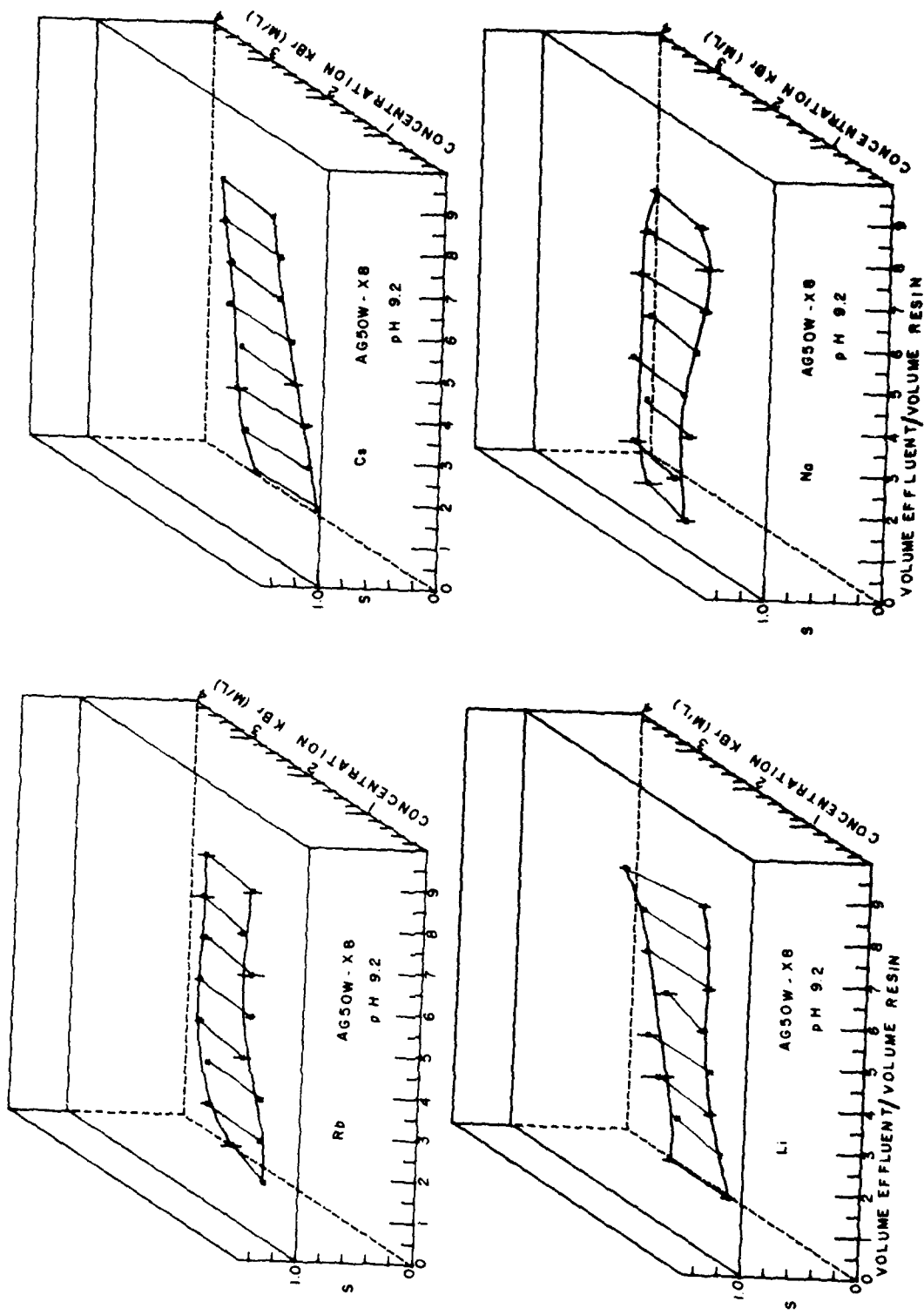


Figure 6: Separation Coefficient Surfaces for  $\text{AG50W-X8}$  from Basic  $\text{KBr}$  Solutions

Thus, a selective ion filter for potassium can be made with these two resins if we operate the Chelex 100 in a basic region and the AG50W in an acidic region. The separation for sodium on Chelex appears to be satisfactory to 6.5 effluent volumes of resin, and the cesium and rubidium appeared to separate well on the AG50W to 8 volumes of effluent per volume of resin.

As mentioned in the preceding section, resins do not exist with the proper order of selectivities for an anion selective ion filter. For halide ions, this requires somewhat different strategy than used for purification of the potassium ion. The anion exchange resins are to perform two functions; first, to remove the transition metal-bromide ion complexes that will form in the solutions, and second to remove other simple monovalent anions. The resins used in the anion exchange columns are Bio-Rex AG 1-X2 and Bio-Rex AG2-X8; these are the analytical grade resins similar to Dowex 1 and Dowex 2. They are both strongly basic anion exchange resins. In the anion purification columns, the first resin encountered by this solution is AG 1-X2 in the bromide form, then, in a second anion exchange column, the AG 2-X8 in a bromide form. The order of selectivity on these resins is similar to Dowex 1 and Dowex 2 (1), but varies slightly due to the differences in cross linkage between the resins used in these columns and those resins studied by Peterson (1). Table 5 gives the order of selectivity in 0.2 M solutions for these particular resins at the specified cross linkage used in this work. In Table 5, the ions which lie above bromide are less strongly bound to the resin than bromide itself. In our usage of the resin, we are concerned with solutions of much higher concentration than used in these preliminary dilute solutions selectivity measurements of a very wide selection of anions. In principle, we attempt to increase the chemical potential of bromide on the

resin lattice to such an extent that it will exchange for ions lying above it in Table 5. Since the potassium bromide solution passing through the columns will be around 1.5 molar as dictated by the potassium selective ion filter, the bromide concentration

Table 5

Dilute Solution Selectivity Order on AG 1-X2 and AG 2-X8  
Anion Exchange Resins

<u>AG 1-X2</u>	<u>AG 2-X8</u>
F <sup>-</sup>	F <sup>-</sup>
CH <sub>3</sub> COO <sup>-</sup>	OH <sup>-</sup>
IO <sub>3</sub> <sup>-</sup>	CH <sub>3</sub> COO <sup>-</sup>
OH <sup>-</sup>	IO <sub>3</sub> <sup>-</sup>
Cl <sup>-</sup>	HCO <sub>3</sub> <sup>-</sup>
NO <sub>2</sub> <sup>-</sup>	Cl <sup>-</sup>
HSO <sub>3</sub> <sup>-</sup>	NO <sub>2</sub> <sup>-</sup>
CN <sup>-</sup>	HSO <sub>3</sub> <sup>-</sup>
Br <sup>-</sup>	CN <sup>-</sup>
NO <sub>3</sub> <sup>-</sup>	Br <sup>-</sup>
ClO <sub>3</sub> <sup>-</sup>	NO <sub>3</sub> <sup>-</sup>
HSO <sub>4</sub> <sup>-</sup>	ClO <sub>3</sub> <sup>-</sup>
Cl <sup>-</sup> /OH <sup>-</sup> ≈ 1.5	I <sup>-</sup>
	Cl <sup>-</sup> /OH <sup>-</sup> ≈ 25

on the resin should be many times that of the bromide ion concentration in the solution. The AG 1-X2 resin is used primarily to remove complex ions from solution and a low cross linkage was chosen to allow good penetration of the large highly charged ions into the resins. The AG 2-X8 is used to scavenge the remaining monovalent anions from the solutions.

The resins come from the manufacturers in the chloride form. The manufacturers ratio of chloride to hydroxide selectivity, the last entry in Table 5, provides an approximate scale for our qualitative order. This ratio for AG 1-X2 is ~ 1.5, but AG 2-X8 binds the chloride to it about 25 times more strongly than hydroxide; therefore, AG 2-X8 will be the most difficult resin on which to invert the selectivity orders. AG 2-X8 will be used as an example to illustrate how this inversion was accomplished. The chloride form of the resin converted into the hydroxide form by treatment with purified 3M potassium hydroxide. With an X8 resin, the swelling was minimal. The resin converts from a light amber color to a very dark chocolate brown in color. The conversion was monitored by observing the pH of the effluent solution. When there was no difference in the pH of the entering and exiting potassium hydroxide solution, the conversion was complete. The resin was washed with copious quantities of deionized water until the pH of the effluent reaches a constant but slightly basic value. Next, a 35% solution of pure hydrobromic acid was passed through the column; the resin converts slowly from its rich chocolate brown to a dark amber color. When the conversion was complete, the effluent acid had the same pH as the entering acid. In this form, AG 2-X8 would convert deionized water to an HBr solution. It was impossible to wash the column free of bromide without converting the resin to the hydroxide form; this can be observed by passing large quantities of water and watching the resins change from dark amber to

chocolate brown as the water washes through the column. That in itself was evidence that the order of selectivities had been reversed. Figure 7 illustrates the removal of  $\text{OH}^-$  from a 1.5 M potassium bromide solution containing 0.1 mole of potassium hydroxide passed through a test bed of AG 2-X8 in the bromide form.

Using ion exchange resins in this way was somewhat unconventional. The first portion of the curve, from 0 to about 0.8 milliequivalents  $\text{OH}^-$  added, occurred as the HBr solution present in the column was eluted by the solution. The region from about 0.8 milliequivalents added to 4 milliequivalents added illustrates the exchange capability of the bromide form of the resin for hydroxide. Up to 4 milliequivalents of  $\text{OH}^-$  added, the column has removed 99% of the hydroxide that was contained in the solution passing through the column and about 31% of the available exchange sites of the resin have been used. The exchange of  $\text{Br}^-$  for  $\text{OH}^-$  is effective until about 80% of the available resin sites have been occupied by hydroxide. The resin behaves very much like an acid buffer with a total capacity equal to 80% of the conventional exchange capacity of the resin. The exhaustion of the exchange capacity can be followed easily with a pH meter monitoring the effluent solution. However, with this particular resin, AG 2-X8, the extent of the exhaustion of the resin bed can be followed visually. As the resin becomes exhausted, it turns from its bromide amber color to the chocolate brown color of the hydroxide form. This occurred when 80% of the active sites had been exchanged for hydroxide. In a long column of the resin, the top portion of the resin was observed turning hydroxide color and that color moved slowly down the resin bed as the bed became exhausted.

The characteristics of the ion exchange resins and the availability of pure chemicals determine the design of the ion exchange system for potassium bromide purification. The time

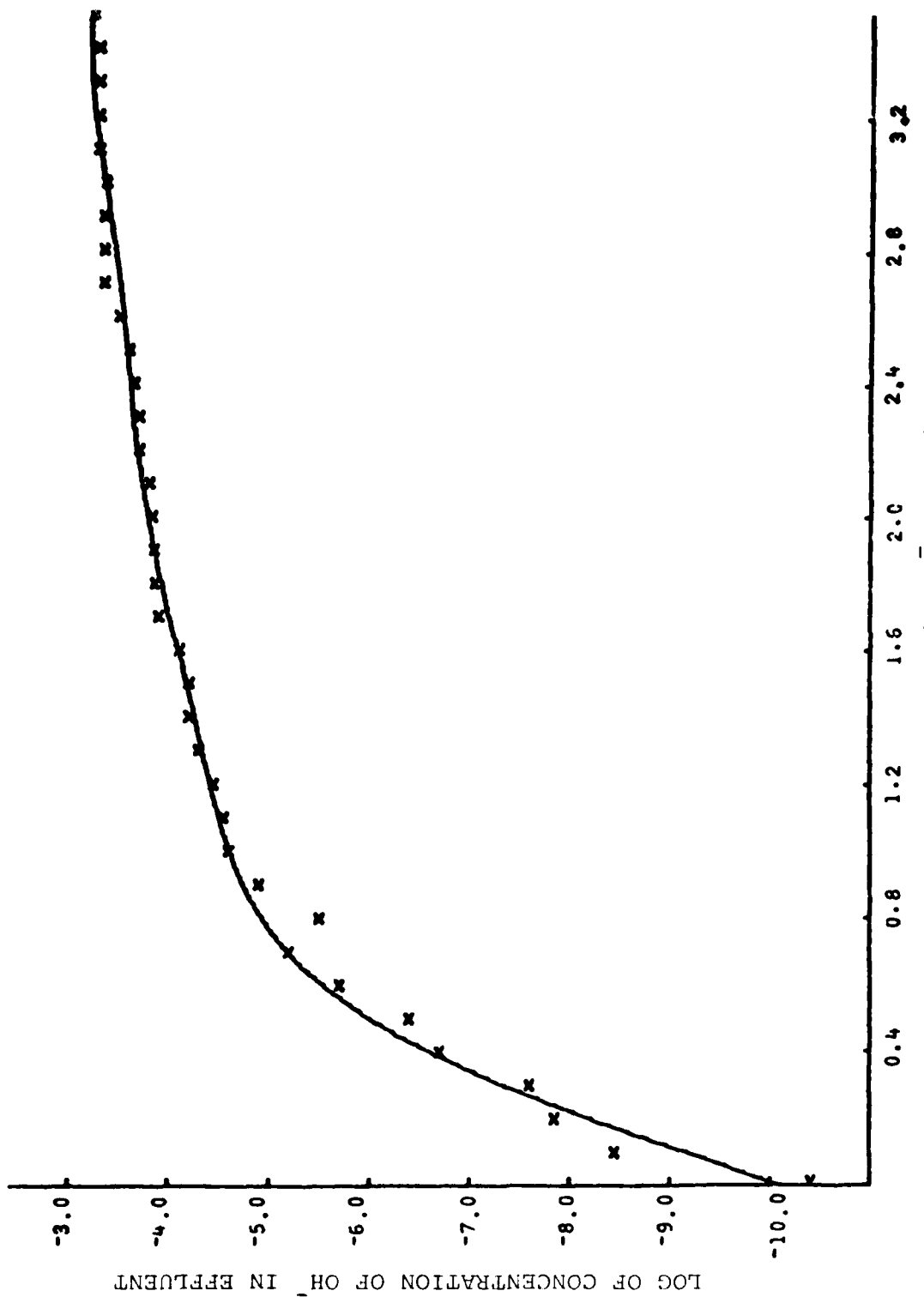


Figure 7. Exchange of  $\text{Br}^-$  for  $\text{OH}^-$  on AG 2-X8

schedule of this program required that the purification system be constructed before the measurements of the characteristics of the resin were completed. Therefore, the ion exchange system had to be designed such that several of the parameters affecting the exchange characteristics of the resin could be controlled. Figure 8 schematically shows such a system. The columns labelled cation 1 and cation 2 constituted the selective ion filter for purification of potassium and the columns labelled anion 1 and anion 2 provided the double exchange system for bromide purification. Columns labelled pH 1 and pH 2 were used to control the pH of the solution passing from the first resin of the selection ion filter to the second resin of the selective ion filter, and the pH of the effluent KBr solution. The central column labelled concentration and pH could adjust both pH and concentration of the solution entering the anion exchange columns. The five reservoirs shown at the top of the figure contained the KBr to be purified, pure potassium bromide for changing the concentration of the solution, potassium hydroxide for increasing pH and for regeneration of various resins, pure water for dilution of the solution and for washing the resins after regeneration, and hydrobromic acid for decreasing pH and resin conversion. All of the regeneration and pH control reservoirs were isolated from each other by teflon check valves, indicated by the circle with the rectifier symbol in it. The circles with crosses are "on/off" and off valves, a dot beside an on/off valve represents a sampling point in the system, the half shaded circles represent flow control valves, the rectangles with F beside them show the location of filters to retain resin particles, the squares labelled M are measuring points which, in this system, contain a combination glass electrode referenced against silver chloride. The reservoirs are maintained under a constant filtered nitrogen pressure and the

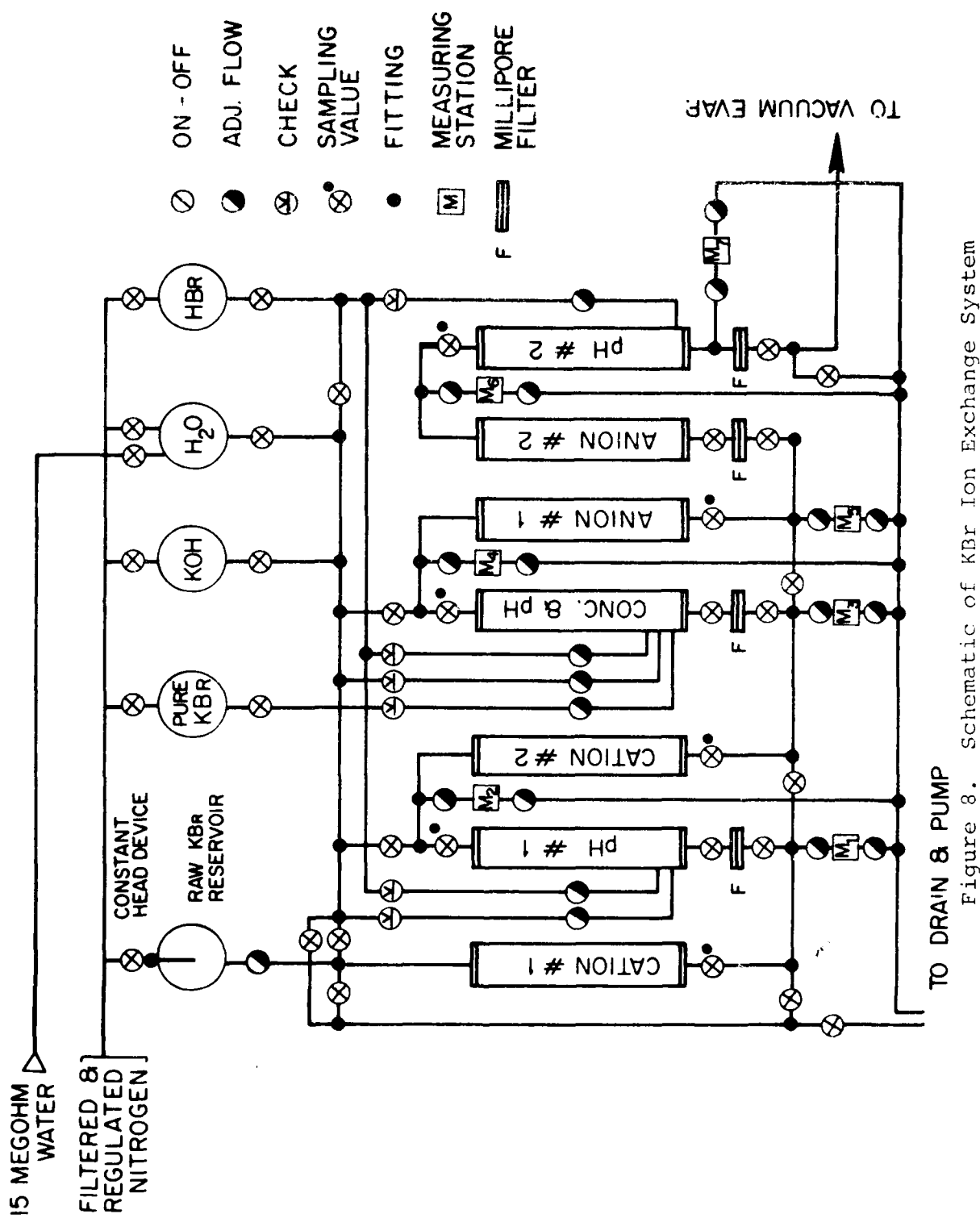


Figure 8. Schematic of KBr Ion Exchange System

pure water is fifteen megohm water supplied by a Millapore Milli-QII purification system, which in turn receives distilled water from the building system.

When operated in the purification mode, the KBr solution flowed from the raw KBr reservoir downward through cation column 1 through the first filter and upward through the pH 1 column. A small amount of the effluent from the cation 1 column passed through M1 and its pH measured, and the solution used for this measurement was discarded because of contamination from the glass electrode. The pH of the effluent from column 1 was adjusted in next column. The solution emerging from pH column 1 was sampled to determine the magnitude of the pH adjustment made in that column and the bulk of the solution passed through cation column 2. The effluent from cation column 2 sampled at M3 and the bulk of the solution passed through the concentration/pH adjustment column, sampled again at M4 before the bulk of the solution passed downward through anion column 1, whose effluent was sampled at M5. The solution then passed through the third filter and through anion column 2, whose effluent was sampled at M6, and finally into the last pH adjusting column whose effluent was measured at M7 with the bulk of the solution flowing through filter F to the vacuum collector. All portions of the solution that came in contact with measuring electrodes were discarded through a constant head device, which is not shown in this diagram. The system was completely closed from the beginning of the purification process until the final evaporation of the solution.

#### IV. MATERIALS OF CONSTRUCTION

A common source of contamination in a purification process is the introduction of impurities from the materials which contact the solution or the melts involved in preparation of pure crystals. In systems used to produce pure salt solutions, a source of contamination might be glass, which itself exhibits some ion exchange properties, and in the presence of strong bases will contribute silicic acids to the solution. The best means of preventing contamination of the solutions is to allow them to contact only materials which they do not wet and which do not strongly absorb impurities that can contaminate subsequent solutions. Many plastics possess these desirable characteristics. However, when using concentrated ionic solutions and strong acids or bases, condensation polymers must be avoided as the ester and amide bonds are hydrolyzed by a strong acid and quickly break down these polymers. This precludes the use of such materials as Nylon or Dalrin. The best polymers for use in these systems are addition polymers such as polyethylene, polypropylene, and teflon. Methylmethacrylate which contains an acid side chain not involved in a polymer bond is also a satisfactory material. It had a lifetime of about ten years in chloride systems and should have a similar lifetime in bromide systems. It fails by swelling and checkering and not by decomposition of the polymer bond; thus it does not release the large amounts of organic materials into solution that the condensation polymers do. The only polymeric material that will withstand exposure to gaseous hydrogen bromide is teflon. The phenomenally unreactive polyolefins added hydrogen bromide to the remaining unsaturated bonds in the polymer. They became brittle and broke down rapidly.

Table 6 gives analyses of a variety of materials used in purification and crystal growth. These are divided into groups

Table 6. Trace Elements in Various Materials by INAA  
 (concentrations in ppb)

Section A - Analyses taken from literature.

Section B - Analyses of material used in this work.

GROUP A		Elements											
Section A		Zn	Fe	Sb	Co	Cr	Sc	Cs	Ag	Cu	Hf		
Teflon	9.3	35	0.4	1.7	<30	<0.004	<0.01	<0.3	22	--			
Acrylics (plexiglass)	<10	<140	<0.01	<0.05	<10	<0.002	<0.06	<0.003	<9.5	--			
Polyethylene Tubing	55	7.4	9000	140	254	11	<100	<300	--	<100			
Polyethylene lab. wave	28	10400	0.18	0.07	76	0.008	<0.05	<0.1	6.6	<0.5			
Polyethylene flip top vials	25	10600	0.83	0.31	19	0.36	<0.15	<0.1	15	<0.5			
Polyvinyl chloride	7120	270000	2690	45	2	4.5	<1	<5	630	--			
Nylon (bulk)	I	I	I	1.4x10 <sup>6</sup>	I	I	I	I	I	I			
Section B		Zn	Fe	Sb	Co	Cr	Sc	V	In	Al	Mn	Au	Br
Tygon Tubing	98000	--	--	3	--	--**	--	--	--	--	--	3.1	540000
Polyethylene Tubing	--	--	--	700	--	21	0.6	--	960	1.1	1.5	75000	
Polypropylene Tubing	320000	--	--	--	--	--	0.002	--	500	0.10	52	--	
Teflon	11000	--	--	--	--	--	0.001	--	--	--	--	0.8	--
Plastic Ware	36000	--	900	--	--	32	0.001	--	10	--	--	0.7	115000

Table 6 (continued)

GROUP B	Elements			Co	Cr	Sc	Cs	Ag	Cu	Hf
Section A	Zn	Fe	Sb	<30	I	<8	<100	1240	<6	---
Surgical Rubber Tubing	3x10 <sup>6</sup>	I	<100	<30	I	<8	<100	1240	<6	---
Neoprene Rubber	1.8x10 <sup>7</sup>	I	290	2300	I	3090	I	1000	--	--
Kimwipe	48800	1000	16	24	500	14	<0.1	>0.8	--	--
Section B	Zn	Fe	Sb	Co	Cr	Sc	V	In	Al	Mn
Polyethylene-Polypropylene O-rings	6.0x10 <sup>7</sup>	--	--	141000	4700	--	0.1	0.8	40	0.07
Viton O-rings	560000	--	--	75000	5900	0.24	0.05	--	0.4	0.01
Kalrez O-rings***	34000	10900	600	--	1190	--	--	--	10	0.01
Buna-S O-rings	4.8x10 <sup>7</sup>	--	--	500	10800	381	--	0.5	150	0.07
Glassine Paper	--	--	700	--	18000	288	0.005	--	400	0.03
Lint Free Paper Texwipe Co.	54	144000	500	14000	1200	21	0.004	--	20	0.6
									14	180000

Table 6 (continued)

GROUP C	Zn	Fe	Sb	Co	Cr	Sc	Cs	Ag	Cu	Hf
Borosilicate Glass	730	2.8x10 <sup>5</sup>	2900	81	I	106	<100	<0.001	--	597
Vycor	I	I	1.1x10 <sup>6</sup>	I	I	I	I	I	I	I
Quartz Tubing										
"Spectrosil"	1.5	395	0.05	0.44	6.5	0.03	1.1	0.05	2	<0.005
"Suprasil"	<1	I	<0.01	<0.01	2.5	0.39	<0.01	<0.01	0.04	<0.005
Quartz Products	I	I	1940	0.89	I	I	1390	<0.1	0.09	<0.01
United States Quartz	21	--	43	0.64	230	0.18	0.30	<0.1	0.05	27
General Electric Co.	33	--	38	1.1	602	0.16	<0.1	0.1	0.03	26

-- not measured or detected  
I interfering radionuclides

\* ppb (1 part/10<sup>9</sup> Host)

\*\* Dashes indicate to photopeaks were observed in samples. A few elements such as Sc and Co were calculated relative to known Sc and Co contents in a standard rock BCR-1. Other elements were calculated by using data such as neutron flux, cross sections, the observed photopeaks of the respective radionuclides, decay schemes, relative photopeak counting efficiencies, etc. Relative concentrations of elements other than Sc, Cr, and Co are considered more accurate than absolute abundances.

\*\*\* Analysis of Kalrez O-ring soaked in saturated KOH at 80°C for 6 mo. Kalrez was the only surviving O-ring from among Kalrez, polyethylene-polypropylene and buna-S O-rings. The Kalrez O-ring indicated 1.68x10<sup>8</sup> ppb of K when removed from KOH rinsed with distilled water. After washing with HNO<sub>3</sub>, then KCH and finally with deionized H<sub>2</sub>O, no K could be detected by INAA.

(Section A analyses from Bawyer, D. T. and J. L. Roberts Jr. "Experimental Electrochemistry for Chemists." Academic Press, New York (1974).)

A, B, and C to separate materials used for similar purposes. The analyses listed under Section A were collected by D. T. Bawyer and J. L. Roberts (2). The section B analyses were made in this laboratory on materials used in the research reported here. The group C analyses are from reference 2. Only United States Quartz and General Electric Quartz were analyzed at OSU. No substantial difference was found between our samples and the earlier results.

Group A of Table 6 shows the analysis of trace elements in various polymeric materials. The materials in group A are those that can be used for construction of the rigid elements of a purification system. The section A entries of Group A represent an older analysis of these materials (2), while those in section B are actual analysis of the materials used for the construction of the systems discussed in this report. Since group A materials were chosen from natural unfilled plastics, most of the contamination should be on the surface with a small amount contained in the materials as residue of their manufacturing process or from plasticizers. The surface contamination arises from the use of mold release compounds or extrusion lubricants in the manufacture of the materials. These are usually heavy metal soaps, which are insoluble salts of metals, such as zinc, with fatty acids, such as oleic or steric. Occasionally, other metals are used in these particular soaps to obtain properties that are required for a particular process. They will not wash off with water, but can be removed chemically. The chemical process consists of using a strong mineral acid to hydrolyze the ester bond in the metal-fatty acid salt. Nitric acid is effective, because the salts it forms with the divalent cations are soluble. The remaining residue of fatty acids can be converted to a soluble soap by treatment with a strong alkali, such as sodium or potassium hydroxide.

Group B materials are soft elastomers used for forming seals and the soft materials used to wipe various pieces of equipment or sometimes to handle crystals. They present a major source of contamination; for example, almost all automatic pipetting apparatus have some type of elastomer in contact with the solution. In general, they contain a large amount of zinc either in the form of a mold release compound, or as a lubricant, or as a filler in the material itself (zinc oxide). Zinc is particularly prevalent in solutions containing these elastomers. Zinc contamination can increase due to the use of an automatic solution dispensing device, such as a Repipet. These contain a buna rubber seal in the pump that delivers a measured amount of solution. In our laboratory this O-ring was washed periodically. When freshly cleaned, it did not add zinc to the solution. But, as it was used, zinc appeared in solutions dispensed by it.

In a purification system, direct contact of the solutions with elastomeric materials should be avoided. The seals should be designed such that the elastomers are in a passive part of the solution flow, if possible. In particular, all solutions must be monitored for zinc to avoid serious contamination problems. Among the group A compounds, it appeared that flexible tygon tubing was very free of cation contamination. Tygon tubing, however, proved unsuitable for use in pure systems because an excessive amount of an unknown substance which decreased the pH leached into the solutions.

As portions of our purification system required the use of extremely strong base, it was necessary to obtain O-rings which would withstand the attack of the alkali. Of the five types of O-ring materials tested, only Kalrez withstood long-term attack by potassium hydroxide. After 6 months, contact with saturated potassium hydroxide at 80°C, all the potassium was located on the surface of the Kalrez O-ring. All other

O-rings dissolved. For other O-ring seals in the system, polyethylene-polypropylene O-rings were used. Kalrez is also the only material that can be used in the reactive gas systems. The other materials harden and decompose by HBr addition to their unsaturated bonds.

The last group of materials in Table 6, group C, are those that would contact the crystals during crystal growth at high temperatures. Contamination from quartz during crystal growth presents a problem only when the salt is not completely dried by a reactive atmosphere prior to melting. In the work reported here, General Electric type 704 quartz was used for the reactive atmosphere container and General Electric semiconductor grade quartz crucibles were used to contain the melt. At no time during the growth of crystals was any devitrification or fogging on the surface of the quartz observed.

## V. SYSTEM COMPONENTS

From consideration of their characteristics, the materials selected for the construction of the purification system were methylmethacrylate for valve bodies, columns, column end plates and fittings; polypropylene or polyethylene was used for interconnecting tubes; porous polypropylene for rough filters and filter supports; filters were Millipore Mytex 5 micron filters. The majority of the tubing used was polyethylene sold under the trade name Tygonthane. The check valves in the control lines were Fluorocarbon Co. teflon check valves. These valves required that the teflon spring be slightly weakened from the standard valve. All O-rings except those in continuous contact with potassium hydroxide were polyethylene-polypropylene O-rings. In those portions of the system continuously exposed

to concentrated KOH, O-rings were of Kalrez, the valve plugs were virgin teflon, and the external drive nuts were Dalrin. Dalrin, a condensation polymer, was chosen because, when attacked by potassium bromide solutions, it turns brown and it provides a means of detecting small leaks in the system by discoloration of the drive nuts.

All tubing seals in the system were constructed as shown in Figure 9. The female fittings for the connection consisted of a 1/2 inch deep hole, 3/8 of an inch in diameter, into which 3/8 inch polyethylene tubing could be forced. A groove cut to contain a number 110 O-ring and a threaded section for the drive nut completed the female fitting. The fitting was assembled as shown in Figure 9, using a Dalrin drive nut, a teflon thrust washer, a number 110 polyethylene-polypropylene O-ring. The nut was of such a length that when its shoulder rested against the valve body, the O-ring was properly compressed. With this type seal, the O-ring is out of the main stream flow and essentially in a passive region.

Figures 9, 10D, and 10E illustrate the basic valve used in these systems. The valve block is methylmethacrylate, the plug is teflon, the bar handle of stainless steel, and the retaining ring of nickel-plated brass. A neoprene O-ring between the retaining ring and the plug provides spring tension on the valve plug. The valve body provided the basic module for all measurement, sampling and access for resin exchange that were needed in the closed system. Figure 10 shows the adaptations used to obtain these functions. The basic control measurement for operation of this system was the measurement of pH. Components A and B shown in Figure 10 illustrate the pH electrode modification of the valve plug. Figure 10A is a completely assembled unit showing the plexiglass guard to prevent breakage of the electrode. Below it, B shows the details of assembly of the unit. C in Figure 10 shows the

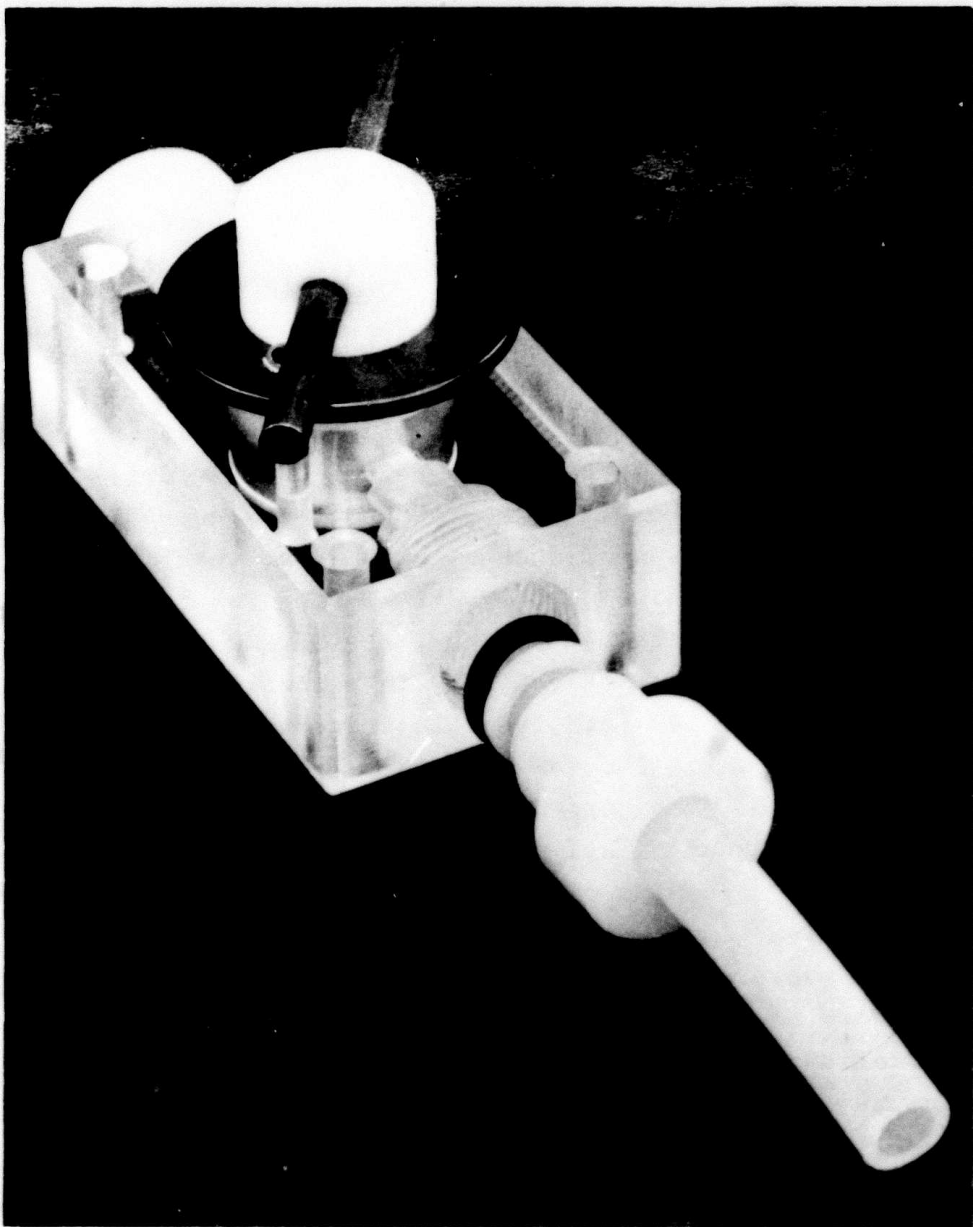


Figure 9. Basic Valve Assembly

method of connecting into the system to add new resin or to remove solution in large quantities from any point at which a valve exists in the system. In these plugs, the hole at a right angle to the plug axis does not pass completely through the plug. The modified plug makes a right angle valve that can accept flow from either side of the valve. F and G in Figure 10 show a sampling plug. With these plugs, a sample can be removed from the closed system without exposing it to the outside ambient. The sample port in the plug opens at 90° to the main flow port of the plug and samples can either be taken upstream or downstream depending on the rotation of the valve. A disposable syringe connects to the sampling plug by a Lura-lock fitting threaded into the sampling section of the valve plug. A final variant of devices made using the basic module is the flow control valve (10E). This consists of the standard plug with a vee-shaped slot across the plug hole to allow adjustable flow with rotation.

Fittings used for interconnections are shown in Figure 11; these three basic fittings provided all connections necessary. Figure 11 shows the construction of the line connections rather clearly and in particular the region that makes the press fit between the polyethylene tubing and the fitting seat can be easily seen.

The ion exchange columns consist of a tube of methylmethacrylate, 2 inches ID, 2-1/4 inches OD, 24 inches long. The top was closed by a plate shown in Figure 12. The disc below the plate is a deflector to prevent direct streaming from the solution onto the resin bed below. The plate bolts to the backboard to support the ion exchange column. The bottom (Figure 13) was closed by a similar plate, except this plate carries a filter disc of porous polypropylene shown above the plate. The porous polypropylene filter was held tightly against the bottom plate by the perforated disc which was

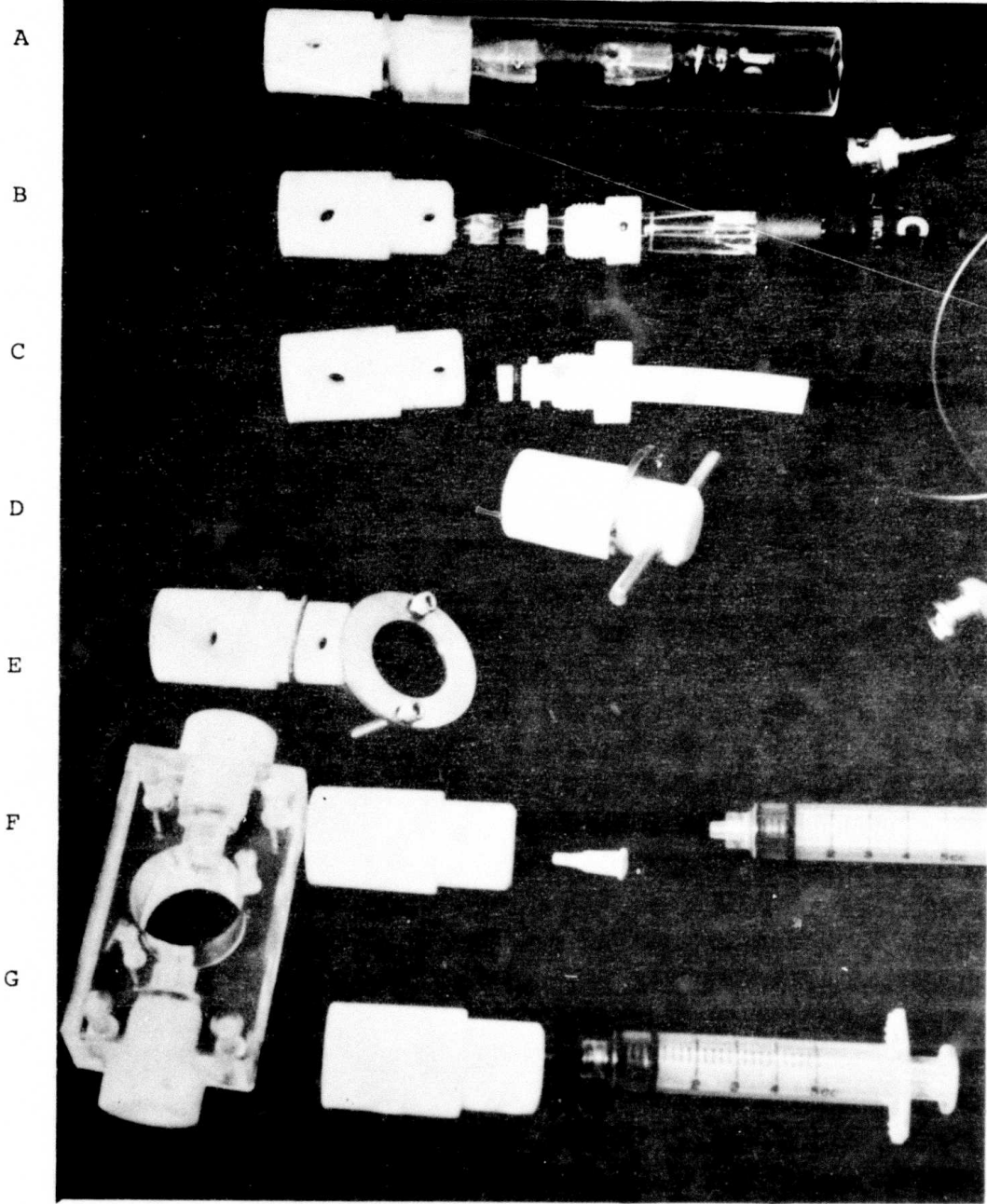


Figure 10. Devices Based on Standard Valve

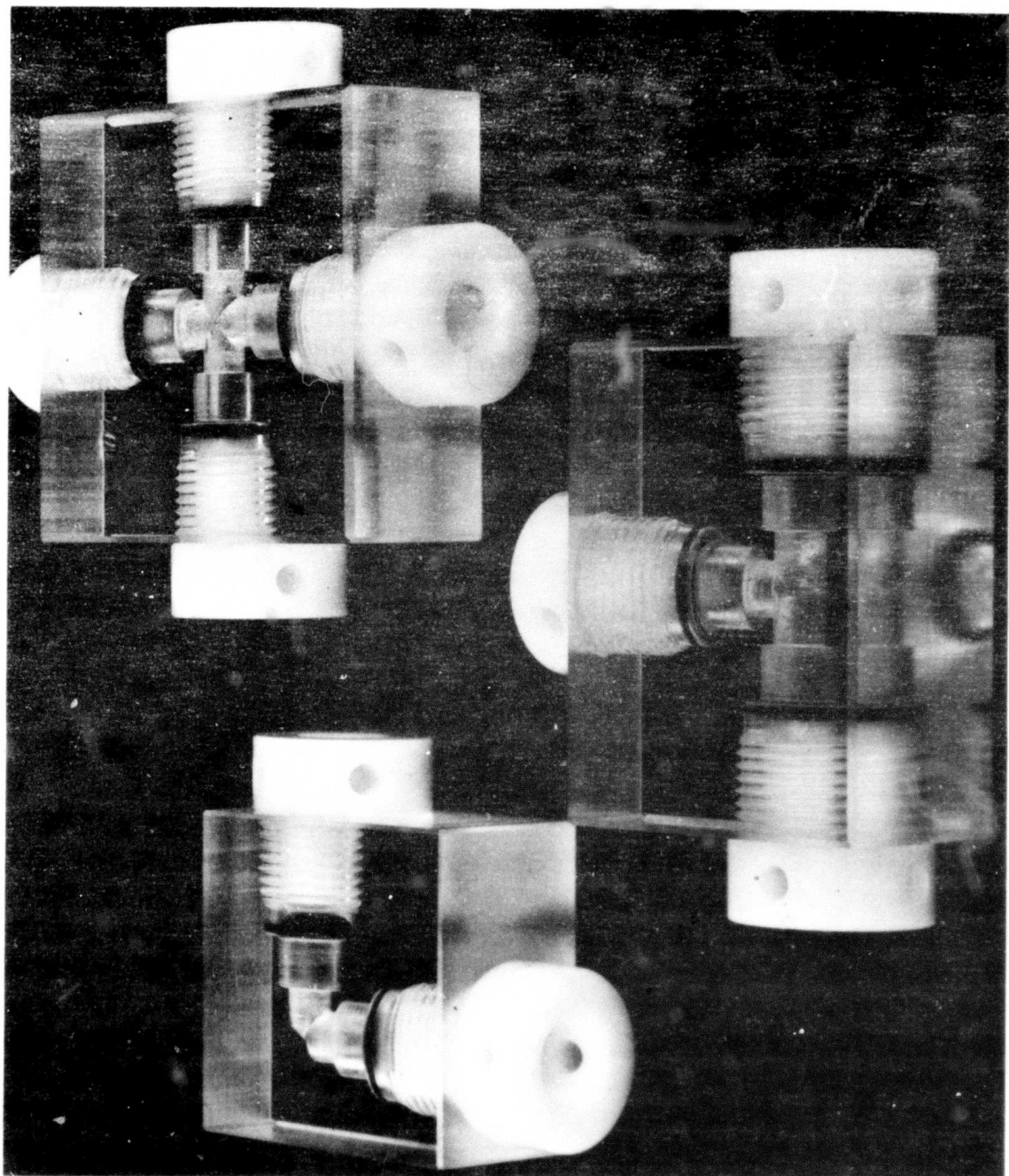


Figure 11. Fittings for Ion Exchange System

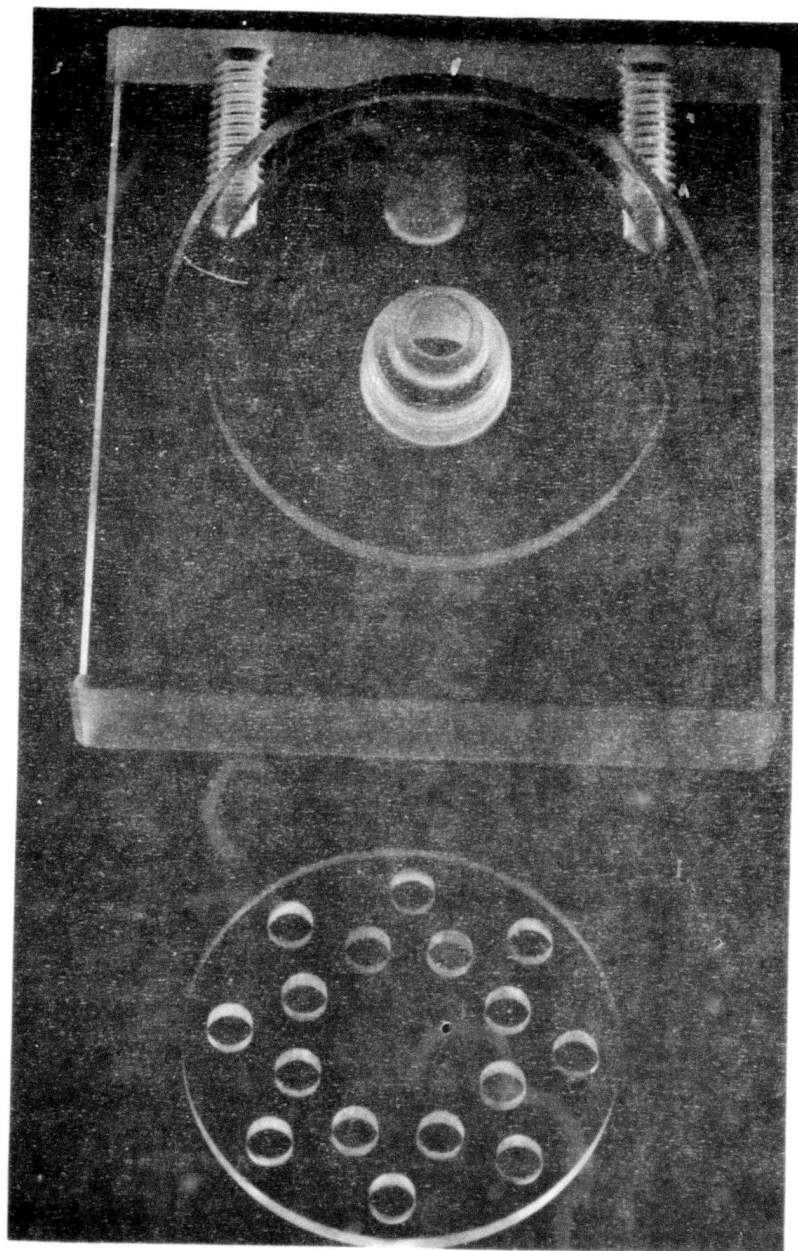


Figure 12. Top Plate for Column

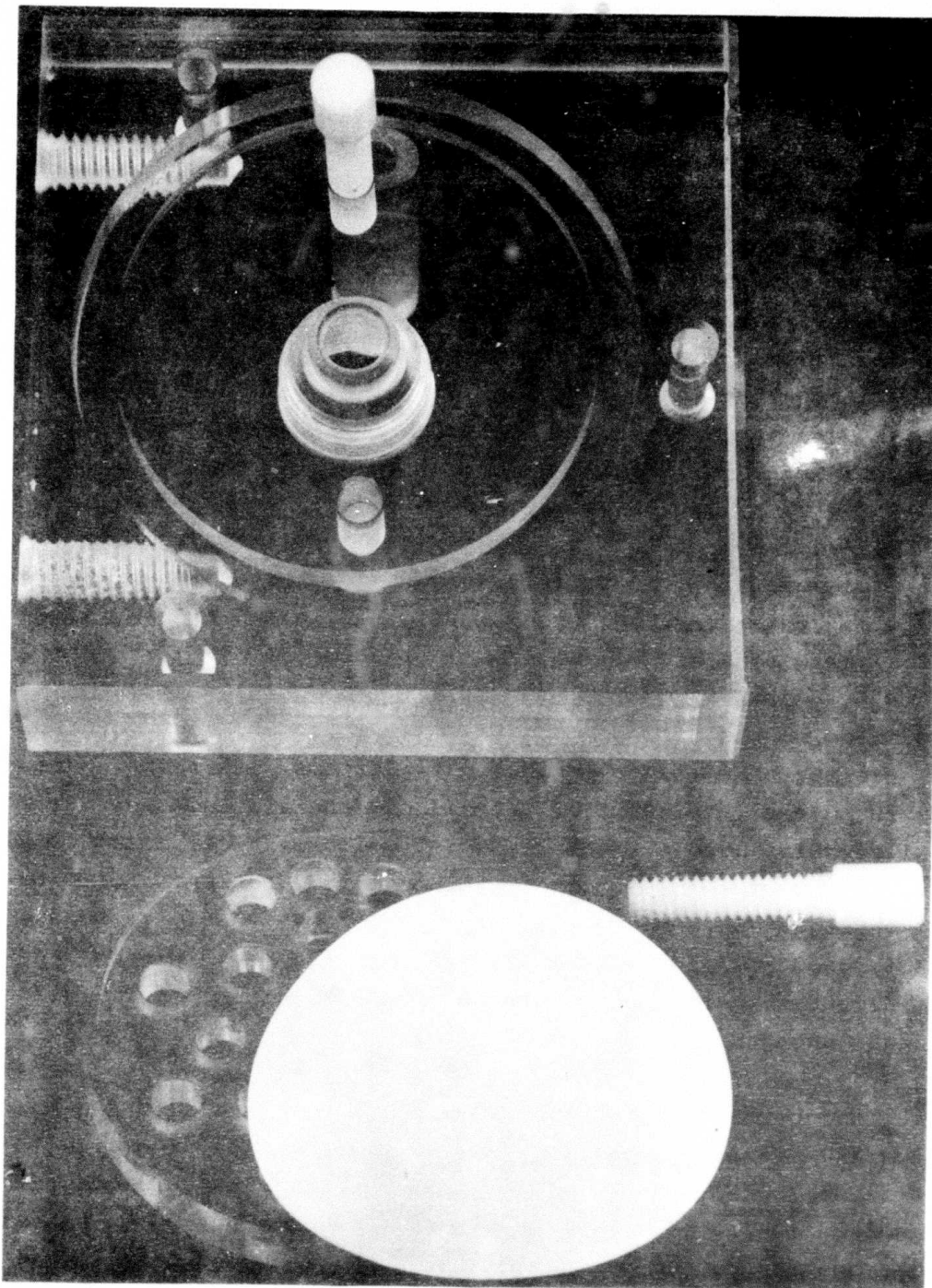


Figure 13. Bottom Plate for Column

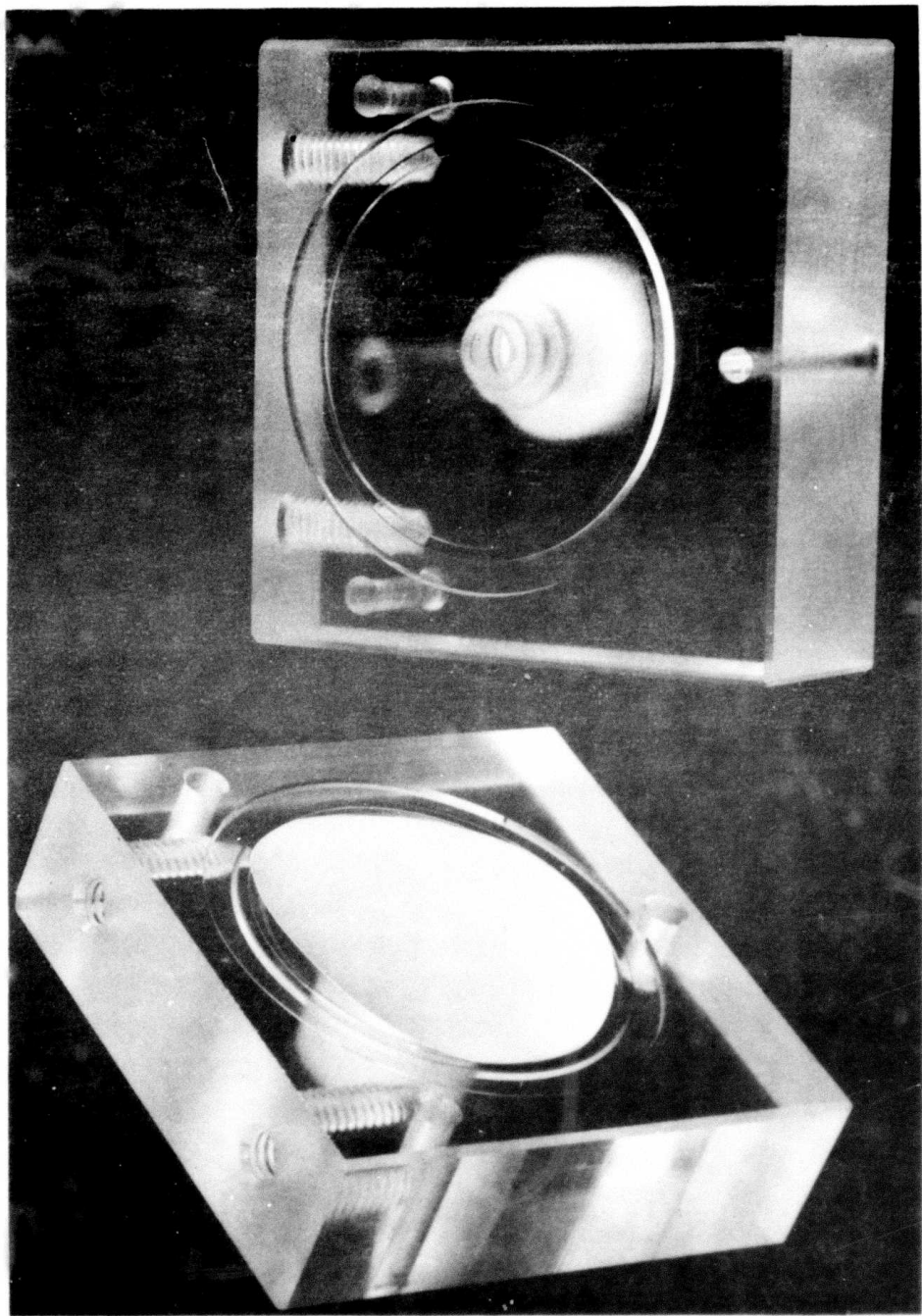


Figure 14. Millipore Filter Case

fastened to the bottom plate by the teflon screws in blind holes on it. The two plates are drawn tightly against the tube by three long stainless steel rods and sealed by polyethylene-polypropylene O-rings. The top O-ring was in the gas space above the solution. The bottom O-ring was in a dead flow region created by the plate and compression disc. The volume of the column is 1.23 liters.

The filters marked F in Figure 8 are shown in Figure 14, the plates making the body of the filter resemble those used for the column ends, except beside the O-ring groove is a rectangular cutting edge that seals the filter tightly to each of the blocks and the center of the blocks are machined on a taper from the circumference to the input/output ports to allow free flow of the solution between them. A typical Mytex filter is shown against one block, each side of this filter was supported by a fine teflon screen to provide mechanical strength for the filter.

Figure 15 shows the method used to introduce the pH and concentration adjusting solutions into the purification process. The plates visible in the column cause mixing of the solutions. The filter holder below the mixing column can be opened to change filters without removing it from the system.

The solution from the purification system was collected in a vacuum chamber containing a polypropylene wide mouth jar; this is shown in Figure 16. The valve at the top right is the input to the polypropylene jar within the container; a polypropylene tube leads into the jar to prevent splashing against the vacuum chamber walls which are polycarbonate. Polycarbonate provides the strength necessary in a transparent plastic vacuum chamber, but is not immune to attack from the solutions used in this work. The tee with the two commercial valves provides a means of allowing filtered gases to enter

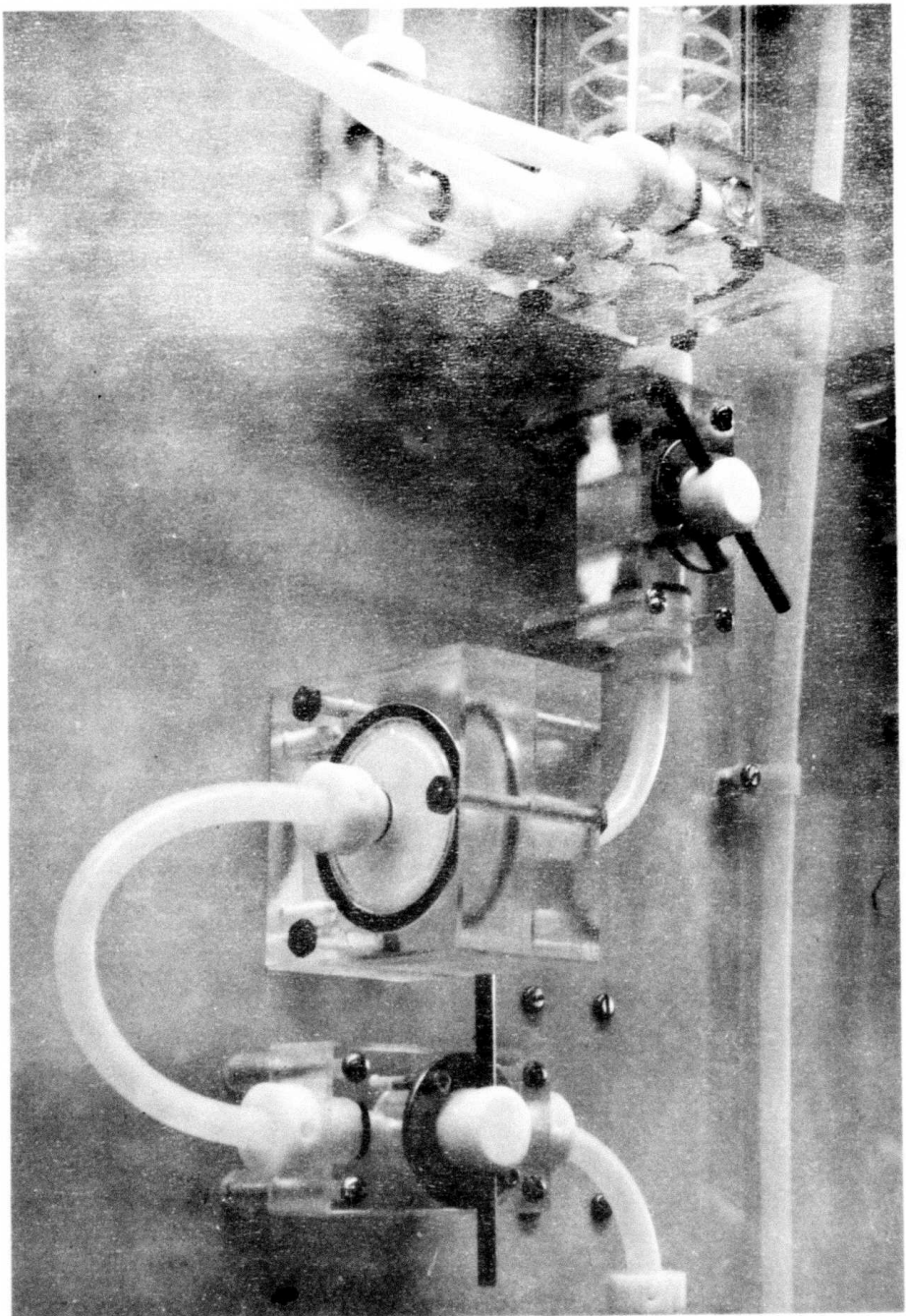


Figure 15. Mixing Column and Filter

the evacuated chamber through the valve on the right. The valve on the left was used to connect the vacuum line to the vacuum chamber. These particular valves are commercial ball valves made of polyvinyl chloride. If the solutions come in contact with them, their life time is approximately two weeks. While satisfactory for gas lines for inert gases, they are completely unsatisfactory when exposed to reactive environments. The valve pointing out of the picture is a check valve of polypropylene that plugs the original port for this vacuum bell. The holes through the top of this chamber substantially weaken the plate, and it is strengthened by 1/2 inch thick methylmethacrylate that fits inside the vacuum chamber and retains the flat neoprene ring used to seal the chamber to the top plate. The valves and tee are fastened through this plate with O-ring seals in the bottom of the valve and the bottom of the tee; otherwise, the components are as previously described.

Two vacuum collectors were made. The system was run until the polypropylene jar was filled, then flow through the system stopped, the valve at the top of the vacuum chamber and the vacuum pumping valve closed, then the chamber disconnected from the system. The entire chamber was transferred to a nitrogen tent and nitrogen admitted through the filtered valve and the jar removed, covered, and a new jar inserted into the vacuum chamber. Next, the vacuum chamber was closed and removed from the nitrogen tent. The jar containing the solution was put into a vacuum oven for complete drying. In the meantime, the second vacuum collector was connected to the ion exchange system to collect the next batch of KBr from the system. In this way, the ion exchange system can operate for long periods producing quantities of purified KBr without long term interruptions.

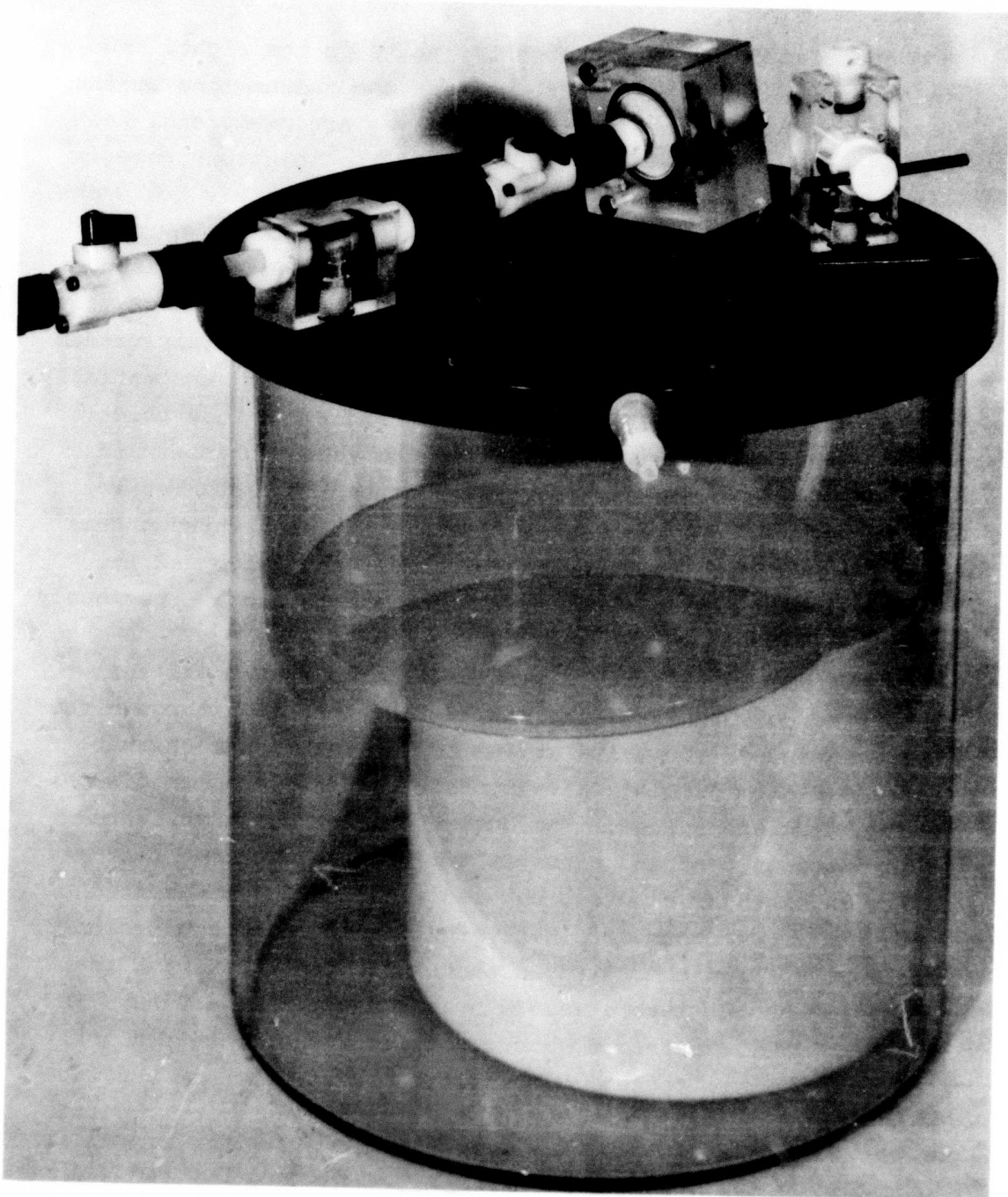


Figure 16. Solution Collector

Figure 17 shows the ion exchange system installed in the laboratory connected to reservoirs on the shelf above it and to the vacuum collector on the floor. The locations of the pH electrodes, the interface amplifiers, and the sampling syringes can be seen. The container on the lower left is the waste reservoir. Behind it is a non-corrodible pump to remove the waste through our normal draining system. In this assembly picture, the direction of flow through column 6 has been reversed from that shown in Figure 8. The additional connections to do this run between the fifth and sixth columns. A constant pressure device in the drain line for the pH electrodes was installed to improve the accuracy of the measurement. Figure 17 shows an early configuration of the resins in which the first column contains AG50W-X8, the third column contains Chelex 100, and the fifth and sixth columns contain AG 1-X2 and AG 2-X8.

The control of the operating conditions of the ion exchange purification system was accomplished by measurement of pH. The sensing element was a Broadly-James 9006 combination glass electrode. The reference junction was silver-silver chloride, the signal from the 1000 megohm pH electrode was conditioned by a buffer FET operational amplifier (40 J Analog Devices). The buffer amplifiers provided an impedance match between the pH electrode and the 4000 ohm input impedance of the Fluke 2240A data logger. They also provided the offset adjustment to set the zero voltage output at a pH of 7 and to set the range over which pH could be measured, and to calibrate the voltage output of the op-amp to correspond with the voltage calculated from a Nernst type equation for this electrode. The circuit for the buffer FET amplifier is shown in Figure 18. Four such amplifiers were built as a unit, and each system requires two buffer amplifier units. The Fluke 2240A contained a scanner card and an A to D converter with sufficient

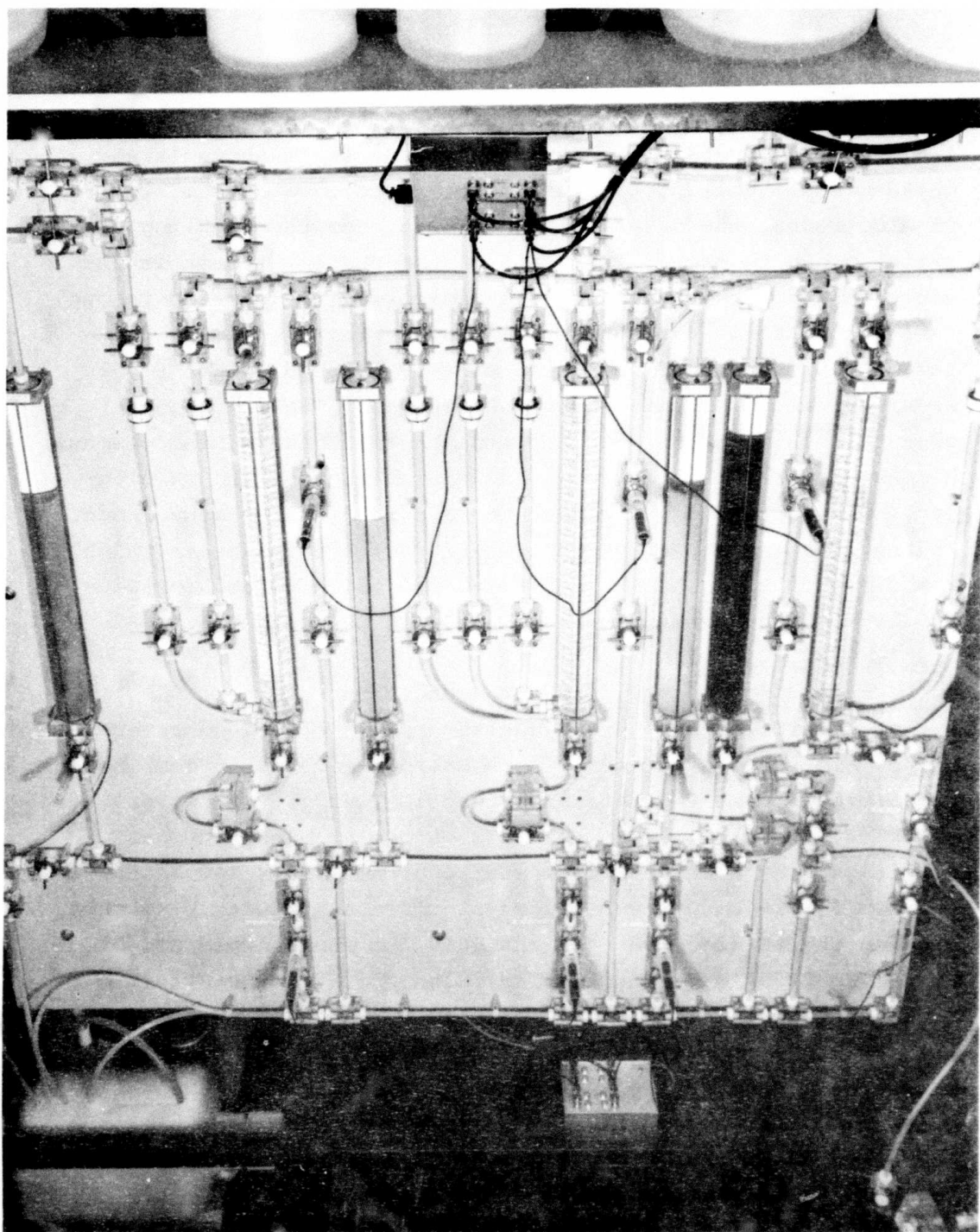


Figure 17. Ion Exchange System Installed in Laboratory

resolution for measurement of pH in this system. It scanned all seven electrodes in a time interval compatible with the response time of the system. The data logger also contained circuitry for operating alarm LEDs. These were mounted behind each pH electrode and could be set for both high and low limits. This alarm circuit was essential in operation of the system. As this potassium bromide purification system contains 58 valves, it is essential that the operator's attention be directed toward those valves that need attention. If a green LED lit, the operator would increase the flow through the adjusting valve for that region of the system; if a red LED lit, the operator would decrease the flow through that valve. While this scheme was certainly not as efficient as automatic valves would be, it was considerably less expensive than all teflon electromagnetic valves, and provided a satisfactory means of control of the system.

The nitrogen used for pressurizing the system was fed from a common source of prepurified nitrogen which passed through a hydrophobic 0.22 micrometer filter and a flowmeter to monitor nitrogen losses from the system. Each reservoir contains a valve that allows control of the pressurization of the individual reservoirs. Each reservoir contains an O-ring and retaining ring to seal the top of the reservoir. This does not form a perfect seal, and there is a slight leakage of nitrogen through that top closure.

As described under components, sampling valves that allow us to sample the solution at various points in the system were designed on the basic valve module. These are located at the points shown in Figure 8 and allow us to take samples of the effluent of each column in a system. The samples can be taken without the introduction of any impurities into the system. The valves are most useful in determining the operation of the system. Connection to the syringe is made through a

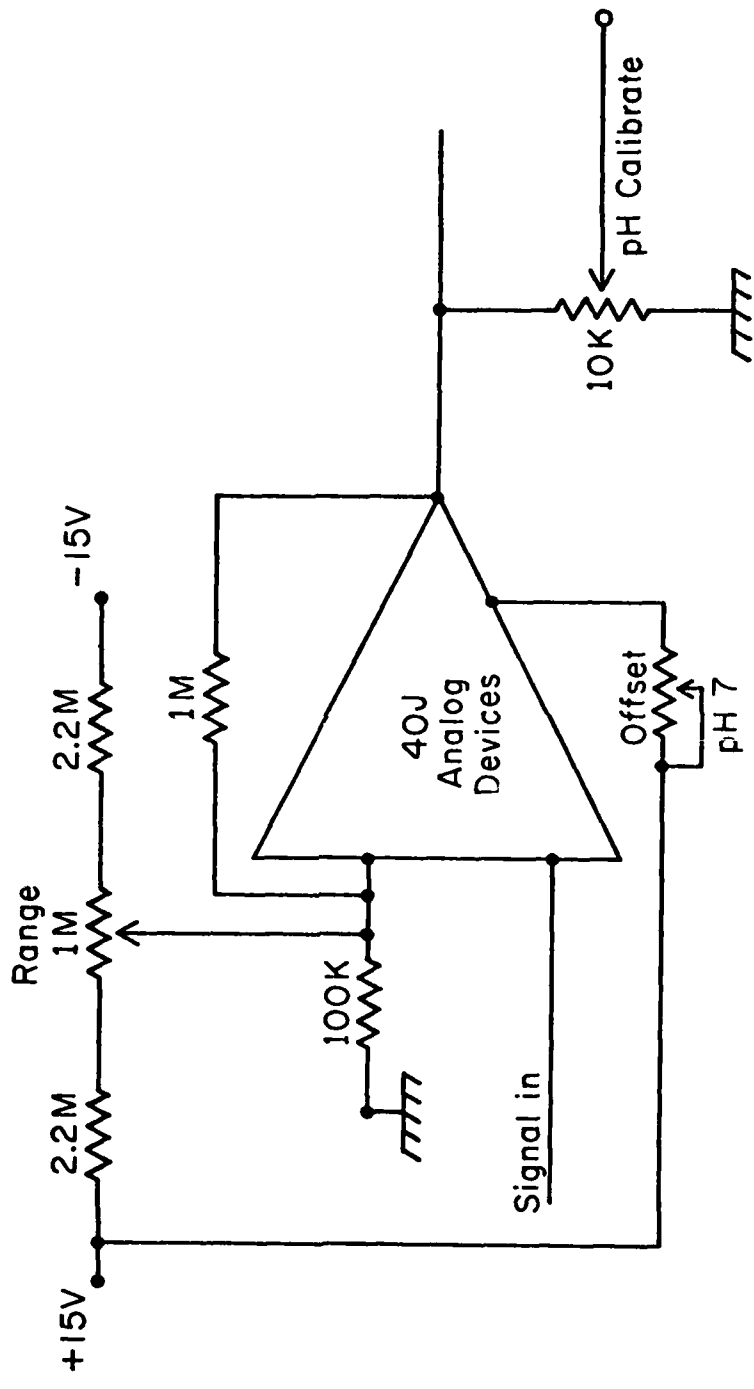


Figure 18. Impedance Matching and Calibration Amplifier

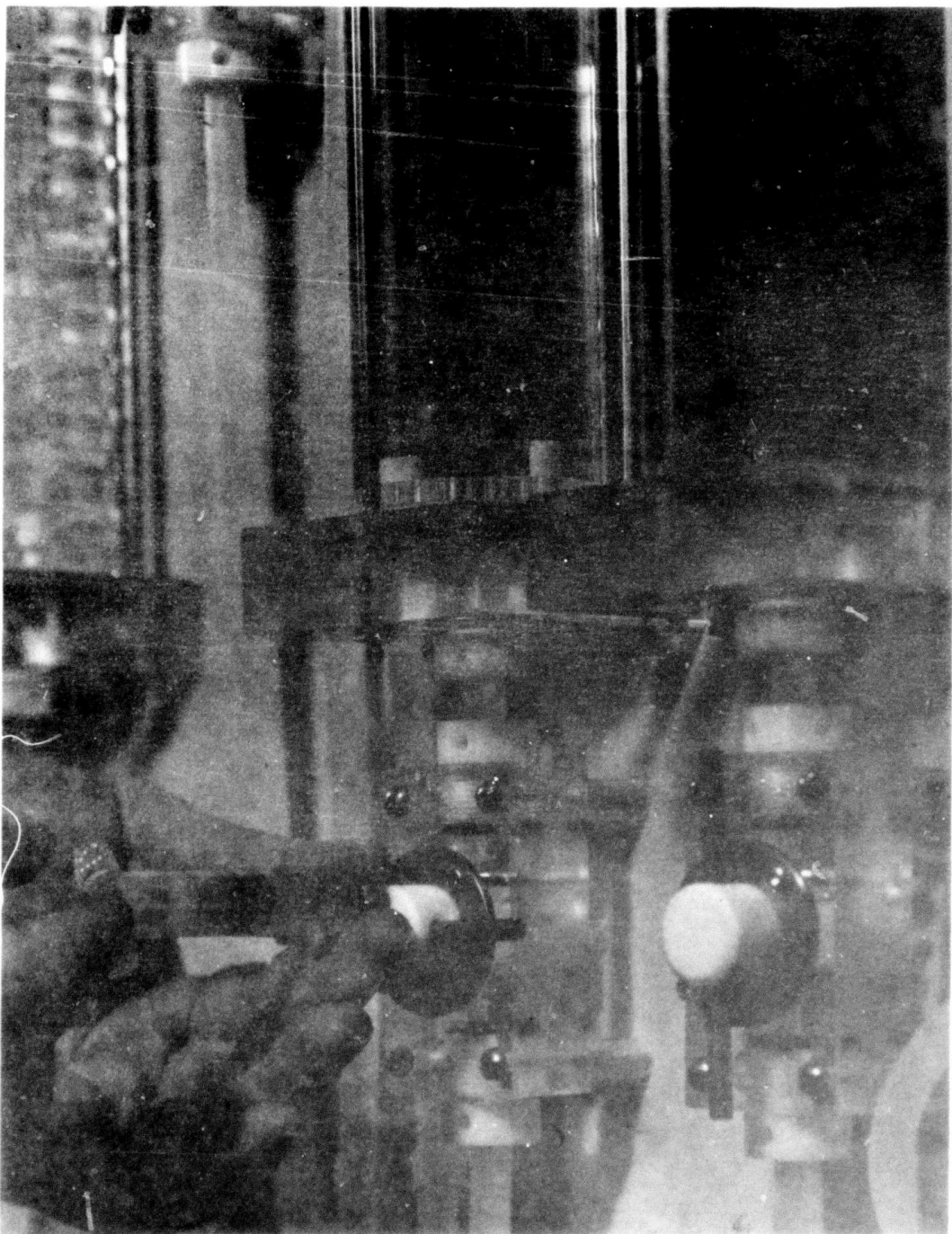


Figure 19. Sampling Technique

Lura-lock fitting which threads into the sampling port with a 5-40 thread and must be carefully supported as shown in Figure 19 while a sample is being drawn. When the system is operating, a syringe must be kept in every Lura-lock fitting to avoid the operator inadvertently turning the valve to a horizontal position and producing a fine stream of highly corrosive fluid. In drawing the sample, one must start the extraction of the syringe plunger, but then the pressure from within the system will push the plunger from its cylinder, so care must be taken to stop the plunger at the appropriate volume level and to close the valve before removing the syringe. Samples were taken directly to a Perkin-Elmer 403 atomic absorption spectrograph and analyzed for any element that was in question.

## VI. RAW MATERIALS AND CHEMICALS

Potassium bromide is basic raw material for this process. As supplied, the quality of the raw material is quite variable among the various manufacturers and will vary somewhat from the same manufacturer with various lots. Table 7 gives the analysis of a reagent grade lot of potassium bromide. The impurity levels are so high in this particular lot that it was only possible to purify a very small quantity before the capacity of the ion exchange system was exhausted. Table 8 shows a more typical analysis of potassium bromide and represents the levels of impurities usually encountered in our raw materials. It contains two samples from one lot, but from different 25-pound containers, and one sample from an entirely different J. T. Baker Chemical Company Analyzed Reagent Postassium Bromide. In both cases, the impurities present in major

Table 7. Levels of Impurities in Mallinckrodt KBr, Lot #WD6K  
 (Expressed as ppm by weight)

Four solutions were made, on days 3-22-77, 2-28-77,  
 4-1-77, and 4-4-77. The values obtained from each  
 solution are shown in chronological order.

<u>Element</u>	<u>ppm</u>	<u>Detection Limit<sup>3</sup></u>	<u>Element</u>	<u>ppm</u>	<u>Detection Limit</u>
Cs	1200 ± 160	242	Cu	5.2 ± .87	1.2
	1350 ± 250			5.1 ± .95	
	1280 ± 154			5.0 ± .83	
	1210 ± 121			6.5 ± .83	
Na	63.8 ± 12	10.9	Fe	91.1 ± 26	22
	68.8 ± 9.3			83.3 ± 10	
	57.9 ± 3.3			75.9 ± 10	
	64.3 ± 6.3			70.1 ± 17	
Li	224 ± 24	23	Mn	2.00 ± .22	.49
	206 ± 4.7			1.53 ± .21	
	186 ± 24			1.92 ± .21	
	181 ± 13			1.88 ± .75	
Rb	247 ± 35	55	Zn	2.30 ± .30	1.7
	246 ± 51			2.42 ± .25	
	238 ± 25			2.21 ± .29	
	350 ± 46			1.71 ± .75	
Ca	24.3 ± 21	16.9	Co	12.1 ± 2.7	1.7
	5.5 ± 1.7			13.1 ± 1.7	
	15.0 ± 14			10.8 ± 0	
	21.7 ± 11			10.8 ± 0	
Mg	1.04 ± 1.34	2.5	Ni	151 ± 50	52.1
	.29 ± 4.7			185 ± 49	
	.58 ± .62			166 ± 25	
	3.30 ± .29			94.4 ± 23	
Cr	0 <sup>2</sup> ± 0.0	1.3			
	0 ± 1.3				
	0 ± 1.2				
	0 ± 1.2				

<sup>1</sup>Four samples run on the AA gave the same peak height.

<sup>2</sup>The peak height was very small, and came where the standard curve intercepted zero.

<sup>3</sup>Detection limit calculated as D.L. =  $\sqrt{2} \sigma$  (samples)  $\frac{dA}{dc}$ .

Table 8  
Levels of Impurities in J. T. Baker Chemical Co.  
Analytical Reagent KBr  
 (Expressed as ppm by weight)

<u>Element</u>		<u>Element</u>	
Cs	42.7 ± 25.6 <sup>1</sup> 0.0 ± 25.6 <sup>2</sup> 0.0 ± 25.6 <sup>3</sup>	Fe	97.4 ± 15.7 131.7 ± 0 70.0 ± 15.7
Na	53.0 ± 8.7 53.0 ± 8.7 175.7 ± 30.0	Mn	32.7 ± 3.5 22.6 ± 4.4 22.6 ± 5.2
Li	153.0 ± 43.0 198.7 ± 12.6 162.2 ± 15.2	Zn	57.4 ± .9 50.9 ± 3.5 63.5 ± 8.7
Rb	187.8 ± 8.7 198.7 ± 12.6 176.5 ± 17.8	Co	90.4 ± 23.5 90.4 ± 23.5 63.5 ± 8.7
Ca	15.2 ± .9 19.1 ± 4.3 17.0 ± 5.7	Ni	188.3 ± 52.6 198.3 ± 4.8 174.8 ± 10.1
Mg	5.2 ± .4 7.0 ± 2.2 6.1 ± 1.3	Cr	4.3 ± 0 7.4 ± 2.6 8.7 ± 4.3
Cu	35.2 ± 12.2 35.2 ± 12.2 20.4 ± 0		

<sup>1</sup>Lot No. 72239, container 1

<sup>2</sup>Lot No. 72239, container 2

<sup>3</sup>Lot No. 52298

quantities are other alkali ions and these are the most difficult to separate by ion exchange.

J. T. Baker Analyzed Reagent grade 47-48% hydrobromic acid was first used for our source of hydrobromic acid. This is a quite pure chemical containing only sodium as an impurity. Since hydrobromic acid will enter the purification system after the Chelex 100 column, which is the sodium removing column, sodium free hydrobromic acid was prepared by dissolving hydrogen bromide in deionized water. The hydrogen bromide source was from our reactive gas manifold and the system produces hydrobromic acid without exposing the hydrogen bromide or the deionized water to external environments. A complete teflon system was used to transport the hydrogen bromide from the reactive gas manifold for solution in a large polypropylene container of deionized water. Analysis of the hydrobromic acid produced in this system showed no detectable impurity elements by atomic absorption spectroscopy.

The preparation of pure potassium hydroxide for use in regeneration and pH control constituted a major problem. Smaller quantities, of course, can be prepared by reacting pure potassium with deionized water, but that is not practical for the large quantities required for regeneration of the columns. Reagent grade potassium hydroxide contains a very high concentration of sodium, cesium, and rubidium. The solid material contains relatively large amounts of divalent ion impurities; many of these are insoluble and can be removed by simple filtering with a fine Millipore filter, but trace divalent impurities remain. The KOH used for regeneration of the columns was passed through a Chelex resin bed in the potassium form and through AG2 in the hydroxide form. In that form, it is an effective anion exchange resin for hydroxide. The effluent from this system was quite free from detectable

anions, such as carbonates, sulfates, and nitrates. However, the Chelex 100 was not sufficient to completely remove the sodium. So the material was not especially satisfactory for use in adjusting pH during a purification run.

The water used in all the work reported here was deionized using a Millipore Milli-Q II system. When functioning correctly, this system produced water in which no cations could be detected by atomic absorption. One batch of replacement ion exchange resins was contaminated, and would not produce water free of cations; a large number of the twin T-90, 0.22 micrometer filters clogged quickly and developed leaky cases. This did not occur with more recent replacement filters of this type. The major source of contamination of the water resulted from our use of Repipet devices for diluting solutions. These have a tendency to introduce zinc into the water from the elastomer seals used in the pump. After the seal was replaced by a Kalrez seal, the contamination vanished. Alternately, the seal was cleaned with nitric acid, followed by potassium hydroxide, followed by washing in deionized water. The contamination would disappear for several months, but eventually would reappear.

## VII. CONVERSION AND REGENERATION OF RESINS

One ionic form of a resin can be converted to any other ionic form only to the extent allowed by the ratio of their selectivity coefficients if both ions remain available to the resin. However, if a conversion reaction is chosen such that its products include a molecular species that effectively removes one of the ions, the conversion will approach completion. As an example, consider the conversion of AG-2 from

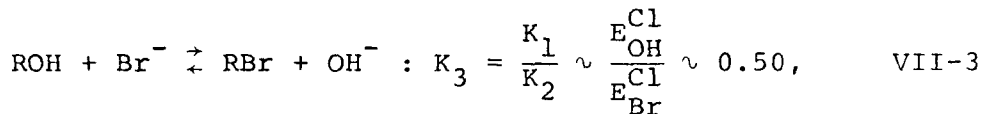
hydroxide form to the bromide form. The competing reactions are:



and



where R is the resin and K an ionization constant. The net reaction for conversion is then:



where the selectivity coefficients E are referred to  $Cl^-$  as the reference ion. If 1 mole of KBr was added to an amount of AG-2 containing 1 mole of exchangeable sites all in the hydroxide form, only 0.414 moles of the sites would be converted to RBr. The pH of the solution in equilibrium with the resin would be 13.6. If the resin was washed and another mole of KBr added, the fraction converted to bromide form would now be 0.637. It would require 23 equilibrium conversions to reduce the amount of  $OH^-$  in the resin to around 1 ppm. The pH of the solution at that point would be 8.14. After 25 treatments, the mole of resin would contain  $4.38 \times 10^{-7}$  moles of  $OH^-$ .

If the conversion is made with excess  $H^+$  present, the three partial reactions are:



where  $K_w$  is the ion product of  $H_2O$ ; the net conversion

reaction is then:



The conversion is essentially complete. In the case of purification of alkali halides, the best conversion reactions are obvious. However, when purification systems for alkaline earths are discussed later, other type reactions will be more useful, but they will be based on the same principles.

After the conversion by reaction 7, the resin contains  $Br^-$  far in excess of the  $OH^-/Br^-$  equilibrium ratio for the resin in pure  $H_2O$  and will exchange  $Br^-$  for  $OH^-$  with  $H_2O$  if an attempt is made to wash it with pure  $H_2O$ . The pH of the effluent is about 0.2 initially (after washing 4 volumes of  $H_2O$  equal to the column volume), then increases slowly until about 0.586 of the resin sites are occupied by  $OH^-$ . At that point, the resin no longer exchanges easily with  $OH^-$  in strong  $Br^-$  solution. Of course, the values of pH measured with a glass electrode in strongly acid or basic solutions are not accurate, but they do provide the useful indications for control and operation of the system.

The conversion reactions and comments on the processes used for each resin in the purification system are given below.

1) Chelex 100



where M is a cation of charge x.

Reference to Table 3 shows the hydrogen form of Chelex to be the most stable monovalent form of the resin. It is also more stable than many of the divalent forms of the resin.

The exchange of  $H^+$  for  $M^+$  is not driven to completion by removal of one of the products by association. HBr was reacted with the resin until the effluent solution had the same pH as the acid added and the volume of resin had reached its minimum value. Then KOH was added until the pH of the effluent was equal to that of the solution added and the volume of the resin reached a maximum. The volume increased by a factor of 2.27 in converting from RH to RK. Initially the resin was converted from the form in which it was supplied (sodium) to RH then to RK in a 2l polypropylene aspirator bottle with 3/8 inch polyethylene tube to connect them to the top of the ion exchange column. The Chelex 100 was converted to RK in this bottle. The reactions were carried out at 80°C to force the equilibrium of VII-8 further to the right than occurs at 21°C, the temperature of the resin in the ion exchange system. Three cycles of reactions VII-8 and VII-9 at 80°C were sufficient to reduce Na in the resin below atomic absorption detection limits. The resin was then transferred to the column and all subsequent regenerations were done with the resin in place.

When regenerating in place, the HBr was added by downflow as the Chelex 100 shrinks. The conversion was considered complete when the pH of the effluent solution was equal to that of the HBr entering the column. The KOH was reacted by upflow because of the expansion of Chelex 100 on conversion from the  $H^+$  form to the  $K^+$  form. The conversion to the potassium form was considered complete when the pH of the effluent was equal to that of the added potassium hydroxide.

2) AG50W-X8

The conversion of AG50W-X8 from the sodium form in which it arrived to the potassium form in which it was used was the

same as that used for the Chelex 100. The initial conversion was carried out in a separate polypropylene aspirator bottle at 80°C, as was done for the Chelex. After the resin was installed in the column, the conversions were done by the same reactions used for the Chelex 100. However, in the case of this X8 resin, the volume changes on going from one form of the resin to another were relatively minor. The acid form is 1.07 times larger in volume than the potassium form. Thus, it makes no difference in the flow direction of interconversion between acid and potassium form.

3) AG1-X2

The conversion reactions for this resin are the same as reaction VII-7 given earlier. The initial conversion from the hydroxide form, in which the resin was supplied, to the bromide form was done at 80°C in polypropylene aspirator bottles. The regeneration of the resin was done in the system. On regeneration, the resin was converted completely to the hydroxide form, then regenerated in the bromide form. The bromide form is 1.12 times larger than the hydroxide form. For this reason, the conversion of hydroxide to bromide was always carried out by upflow of the HBr. Other of the anion resins characteristically entrap small amounts of the nitrogen, with which the system was filled, and the backwashing tends to remove the entrapped nitrogen from the resin.

4) AG2-X8

This resin was supplied as a hydroxide. It is converted to the bromide by reaction VII-7. The process is carried out as it was with AG1-X2. The volume change with the X8 resin is insignificant; however, because of its tendency to entrap nitrogen bubbles, the hydrogen bromide was put into the column

in an upflow direction to remove any of the bubbles that could cause channeling of the resin bed by the solution.

An indication of the condition of many resins can be obtained by noting color changes of the resin. The Chelex 100 is white when in the potassium form and slightly off-white in the hydrogen form. The color change is subtle and difficult to see. When the resin ages it may yellow and, in that condition, it is replaced with new resin. The color change indicates the polymer is beginning to deteriorate. The AG50W-X8 is an amber resin and a little lighter in color in the potassium form than when in the hydrogen form. It is not possible to detect the onset of deterioration of the polymer base for the resin by a color change. Samples of the elutent must be analyzed for content of organics to detect this. The AG1-X2 is a cream colored resin in both the hydroxide and the bromide form. It yellows with age, and this can be used as an indication of the time to change the resin. AG2-X8 is a dark brown resin when in the hydroxide form and an amber resin in the bromide form. All resins used in this work were of 50-100 Mesh. The exchange capacities of the resin are given in the table below:

Table 9. Capacities of Resins in Milliequivalents

	meq/dry gm*	meq/ml**
Chelex 100	2.9	0.7
AG50W-X8	5.1	1.7
AG1-X2	3.2	1.4
AG2-X8	3.5	0.8

\*In potassium or bromide form of 5-100 Mesh (dry) resin.

\*\*Fully hydrated resin.

Currently, the purification system contains 730 meq of Chelex 100, 1188 meq of AG50W-X8, 659 meq of AG1-X2, and 1396 meq of AG2-X8. These may appear to be rather small capacities, but the smallest capacity column (AG1-X2 at 659 meq of monovalent ion) will treat about 3580 l of 2M KBr containing 1000 ppm/l of  $\text{SO}_4^{2-}$  before exhausting its capacity. In practice, 75 l of 1.5 to 2M KBr are purified between each regeneration. The resins are never operated near their capacity limits because, in this process, it is essential to maintain the chemical potential at a high level in the resin.

#### VIII. OPERATION OF PURIFICATION SYSTEM

The separation coefficients show that KBr can be purified using the resins selected. However, they do not indicate the best resin order for stable operation of the system.

The selective ion filter can be operated with either resin first. With AG50W-X8 as the initial resin, the raw KBr can be stored in the reservoir at an acid pH. This had the advantage that it prevented absorption of atmospheric  $\text{CO}_2$  and the formation of bicarbonates and carbonates in the potassium bromide. It had the disadvantage that the effluent from the AG50W-X8 had to be made basic before it could enter the Chelex 100 column. The effluent from the Chelex 100 would have to be made acid before it could enter the columns containing anion exchange resins. The alternate order was to put the solution through Chelex 100 first, then through AG50W-X8. That scheme had the disadvantage that the KBr in the initial reservoir must be basic and thus can absorb carbon dioxide from the atmosphere. But, it had the advantage that only HBr needed to be added to the system in the column between the Chelex 100

and AG50W-X8. Both orders were tried. Initially the AG50W-X8-Chelex 100 scheme was used. This proved unstable and difficult to control because of the time required for solution to flow between successive electrodes of the mixing column. The large volume of the mixing column induces a long delay time which makes adjustment of the proper amount of additive chemical difficult. Once the set point was overshot, it required considerable time for the system to clean itself and a new adjustment made. In a revised system, these mixing chambers should be made much smaller. In the original design they were made their present size so they could double as an added resin column, if it proved necessary. In addition to difficulty of control with that order of operation, it was necessary to add potassium hydroxide in the first pH adjusting column. Potassium hydroxide cannot be prepared with a purity equivalent to that of the hydrogen bromide manufactured in the laboratory with high purity and with relative ease. The principal impurities in potassium hydroxide were sodium and iron. These were removed on the Chelex, but exhausted the resin quickly. If the correction of the pH of the effluent from the AG50W-X8 was not sufficient, the solution remains acid and, when it enters the Chelex 100 column, the hydrogen ion replaces the potassium ion and quickly exhausts the effectiveness of the resin. The disadvantages of this scheme far outweighed the advantage of not forming carbonates in the initial raw KBr reservoir. This scheme was abandoned.

The best resin order for purification of KBr was Chelex 100 in the first column, and AG50W-X8 in the third column. The order of the anion exchange resins was not critical. There was a slight advantage in using AG1-X2, the less polymerized resin, before AG2-X8. The X2 resin was more effective in removing complex ions than the X8 resin. With AG1-X2 in the fifth column and AG2-X8 in the sixth column, the pH of the

KBr solution decreases as it progresses through the system. Only HBr need to be added in the second column with this resin order.

The sole disadvantage of that scheme was that the basic potassium bromide feed solution must be freshly prepared to avoid CO<sub>2</sub> absorption on solution storage. The formation of carbonates in the basic solution was minimized by deaerating the solution with nitrogen and storing the basic solution under a nitrogen atmosphere. The initial 5 gal of solution stored in the reservoir above the ion exchange system is under nitrogen at 5 psi.

Initial start-up of the system or initial operation of the system after regeneration required the wastage of a sizeable amount of solution, as each column must be filled with the KBr solution and its effluent discarded until stable operation at the proper pH was achieved. During this initial stage, the pH of the effluents of various columns changed rapidly and on occasion oscillated. The initial pH readings have relatively little meaning because the rapidly flowing solution across the electrode induced charges on the glass electrode which distorted the reading. Shortly after all the original solution in the column was displaced, the electrode fluctuations decreased and the flow through the electrode reduced so that accurate pH readings could be made. When the column had suitably stabilized, the solution was passed to the next column and the same procedure followed until it in turn stabilized. The initial adjustment of the columns system required about four hours and used about three gallons of potassium bromide solution. None of the columns have been run to exhaustion in our operation. They were always regenerated when only a very small fraction of the resin had been exhausted. When exhaustion does occur, there is a sharp change in the pH of the effluent and it is easily detectable;

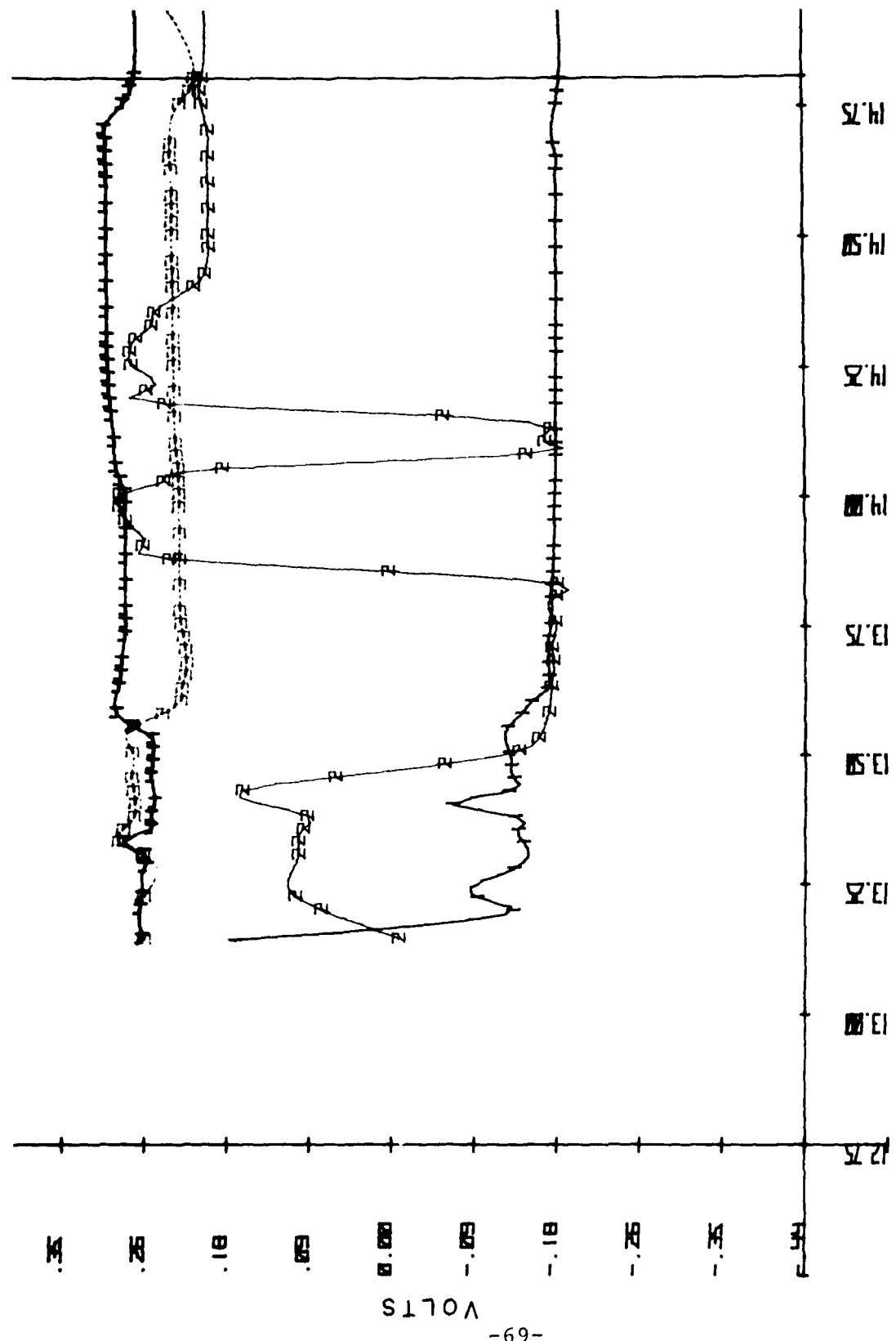


Figure 20. Voltages of pH Electrode During Run 318 for Electrodes 1, 2, 3, 4.

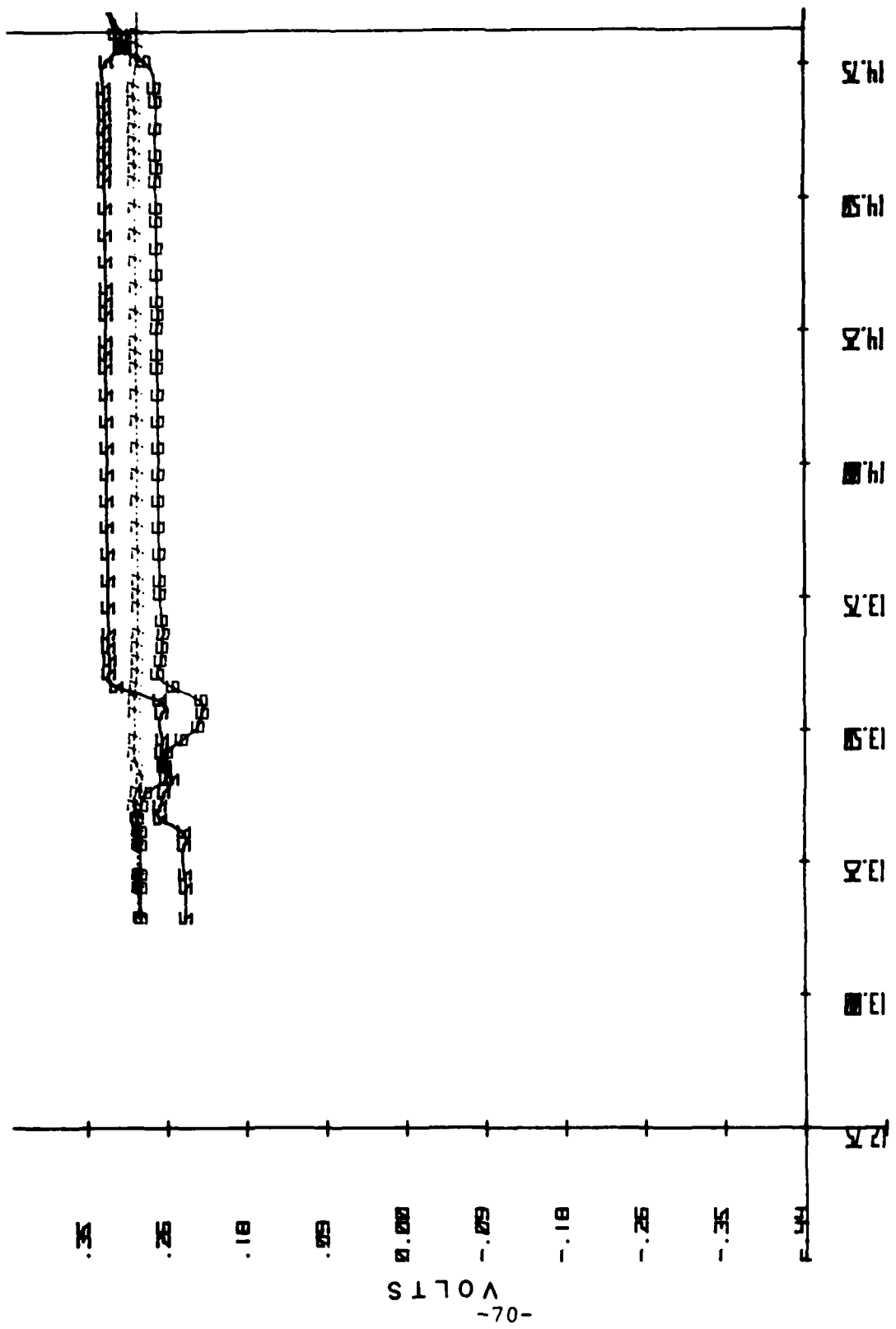


Figure 21. Voltages of pH Electrode During Run 318 for Electrodes 5, 6, 7,

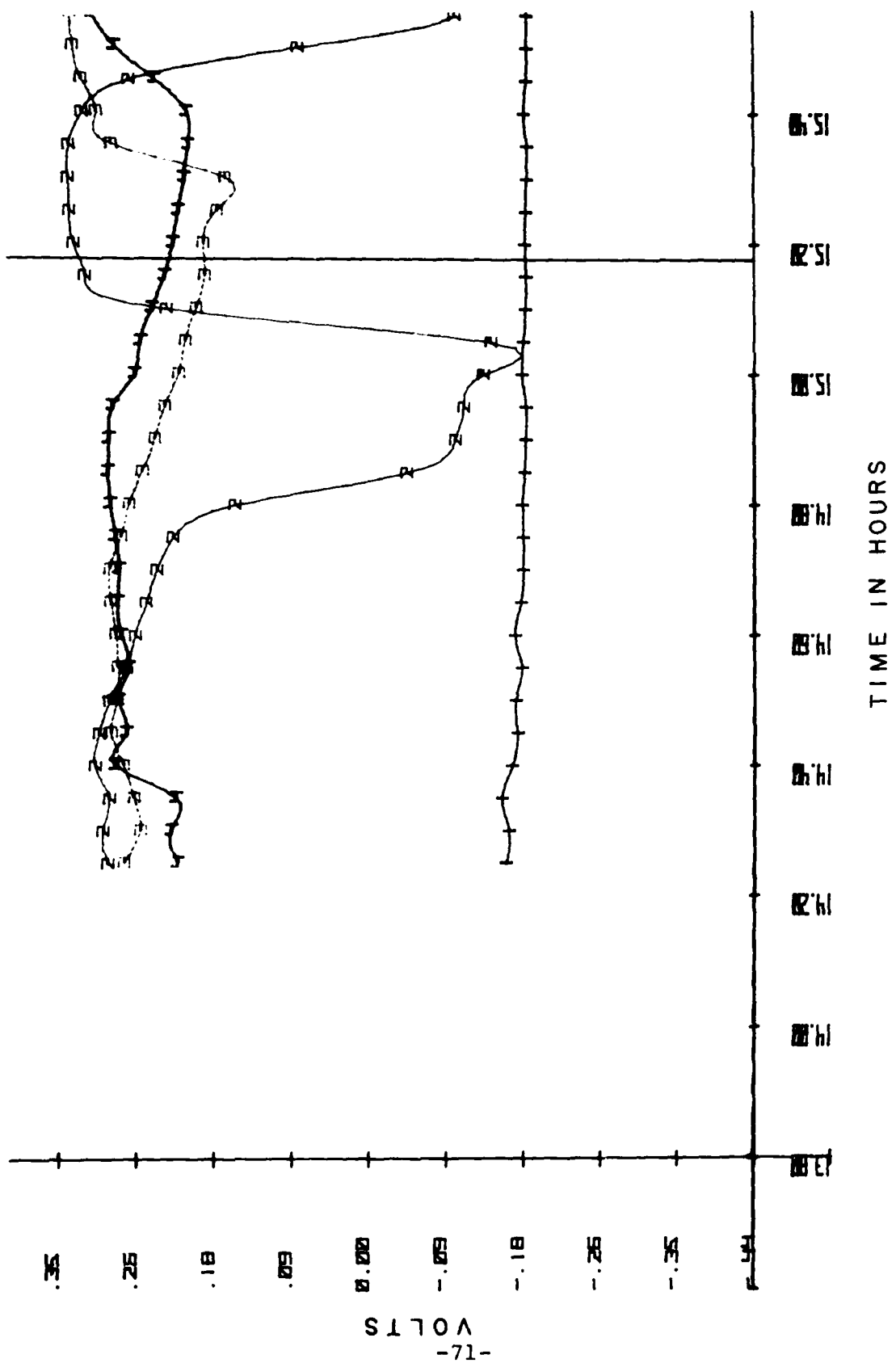


Figure 22. Voltages of pH Electrodes During Run 319 for Electrodes 1, 2, 3, 4.

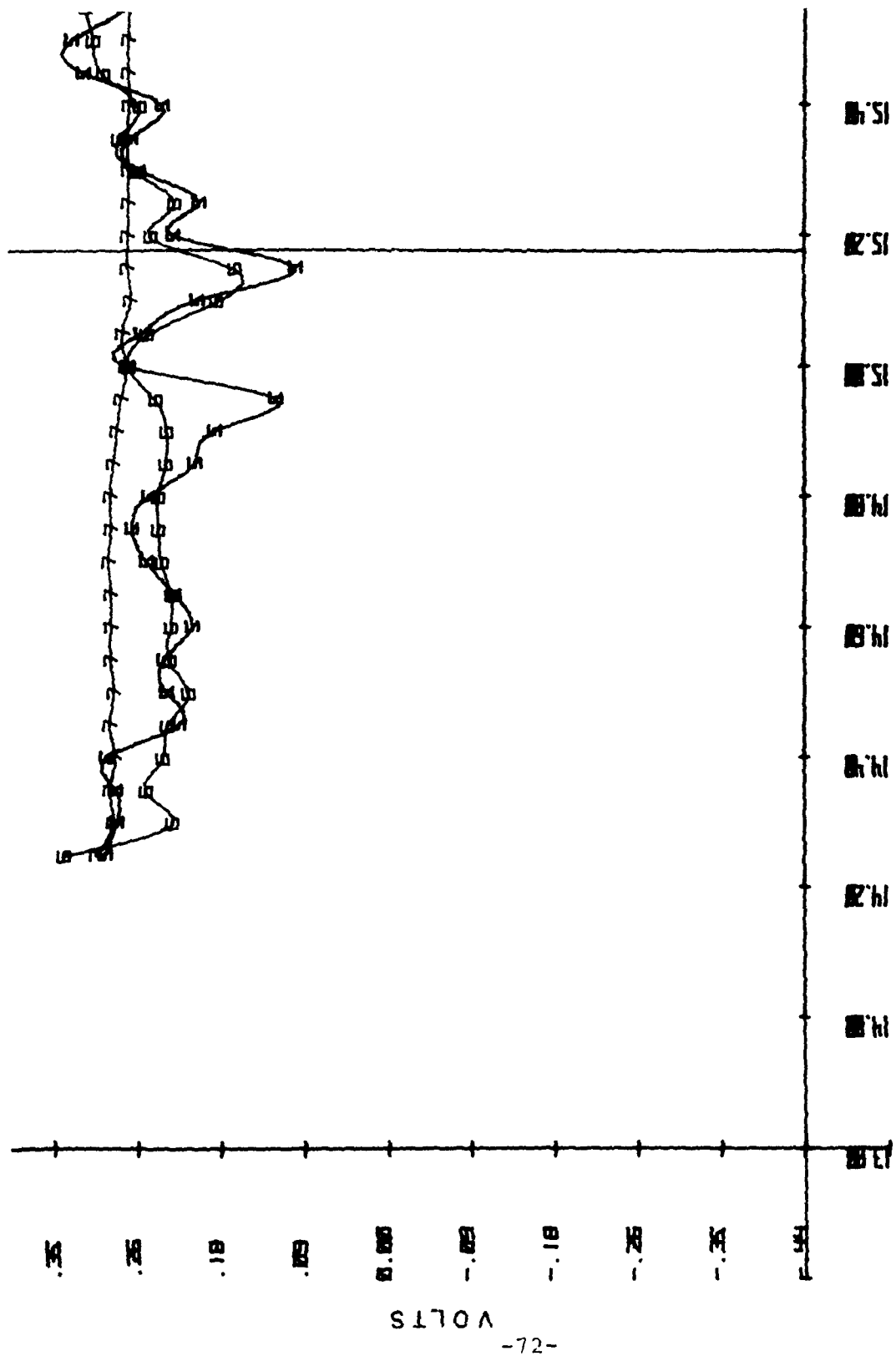


Figure 23. Voltages of pH Electrode During Run 319 for Electrodes 5, 6, 7.

however, for most of the columns, simple observation of the resin will give an indication on how far the process has progressed. For example, as the Chelex 100 became exhausted, it shrank considerably in volume, much like the volume changes it underwent during conversion. That was because the divalent ion forms of the resin have a smaller volume than the monovalent form. Also, discoloration of the resins occur as they are exhausted. These changes were always observed at the top of the resin bed. They varied in exact color and amount from run to run, but in all runs they were confined to the first few centimeters of the resin bed; then the column was regenerated.

Some atypical operation curves are shown in Figures 20 and 21 for one operation of the system, and in 22 and 23 for operation of the columns on the succeeding day. The numbers on the curve indicate the electrode number in the system starting with number 1 measuring the effluent of column 1, number 2 the effluent of column 2, etc. The ordinate gives the voltages as measured on the Fluke Data Logger. These were the parameters used for control, but if it is necessary they can be converted to pH by the following equation:

$$\text{pH} = -16.976V + 7,$$

where V is the voltage read on the Fluke Data Logger. Note the constancy of electrode 1 on run 318, then the rapid change of that electrode 1 during the initial start-up of 319, and that short curve and the erratic voltages at the beginning of the run represented the wash-out of the lines and some of the column during the start-up. The atypical feature in these runs was electrode 2 at the output of the pH adjusting column. Note that at about 14.8 hrs the pH began to increase markedly, indicating that the output of column 1 was not being corrected by the addition of a sufficient amount of acid. The problem

was soon discovered to be a sticking check valve which was corrected during this run and the following run by first tapping the valve to unseat it and later in the second run by bypassing it and adding acid through a secondary valve in column 2. After these two runs, the problem was corrected by shaving the teflon valve spring to allow the valve to open at a much lower pressure. An interesting feature observable in this run was the time at which the pH indicated by the second electrode begins to increase and the accompanying slow increase in pH of the effluent from column three; then when two is corrected, the delay between the correction and change in electrode three. A comparison of those curves gives good illustration of the delay time in the system which made it difficult to adjust easily. After run 319, the columns ran correctly and all electrodes produced constant voltages throughout the runs. The system was operated at 5 lbs positive pressure of filtered nitrogen. During operation, the combined nitrogen leakage and flow through the system was about 0.4 of a cubic foot per minute.

The effluent from the system was collected in 2 gallon lots in the vacuum chambers shown earlier. When the salt was dry, the vacuum oven was opened under positive pressure of nitrogen and the cap pushed down on the salt container which was immediately transferred to the nitrogen tent where the salt was put into polypropylene storage containers until required for crystal growth. Because the effluent of column 7 was highly acid, the resulting solid contains a substantial amount of hydrogen bromide, and if dissolved in water will produce an acid solution.

## IX. REACTIVE GAS TREATMENT AND CRYSTAL GROWTH

In the crystal growth process used in this work, the reactive gas treatment occurred as an integral part of the melting cycle and in the same apparatus as that in which the crystal was grown. It is shown in Figure 24. The details of furnace construction are shown in Figure 25. In this work the rotating crucible platform was lowered to the bottom of the furnace and the graphite ring placed on it to hold the bottom of the quartz test tube shaped reactive gas chamber. During a portion of the process, the reactive gas chamber and melt were under low pressure. To avoid leakage of the ambient atmosphere into the chamber, the cold finger seal shown in Figure 25 was replaced with a three-stage seal shown in Figure 26. The first stage of that seal was maintained at the pressure and atmosphere of the growth chamber, the second stage was maintained at 5 lbs pressure of the reactive gas, and the final stage was maintained at 10 lbs pressure of argon. Thus, any leakage into the reactive gas chamber was either the reactive gas itself or argon. All metal parts that came in contact with the reactive gas were of nickel 200. Initially, the cold finger was nickel 200 plated with rhodium. That particular couple had proved very effective in avoiding corrosion due to chlorine. It did not work well with hydrogen bromide and bromine; nickel 200 proved superior. The elastomers in the first two stages of the seal and the elastomers used in the tube seal were DuPont Kalrez perfluoroelastomer. The seal between the reactive gas chamber and the furnace was Viton, which neither contacted the reactive atmosphere nor the salt. The furnace element was of reactor grade graphite. Originally the furnace element was 4.5 inches long, made of 1/8 inch thick graphite, later changed to a 6 inch tube made of 1/16 inch thick graphite. The change was to permit the

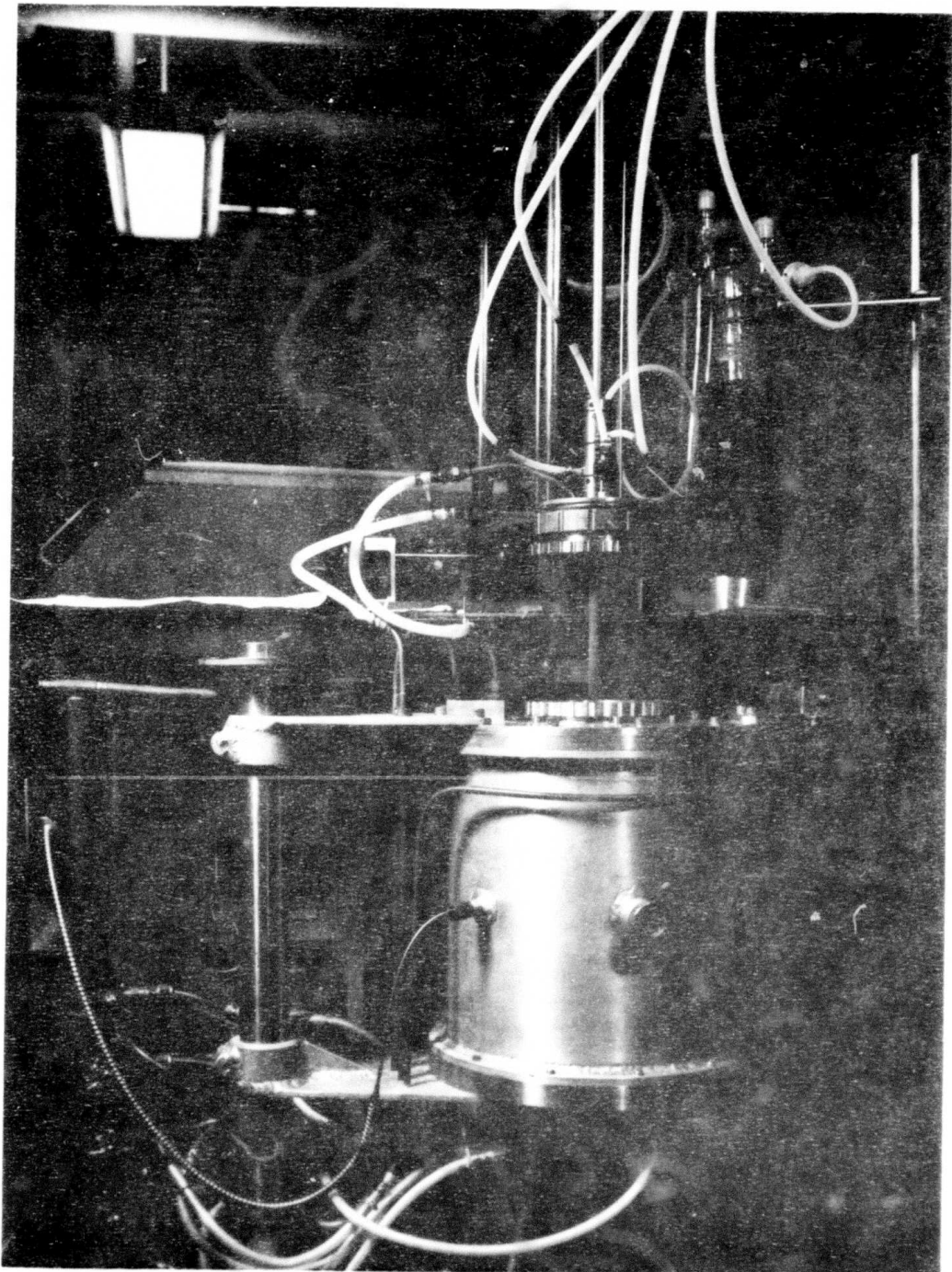


Figure 24. Crystal Growing Furnace

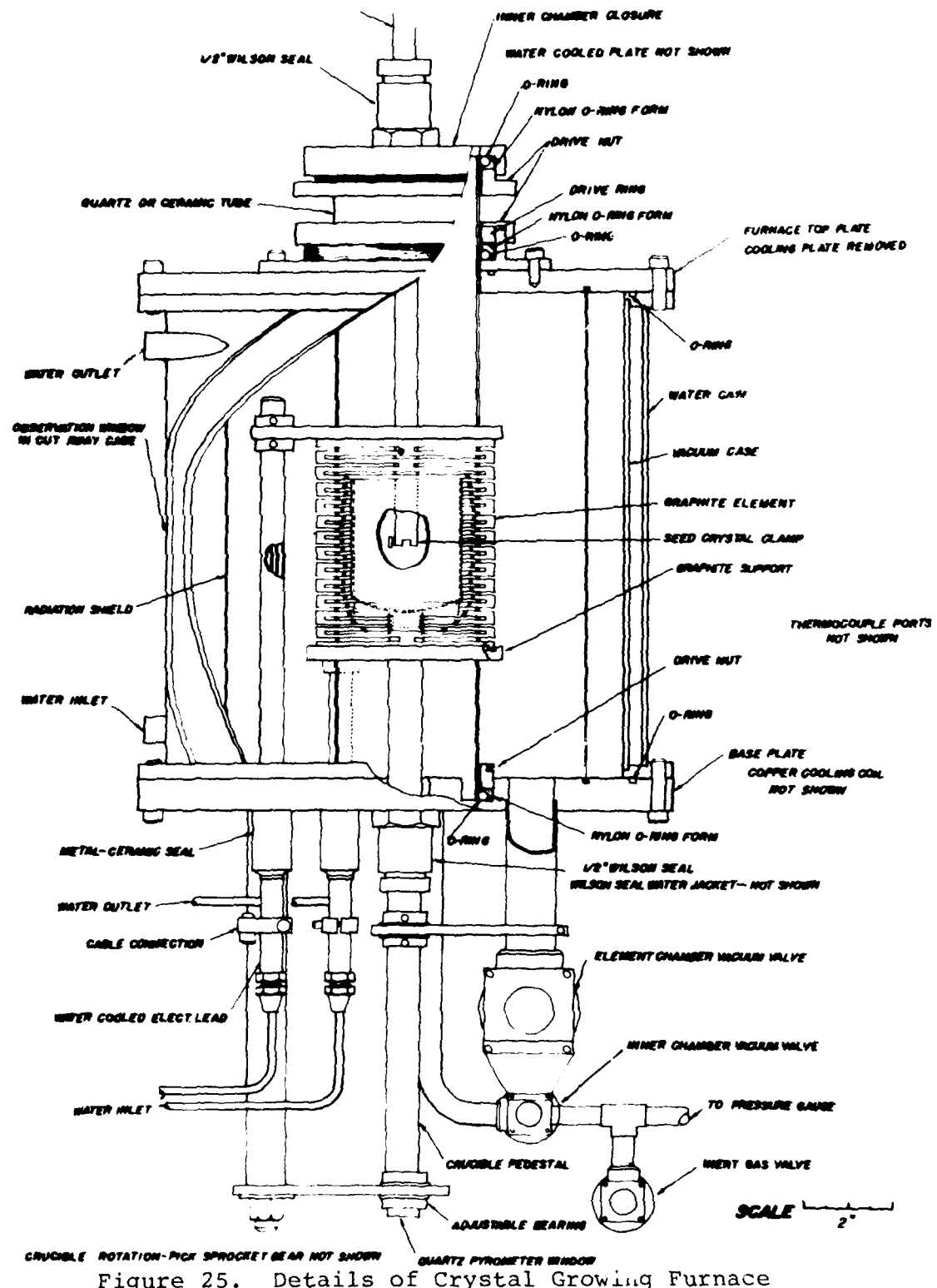


Figure 25. Details of Crystal Growing Furnace

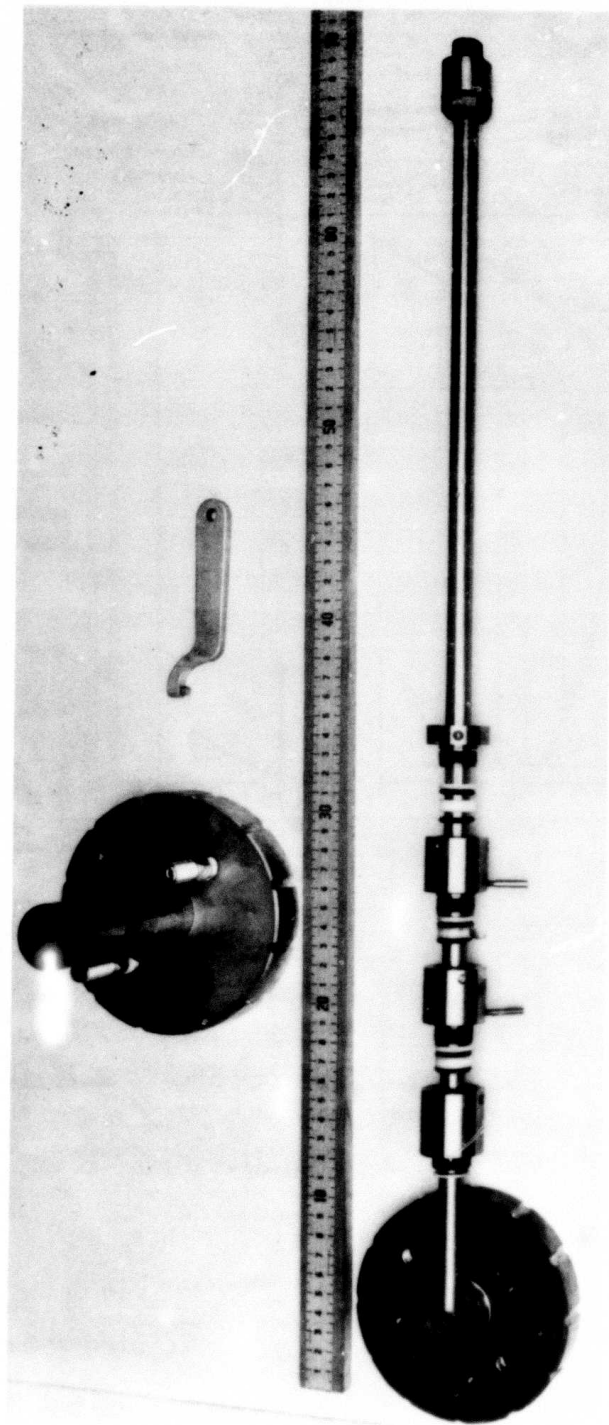


Figure 26. Three Stage Seal

growth of longer crystals and still maintain the flat growing interface which was used in the process.

The reactive gas manifold is shown in Figure 27. The mixing portion of the reactive gas manifold was constructed of pyrex, all valves were teflon-glass valves, all O-rings were perfluoroelastomers, all plastic connections and tubing used in the system were teflon. The safety lines from the regulators bonnet vents were polypropylene as was the waste gas line vented to a laboratory hood system. The regulators and all metal parts in the system were Monel or nickel. The three cold traps provided means of distillation of hydrogen bromide and storage of hydrogen bromide used during reactive gas treatments. As high purity hydrogen bromide was unavailable, it was essential that it be distilled or treated in some way to clean the gas. The mass spectrum of the gas showed it to be relatively pure, containing a few parts per million of water and a trace of bromine, and some nitrogen. The hydrogen bromide was purified by three condensations and distillations

The reactive gas treatment followed a long schedule. On the night before the crystal was to be grown, the purified potassium bromide was placed in a semiconductor grade quartz crucible, 6.5 cm diameter by 7.86 cm high, in the nitrogen tent. While in the tent the crucible containing the salt was placed in a beaker, and covered with a plastic bag, through which special crucible pliers extended. The crucible was placed in the crystal growing system. The mouth of the large bag containing the crucible and beaker was stretched over the entrance of the 46 cm x 8 cm diameter quartz tube used as the reactive gas chamber of the furnace. The pliers were then used to place the crucible on a quartz pedestal in the bottom of this tube. A watch glass was placed over the mouth of the tube and the bag removed. The seal for the reactive gas

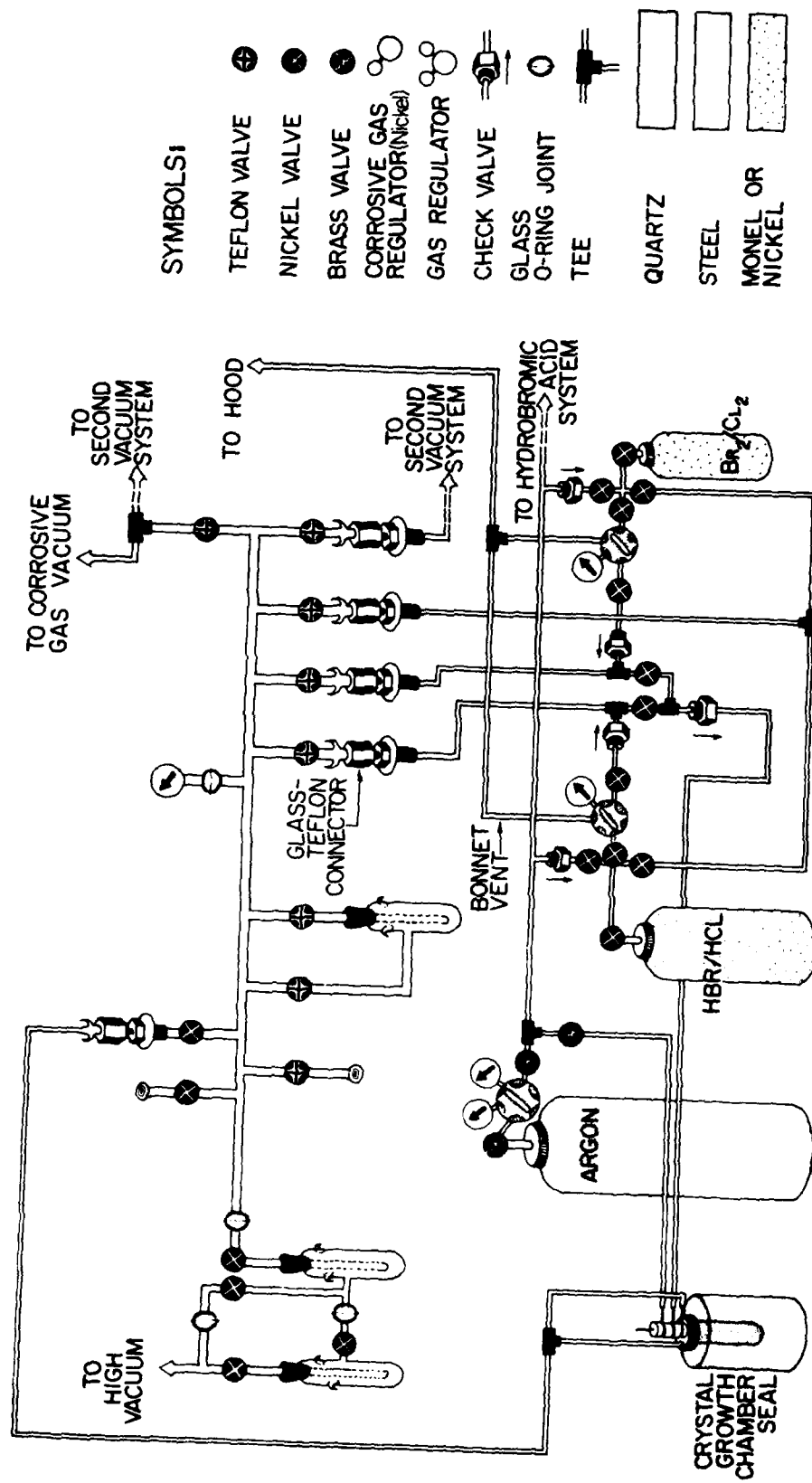


Figure 27. Reactive Gas Manifold

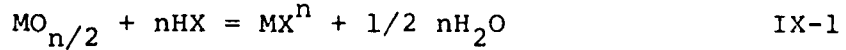
closure, which had been previously assembled on the cold finger containing the seed, was lowered directly above the watch glass. The closure was placed on the quartz tube immediately after the watch glass was removed. This operation was done under a plastic cover to avoid contamination from dust particles in the atmosphere.

This technique, while not totally eliminating contamination, minimized the amount of dust that could reach the salt or the interior of the crystal growing apparatus during assembly. The seal was closed and connected to the reactive gas input and the waste gas disposal system. The disposal system is not shown on the reactive gas drawing. The waste gas system connected to the seal opposite the reactive gas input seal. The waste gas first passes through a cold trap adjacent to the crystal grower and from there to the waste vacuum system. It was important to use a separate waste system because, during the reactive gas processing, impurities were transported out the exit tube. If the exit tube was used for both filling and emptying, these would be blown back into the chamber when new gases were admitted. The tubes to the three-stage seal were connected and the seal evacuated, then filled with appropriate gases. The system was evacuated and flushed with argon several times, then the temperature was brought to 100°C. During the initial drying, several hundred microns pressure of water vapor and HBr were given off by the salts. This was trapped in the cold trap immediately adjacent to the crystal grower and the system left in this initial drying configuration overnight. When the pressure had dropped to the base pressure of the vacuum system, the salt was ready for reactive gas treatment. The specific reactive gas treatment depends somewhat on the source salt being grown. In this work crystals were grown from three salts: raw J. T. Baker Analytical Reagent KBr, KBr supplied by Dr. Phillip Klein of

the Naval Research Laboratory, and the potassium bromide purified in this laboratory. Each type of potassium bromide has certain individual characteristics that dictated the best reactive gas treatment.

The principal anionic impurities in these salts should be other halides, but if the salt had been heated to a sufficiently high temperature, a reaction would occur between residual water and the salt which produced hydroxides and oxides in trace quantities. For that reason, it was important that the drying of the salt by a reactive atmosphere be initiated at relatively low temperatures and continued during the melting of the salt. In the case of any of the alkali halides, this drying can be effectively accomplished by treatment with the hydrogen halide. These will also effectively convert many of the oxides to the halides. These reactions can generally be summarized as follows.

The reactions of hydrogen halides with oxides as given by the reaction



will proceed if  $\Delta G$ , given by

$$\Delta G = \Delta G_f^\circ(MX_n) - \Delta G_f^\circ(MO_{n/2}) - n[\Delta G_f^\circ(HX) - 1/2\Delta G_f^\circ(H_2O)] \quad IX-2$$

is negative. Thus a set of general conditions can be expressed as

$$\Delta G < \Delta G_f^\circ(MF_n) - \Delta G_f^\circ(MO_{n/2}) + 36.55 \text{ Kcal mol}^{-1} \text{ for fluorides;}$$

$$\Delta G < \Delta G_f^\circ(MCl_n) - \Delta G_f^\circ(MO_{n/2}) - 5.972n \text{ Kcal mol}^{-1} \text{ for chlorides;}$$

$$\Delta G < \Delta G_f^\circ(MBr_n) - \Delta G_f^\circ(MO_{n/2}) - 16.01n \text{ Kcal mol}^{-1} \text{ for bromides; and}$$

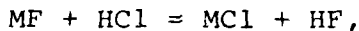
$$\Delta G < \Delta G_f^\circ(MI_n) - \Delta G_f^\circ(MO_{n/2}) - 28.91n \text{ Kcal mol}^{-1} \text{ for iodides.}$$

The reaction of the gaseous halides with alkali metal oxides,  $H_2O$ , the alkaline earth oxides, including  $MgO$  and zinc and cadmium oxides are all strongly exothermic. Hydrogen halides react with other alkali metal halides by the reaction:

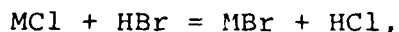


IX-3

All alkali metal fluorides, except lithium, should react with hydrogen chloride to give the chloride and hydrogen fluoride; again with the exception of lithium, they should all react with hydrogen bromide to give the bromide and hydrogen fluoride. Potassium fluoride, rubidium fluoride and cesium fluoride will all react with hydrogen iodide to give the corresponding iodide and hydrogen fluoride. The reactions are exothermic, and for all salts except the iodides, should therefore go as desired. For example:

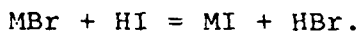


IX-4



IX-5

and



IX-6

The reactions used to reduce hydroxide and oxide impurity concentration of the salt are carried out over a temperature range from  $100^{\circ}C$  to the melting point of potassium bromide. In general, increasing the temperature decreases the extent to which the reaction proceeds in a favorable direction. These changes are summarized in Table 10.

Table 10

Reactions of Hydrogen Halides with Alkali Metal Salts\*

	HCl + KOH $\rightleftharpoons$	H <sub>2</sub> O + KCl		IX-8
	HBr + KOH $\rightleftharpoons$	H <sub>2</sub> O + KBr		IX-9
T(°K)	300	500	700	900
Kcal ΔG(8)	-38.59	-38.66	-37.86	-36.16
ΔG(9)	-43.28	-42.37	-41.02	-39.41
				1100
	2HCl + K <sub>2</sub> O $\rightleftharpoons$	H <sub>2</sub> O + 2KCl		IX-10
	2HBr + K <sub>2</sub> O $\rightleftharpoons$	H <sub>2</sub> O + 2KBr		IX-11
T(°K)	300	500	700	900
Kcal ΔG(10)	-127.2	-121.7	-116.0	-110.0
ΔG(11)	-133.2	-127.8	-122.3	-116.6
				1100

\*ΔG calculated from data given in reference 3.

The other function of the reactive gas is to reduce the concentration of unwanted halides that may pass through the columns. While these should be very low, the columns are not remarkably effective in removing chloride or fluoride ion; however, HBr is effective in converting potassium fluoride or potassium chloride to potassium bromide, but will not convert the iodide to the bromide. Fortunately, the iodide was very effectively removed in the ion exchange column system. Table 11 shows the free energy of these reactions as a function of temperature.

Table 11

Hydrogen Bromide Reactions with Other Potassium Halides\*

HBr + KX $\rightleftharpoons$ HX + KBr						IX-12
	T(°K)	300	500	700	900	1100
Kcal	ΔG(Cl)	-2.980	-3.066	-3.251	-3.251	-3.539
	ΔG(I)	+3.015	+3.444	+3.886	+4.329	+5.280
	ΔG(F)	-11.61	-11.76	-11.94	-12.14	-12.70

\*ΔG calculated from data given in reference 3.

The quantities calculated for the above tables were based on the presumption that the hydrogen bromide was at 1 atm and at the temperatures indicated in the tables. They represent the reactions of the gas with the solid phase salt reasonably well. However, these reactions were limited by diffusion of the hydrogen bromide into the crystalline salt and the diffusion of the product out of the salt. This is a relatively slow process at low temperature, and most of the low temperature reactions occurred on the surface of the crystal and consisted of removing adsorbed water. Higher temperatures enhanced diffusion, but decreased the equilibrium constant significantly (Table 10).

Hydrogen bromide was extremely soluble in the molten potassium bromide. Thus the concentration of HBr reacting with impurities in the KBr increased greatly. Data on the activity of HBr in molten potassium bromide are not available; however, the solution appeared to be quite non-ideal. The volume of the melt decreased slightly as HBr was absorbed.

When quartz crucibles were used as the container for the melt, it was extremely important that the reactive gas treatment begin at relatively low temperatures. Any hydroxide

present in the salt caused the quartz to devitrify. When hydrogen halide treatments were begun at temperatures of 100-150°C, there was no reaction of the salt or its melt with the quartz. If the introduction of HBr was delayed until the salt was heated to 450-550°C, the quartz crucible developed a cloudy appearance. The absence of devitrification provides a good test of the effectiveness of the hydrogen halide treatment.

One of the advantages of quartz crucibles over vitreous graphite was that the quartz contributed no carbon to the melt. All alkali halides contain carbonaceous materials that decompose to form small particles of graphite in the melt. In chlorides it was easily removed by treatment with chlorine gas. Treatment with bromine was not practical because of its tendency to collect in cooler parts of the gas treatment system. However, some bromine treatment cannot be avoided, because at the melt temperature of KBr hydrogen bromide is about 5% dissociated. This provided some oxidation of the carbonaceous materials by bromide at the melting point, but it was not especially effective.

Two series of crystals were grown using HBr as the reactive gas and two series of crystals using both HBr and pure O<sub>2</sub> as reactive gases. The oxygen was effective in removing carbonaceous material from the salt. A typical reactive gas treatment consisted of three hydrogen bromide treatments at a pressure of 1 atm starting the first at 100-150°C. The hydrogen bromide was exchanged at 5 min intervals. Around 300°C, the hydrogen bromide was removed, the reactive gas chamber flushed with argon until free of hydrogen bromide, and 1 atm of pure oxygen added. Oxygen was exchanged three times while the temperature increased from around 300 to 400°C. The salt was held at around 400°C, and the system flushed with argon until free of oxygen. Then hydrogen bromide treatments began again with bromide exchanged at 5 min intervals for fresh HBr. Five such

treatments generally occurred before the salt melted. On melting, three additional hydrogen bromide treatments were administered to the molten salt. During the final treatment the temperature of the melt was adjusted to the temperature required for initiating crystal growth. Then the system was pumped by a cryogenic trap until pressure was around  $3.0-3.5 \times 10^{-2}$  torr. The crystal chamber was then filled with argon to -2 inches gauge pressure.

After the salt was melted, cold water was turned on in the cold finger and it was moved from its storage position against the top seal of the tube and lowered into the melt. About 2 mm of seed was immersed in the melt. The seeding process was observed through the melt level window on the side of the furnace case. Temperature was read on a blind thermocouple that extended through the outside case to the graphite heating element. The temperatures read were not the true temperature of the melt, but were usable for control of the furnace, and for monitoring various processes. The seed was immersed in a melt that was about  $10^{\circ}$  above the temperature at which the salt was observed to melt. The temperature was lowered until the seed enlarged after its initial melt-off; once a growth temperature was established, it was maintained within  $\pm .25^{\circ}\text{C}$  by a Leeds Northrup control system. This consisted of a millivolt set point unit, Leeds Northrup Model 10810, a three action control unit, Leeds Northrup #10877, and a DC null detector, Leeds Northrup #9834-2. The output signal of the controller drives a magnetic amplifier which controls the input to a step down transformer. The original system was designed to function at much higher temperatures than used in potassium bromide growth, but the controller maintained a constant temperature extremely well. The temperature was brought to the melting point manually. Once the crystal started to grow, the temperature must be

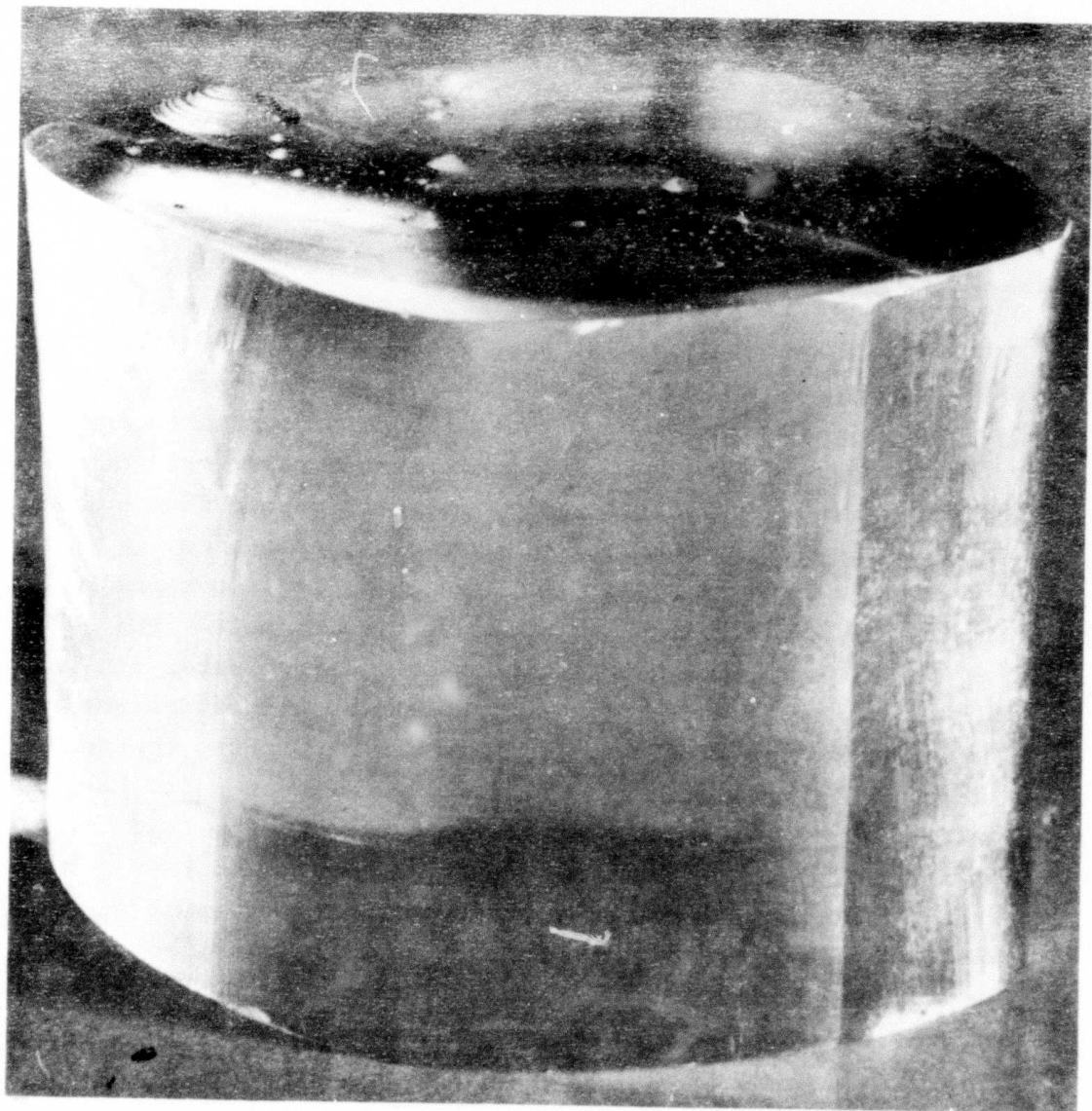


Figure 28. A Portion of a Crystal

adjusted occasionally to maintain a relatively constant diameter of the crystal. This was done by a manually operated clock motor drive on the set point control. The crystals were pulled at a rate of about 1 cm per hour. Pulling rate and temperature were adjusted so that the interface between the crystal and the melt was horizontal. Because the crystals grow near equilibrium growth conditions, they were approximately square with flat  $<100>$  faces. On the  $<100>$  faces thin rectangular terraces formed by the intersections of  $<011>$  and  $<0\bar{1}\bar{1}>$  steps were observed. If the temperature increased sufficiently to cause the crystal to shrink in cross section, the  $<100>$  faces decreased in area and a line appeared, formed by the intersection of  $<110>$  and  $<\bar{1}\bar{1}0>$  faces. This line was displaced slightly from the center of the crystal. The amount of displacement depended on the rotation speed. When the temperature decreased, this line disappeared and the surface features returned to their normal appearance. Often, these crystals did not show the growth rings usually seen on pulled crystals. Some of these features can be seen in Figure 28. When the melt reached within 5 mm of the bottom of the crucible, a rapid increase in temperature was necessary to prevent the crystal from freezing in the melt. Generally, the crystal was pulled from the melt at this point. The pulled end showed a relatively flat growth face with the small drop of the residual melt hanging to it.

Reactive gas treatment and growth of the crystal were always completed without interruption. The total time required for the entire process was 14-16 hours. When all conditions were favorable, a crystal of about 10-11 cm long and 2.5-3 cm across the flat  $<100>$  faces was obtained. More often the crystal grew to about 8 cm in length before the melt was exhausted.

The most striking feature of the J. T. Baker Analyzed Reagent salt was that when left overnight at 100-150°C a thin layer of a white material sublimed from the salt onto the upper portion of the reactive gas chamber. However, the system pumped to the base pressure of the vacuum system used initially to remove moisture from the salt. As the temperature was raised at about 300-364°C, a large amount of white material sublimed from the salt. This occurred even if the salt was treated with HBr before heating to 300-364°C. The material was not KBr, because the temperatures were far too low. It has not been possible to analyze the material that comes from the J. T. Baker Analyzed Reagent potassium bromide. When viewed at a glancing angle, it appeared to be on the outside surface of the quartz. When potassium bromide sublimed, it appeared to be on the inside of the quartz tube. During reactive gas treatment, a considerable amount of material sublimed from this salt and a large amount of moisture was initially present. The crucible will remain only about 5/8 full after the salt has been melted; the rest has been lost as moisture or sublimate. The melted salt contained a modest amount of organic residue as graphite. Also, organic materials were deposited just above the seal of the tube to the furnace chamber. These products were partially decomposed and had a brownish to blackish appearance. They were soluble in alcoholic KOH. The amount of carbon left in the melt was relatively minor and only occasionally was occluded in a pulled crystal. Treatment with oxygen did remove most the residual carbon.

The Navy Research Laboratories' potassium bromide was much purer; no sublimate was formed until the final outgassing of HBr from the salt at a temperature well above its melting point. This salt did deposit organic matter on the cooler portions of the graphite tube. It was partially decomposed and

brownish to black in color. This residue was more difficult to remove than J. T. Baker Analyzed Reagent KBr residue. An oily substance condensed on the water cooled nickel closure at the top of the reactive gas chamber. The shrinkage of the salt on melting was considerably less than that of J. T. Baker Analyzed Reagent KBr. The melt contained appreciably more carbon and it often occluded on the seed when it was initially immersed in the melt and remained there during pulling. Occasionally graphite or carbon particles were picked up in the crystal from the salt. Treatment with oxygen during the initial stages and during the melt did remove carbon fairly effectively, but some always remained in the melt.

Ion exchange purified salt contained a large amount of hydrobromic acid, which had to be removed during the initial pump out. To avoid condensation of hydrobromic acid on the various components of the reactive gas system, the water to the top seal to the reactive gas chamber was shut off and the seal allowed to heat to about 100°C. This was sufficient to prevent condensation of the acid on the seal. The acid was collected in a liquid nitrogen cooled cold trap immediately adjacent to the exit port of the crystal growth chamber. The salt pumps down to the base pressure of the system overnight. No sublimate was observed on the tube. No sublimate formed until the final pump out of the HBr from the melt at a temperature well above the melting point of the salt. The shrinkage of the salt was not as great as J. T. Baker Analyzed and was only slightly greater than that of the Navel Research Laboratories KBr. There was noticeable difference in the growing temperature of the J. T. Baker Analyzed Reagent, the NRL, and the ion exchange purified salt; the latter two grew at a substantially higher temperature on the blind thermocouple.

The ion exchange salt had variable amounts of organic matter in it, depending on the quality of the filters in the

ion exchange system. Without micrometer Millipore filters, the amount of organic material exceeded that of the NRL salt; with micrometer Millipore filters, the amount of organic material was less than in the NRL salt. After initial aging, the quantity of organic compounds reached a minimum and remained constant.

## X. RESULTS

Crystals of KBr grown from J. T. Baker Analyzed Reagent, Naval Research Laboratory, and ion exchange purified were sent to Dr. J. Harrington of Hughes Research Laboratories and to Dr. D. Edwards of Los Alamos Laboratories for laser optical measurements. Similar crystals were spectrophotometrically studied here. Samples of some of these crystals were sent to the Missouri Reactor for irradiation and returned to OSU for counting. The results of the testing program are beginning to become available.

### (a) Analysis of Crystals.

Small samples (2 mm cubes) of various KBr crystals were sealed in quartz tubes. Each tube contained five or six samples. Generally, duplicate samples were placed adjacent to each other in the same tube. Occasionally such paired samples were placed in different tubes or paired samples from crystals grown from different source materials were placed in the same tube. The reason for arranging crystals in this manner was to expose errors caused by residue left in the tube from improper cleaning or introduced from equipment used in handling the samples. Many of the analyses were for impurities

present in ppb ( $10^{-12}$ ) by weight and careless treatment could introduce significant amounts of impurities.

Induced neutron activation analysis of KBr was not as easily accomplished as analysis of KCl. The crystals were very hot when removed from the reactor due to the bromine and were left to decay for 60 days before being counted at Oregon State University. Therefore, Na was not detectable nor were the  $n,\gamma$  products of the alkaline earths [ $^{27}\text{Mg}$  (9.5 min),  $^{49}\text{Ca}$  (8.8 min),  $^{87\text{m}}\text{Sr}$  (2.8 h),  $^{89}\text{Sr}$  (2.81 min),  $^{139}\text{Ba}$  (85 min),  $^{131}\text{Ba}$  (11 d)]. Sodium and alkaline earths are now in process in OSU's small reactor so that  $^{24}\text{Na}$  (15 h) can be counted and alkaline earths precipitated as carbonates to separate them from interference by the bromide. This technique should detect  $\text{Sr}^{2+}$  and  $\text{Ba}^{2+}$ , but is questionable for  $\text{Ca}^{2+}$  and  $\text{Mg}^{2+}$ .

Table 12 gives the results of the present stage of the analysis of these crystals. These results report all detectable species found in the crystals after a 60 day decay before counting. Of the analyses attempted, two tubes containing five samples were rejected because all samples showed excessive Zn contamination while the other sample of a split pair did not show excessive Zn. The distribution of Zn in one of these rejected tubes varied from 1030 ppb in an NRL crystal at the suspected contamination source to 29 ppb in an ion exchange crystal located the greatest distance from the source.

The current stage of the analyses show the only cation impurities present in the ppm range are  $\text{Rb}^+$  and  $\text{Fe}^{2+}$ . Rubidium is the most difficult ion to remove from potassium salts and four to five ppm remaining in the finished crystal is not unusual, but the ion exchange system should be capable of reducing it to less than one ppm when operating at maximum efficiency. The 0.03 to 0.05 ppm of iron found in these crystals must be introduced after the ion exchange process, as this exceeds the amount found in the control samples taken

Table 12  
Analysis of KBr Crystals by Induced Neutron Activation Analysis

Crystal type	Rb x10 <sup>6</sup>	Fe x10 <sup>6</sup>	Ag x10 <sup>12</sup>	Cr x10 <sup>12</sup>	Sb x10 <sup>12</sup>	Co x10 <sup>12</sup>	Cs x10 <sup>12</sup>	Zn <sup>1</sup> x10 <sup>12</sup>
BA <sup>2</sup>	5.2	0.06	< 1	4.2	0.5	0.2	0.3	9
3	(±0.5)	(±0.3)		(±4)	(±0.5)	(±0.1)	(±0.2)	(±4)
NLR <sup>4</sup>	6.0	0.14	< 1	5.6	0.38	0.1	0.5	11
	(±0.9)	(±0.2)		(±4.9)	(±0.16)	(±0.1)	(±0.2)	(±3)
OSU <sup>5</sup>	4.9	0.04	< 1	0.3	0.34	0.06	0.27	8
	(±0.8)	(±0.01)		(±0.2)	(±0.26)	(±0.05)	(±0.1)	(±3)
RAW	187	100	NA	6.8(10 <sup>6</sup> )	NA	81(10 <sup>6</sup> )	14(10 <sup>6</sup> )	57(10 <sup>6</sup> )
BA <sup>6</sup>	(±20)	(±56)		(±4.1)		(±29)	(±45)	(±12)

<sup>1</sup>Zn suspected as residual impurity on quartz analysis tubes.

<sup>2</sup>Baker Analyzed KBr. Crystals grown by Czochralski method at Oregon State University. Mean value of six analyses (two samples from three crystals).

<sup>3</sup>95% confidence limits calculated as  $ts/\sqrt{N}$ .

<sup>4</sup>Naval Research Laboratory KBr. Crystals grown by Czochralski method at Oregon State University. Mean value of ten analyses (two samples from five crystals).

<sup>5</sup>Baker Analyzed KBr purified by ion exchange. Crystals grown by Czochralski method at Oregon State University. Mean value of ten analyses (two samples from five crystals grown from five different batches of purified KBr).

<sup>6</sup>Analysis of three lots of Baker Anzlyzed KBr before purification by atomic absorption. Data taken from Table 10 of Volume I of this report. This raw KBr also contained Ni (187±21), Li (171±44), Na (93±129), Cu (30±16), Mn (22±1), Ca (17±3.6), Mg (6.1±1.6), which would not have been detected by the INAA technique used.

from the ion exchange system. The sources for iron were the drying oven used in cleaning the quartzware or possibly the monel closure on the reactive gas chamber. However, if the closure was the source of iron, the crystal would also contain nickel. Quartzware will be cleaned using a different process.

All other cationic impurities detected occurred in the parts per billion range. Of these, only  $Zn^{2+}$  consistently was detected in the  $10^{-11}$  gm per gm KBr range. The most common source of Zinc contamination is elastomers. The zinc content of ion exchange purified crystals is generally lower than unpurified crystals. On occasion excessive amounts of zinc were found in a sample placed in one irradiation tube, but a different sample cut from the same crystal irradiated in a different tube contained much less zinc. When one crystal in a tube contained excessive zinc, all other would show a high zinc content. These observations suggest the zinc quantities given in Table 12 reflect the residue from cleaning these small tubes rather than the actual zinc content of the crystal. The same may be true of antimony. Because antimony is trivalent two compensating cation vacancies must be introduced in KBr. Therefore,  $Sb^{3+}$  is not often found in alkali halides while it is commonly found in the insoluble soaps used as mold release compounds.

Neutron activation analyses for oxygen and silicon had to be abandoned because Oregon State University's 14 meV neutron source was shut down just as the analyses were started. During the course of growing crystals, it was found that all melts contained carbon. This was present regardless of the source of the salt. The amount in the finished crystal appeared to be very small. The usual method of analysis for carbon is by a  $^{12}_6C(n,2n)$  reaction to produce  $^{11}_6C$  which is detected by positron emission. This is not an especially sensitive analysis (10 to 50  $\mu$ gm per gm). No carbon was

Table 13. Laser Calorimetric Absorption Measurements

Sample No.	Source KBr <sup>3</sup>	$\beta(10.6 \mu\text{m})$ ( $\times 10^4 \text{ cm}^{-1}$ )	$\beta(9.27 \mu\text{m})$ ( $\times 10^4 \text{ cm}^{-1}$ )	Notes
396	B.A.	$8.23 \pm 0.8$	$21.76 \pm 0.4$	1
493	B.A.	$3.72 \pm 0.1$	$23.65 \pm 0.7$	2
429	N.R.L.	$4.48 \pm 0.3$	$6.55 \pm 0.6$	1
491	N.R.L.	$4.68 \pm 0.26$	$9.76 \pm 0.5$	2
318/460	O.S.U.	$2.90 \pm 0.19$	$15.77 \pm 0.4$	2
319/464	O.S.U.	$3.20 \pm 0.27$	$9.06 \pm 0.46$	1

NOTES:

1. Crystals treated with a minimum of 12 HBr exchanges between 150°C through melting. The final 3 applied after salt melted. The crystal was grown under argon atmosphere.
2. Crystals treated with three HBr exchanges, flushed with argon until free of HBr, then three pure O<sub>2</sub> exchanges were applied to unmelted salt. Six additional HBr exchanges were made before melting and three after melting. The crystal was grown under an argon atmosphere.
3. B.A. is J. T. Baker Analyzed Reagent.  
N.R.L. is Naval Research Laboratory.  
O.S.U. is Oregon State University.  
Sample Number means purification batch/crystal.

detected in any of the crystals at this high concentration. As noted below, if carbon is present in the crystals, not much of it is in a chemically combined form.

(b) Optical Absorption Spectra

The absorption spectrum at room temperature was measured from 205 nm to 20  $\mu\text{m}$  in all KBr crystals grown. In this spectral region, no absorption bands were detected in any of the crystals. The spectra consisted of featureless noise lines, even with the transmission multiplied by a factor of five. The percent transmission was independent of the thickness of the crystal.

(c) Laser Absorption Measurements

Six crystals of KBr were sent to Dr. J. A. Harrington of Hughes Research Laboratory for Laser Calorimetric absorption Studies. The crystals were approximately 2.5 cm square and, after the ends were removed by string sawing with HBr, they were between 8.5 and 9.5 cm in length. At Hughes, the cut ends were mechanically polished and absorption measured at two wavelengths. The results of these measurements are given in Table 13.

## XI. DISCUSSION

The measurements of most interest here are the absorption coefficients of Table 13. In Table 15, some of the "lowest measured" values from the literature (4,5,6) have been collected for comparison. It was not possible to identify exactly all the measurements or the sources of crystals that appear in the summary tables in the two review articles used as primary

Table 14  
Analysis of Crystals Used for Absorption Measurement<sup>1</sup>

Crystal	Rb x10 <sup>6</sup>	Fe x10 <sup>6</sup>	Ag x10 <sup>12</sup>	Cr x10 <sup>12</sup>	Sb x10 <sup>12</sup>	Co x10 <sup>12</sup>	Cs x10 <sup>12</sup>	Zn x10 <sup>12</sup>
396	5.3 (±0.3)	0.05 (±0.05)	< 1	10 (±3)	< 1	0.2 (±0.1)	0.5 (±0.1)	4.1 (±1.3)
429	6.2 (±0.4)	0.06 (±0.06)	< 1	20 (±2)	0.1 (±0.1)	0.1 (±0.1)	0.6 (±0.1)	6.1 (±0.5)
491	5.1 (±0.3)	0.05 (±0.02)	< 1	0.1 (±0.1)	0.7 (±0.2)	0.0 (±0.1)	0.5 (±0.2)	8.6 (±0.9)
460	4.4 (±0.3)	0.03 (±0.01)	< 1	< 3	< 1	0.0 (±0.1)	0.4 (±0.3)	8 (±1)
464	5.0 (±0.3)	0.02 (±0.01)	< 1	0.1 (±0.1)	0.3 (±0.1)	0.1 (±0.1)	0.2 (±0.1)	8 (±1)
22477 <sup>3</sup>								
edge	5.9 (±0.4)	0.13 (±0.04)	< 1	6 (±5)	0.4 (±0.1)	0.4 (±0.1)	7 (±0.4)	15 (±2)
center	4.9 (±0.3)	1.4 (±0.2)	< 1	1.2 (±0.6)	0.6 (±0.1)	1.6 (±0.2)	1.2 (±0.2)	5.2 (±1.5)
middle	5.9 (±0.4)	0.03 (±0.02)	< 1	< 1	0.6 (±0.1)	0.6 (±0.1)	1.8 (±0.2)	10 (±1)

<sup>1</sup>Determined by instrumental neutron activation analysis: radio-nuclides measured were 27.7d <sup>51</sup>Cr (320 keV $\gamma$ ); 44.5d <sup>59</sup>Fe (1099.2 keV and 1291.5 keV $\gamma$ ); 5.27y <sup>60</sup>CO (1173.2 keV $\gamma$ ); 224d <sup>65</sup>Zn (1115.5 keV $\gamma$ ); 18.7d <sup>86</sup>Rb (1076.6 keV $\gamma$ ); 252d <sup>110m</sup>Ag (657.7 keV $\gamma$ ); 60.2d <sup>124</sup>Sb (1691.1 keV $\gamma$ ); and 2.06y <sup>134</sup>Cs (604.7 keV).

<sup>2</sup>Standard deviation.

<sup>3</sup>Analysis sections of NRL-KBr crystal supplied by Dr. P. Klein.

Table 15. Absorption Coefficients of Laser Window Materials

Materials	$\beta(10.6\mu\text{m})$	$\beta(9.27\mu\text{m})$	$\beta(5.25\mu\text{m})$	$\beta(3.8\mu\text{m})$	$\beta(2.7\mu\text{m})$
KBr	$4.2 \times 10^{-4}$ (1a)		$2.1 \times 10^{-4}$ (a)	$1.6 \times 10^{-4}$ (1b)	$1.2 \times 10^{-4}$ (1c)
	$4.2 \times 10^{-4}$ (2)		$2.1 \times 10^{-4}$ (2)		
	$1.4 \times 10^{-5}$ (3a)			$2.2 \times 10^{-4}$ (3b)	$1.2 \times 10^{-4}$ (3b)
	$2.9 \times 10^{-4}$ (4)	$15.7 \times 10^{-4}$			
	$3.2 \times 10^{-4}$ (4)	$9.06 \times 10^{-4}$			

- 1) Bendow, Bernard. Multiphonon Infrared Absorption in the Highly Transparent Frequency Regime of Solids., in "Solid State Physics," 33 (Eds. Ehrenreich, H., Seitz, F., Turnbull, D.) Academic Press, New York (1978) p. 308.  
(a) Deutsch, T. F. (b) Harrington, J. A. (c) Unidentified.
- 2) Sparks, M., "Theoretical Studies of Materials for High Power Infrared Coatings." Sixth Technical Report, 31 December 1975, p. 226 (measured on Raytheon CO<sub>2</sub>/CO laser calorimeter).
- 3) Klein, P. M., Growth of Lowloss KBr in Halide Atmospheres. A Xerox copy. Publication source not known. (a) unidentified (b) Harrington, J. A. (University of Alberta calorimeter).
- 4) From Table 13 in this report. (Harrington, J. A.) (Hughes calorimeter).

references. However 15 does provide a useful comparison of various results. Clearly, Klein's reported value of  $10.6\mu\text{m}$  is the lowest  $\beta$  yet obtained. Dr. Klein provided some of the same salt used in those crystals from which were grown Czochralski crystals with HBr as the reactive atmosphere. The lowest absorption coefficient measured at 10.6 nm and crystals grown from NRL salt was  $4.48 \times 10^{-4}$  which compares with  $2.9 \times 10^{-4}$  at 10.6 nm for the OSU purified salt.

In Table 12 are presented the analysis of the three types of crystals grown here as well as the analysis of the raw salt. The crystals grown from NRL salt appear to have a significantly greater amount of iron present than either the BA or the OSU. However, that is somewhat misleading in that the range of iron concentration found in the BA salt was significantly larger than that found in the NRL salt, both of which were twenty or thirty times greater in range than that found in the OSU salt. This means that of the samples analyzed the concentrations found in individual samples of crystals varied greatly in both BA and NRL, while the OSU crystals were relatively uniform. It is typical of crystals containing divalent impurities for the impurities to cluster small regions in the crystals with excessively high impurity content. That results in rather large 95% confidence limits for a particular set of samples. While the OSU Salt is lower in iron content than the others and much more uniform, the  $4 \times 10^{-8}$  gram per gram of KBr was somewhat larger than expected. As mentioned earlier, the iron was apparently introduced during crystal growth due to contamination from ineffective cleaning of quartzware or the drying oven.

The other major impurity found in these analyses was rubidium. The crystals are essentially all similar in rubidium contamination. The OSU crystals are slightly lower in rubidium content, but not by a significant amount.

The minor impurities occur in the parts per billion range. Chromium appears in concentrations from 4 to 6 ppb in the BA and NRL salts. Again, the 95% confidence limit is large, indicating there was a wide range of concentrations present in these salts. The OSU salt has relatively little chromium. The zinc and antimony reported are probably contaminants left from cleaning the small quartz irradiation tubes. The argument for this has been given earlier. In every case the zinc was high,

it was distributed from a point in the tube to other crystals present. Antimony exhibited the same characteristics. For that reason, it is likely that these two elements were carried into the analysis from the cleaning procedures of the quartz tube. The other impurities all occur at less than a part per billion, and probably would not significantly alter the optical properties of the crystals.

Table 12 illustrates the effectiveness of the crystal growing system for reduction of impurities in a crystal. All the elements detected here were present in the parts per million range in the raw J. T. Baker Analyzed Reagent salt. Comparison of the first entry in Table 12 with the raw J. T. Baker Analyzed Reagent data given in the last entry of Table 12 illustrate the effectiveness of the Czochralski method used for growing the crystals. Unfortunately, the samples sent for analysis of the other two salts prior to crystal growth were lost due to fracture of the irradiation tube. Compare the analysis of the crystal labelled 22477 in Table 14 with the NRL labelled entry in Table 12 to observe the differences in a Czochralski crystal and a Stockbarger crystal. Crystal #22477 was grown at the Naval Research Laboratory. The values entered in Table 14 are the lowest value for two samples taken from the edge, center, and middle labelled portions of the crystal sent to us. The quantities found in these samples varied considerably when the two edge pieces were compared, or the two middle pieces, or the two center pieces; for that reason, we chose to list the lowest values. The reason for the variation is the inability of the impurities to escape from the melt. The crystal is zone refined by Stockbarger growth, but the impurities remain in the crystal. For example, the better edge sample had 6 parts per billion chromium, while the poor edge sample had 64 parts per billion chromium. The values reported in parentheses are the standard deviations

based on the counting statistics. There were not enough samples analyzed to establish confidence limits as was done in Table 12.

Aliovalent impurities in alkali halides should not affect absorption seriously at the long wavelengths of interest for laser windows. Some of them do have absorptions in the visible, but most of the absorption bands due to cationic impurities are in the ultraviolet. If the clustering phenomena occurs to a large extent, it could degrade optical properties to a significant degree. It is doubtful whether impurities present in the parts per billion range would produce significant effects from that phenomenon. However, some crystals appear to have enough iron present that, if it were clustered in the region used to transmit laser radiation, some significant deterioration of the optical properties would occur. One of the adverse features of aliovalent ions in alkali halides is their tendency to form very stable complexes with hydroxide and other anionic species within the lattice. These can make it more difficult to remove hydroxide by reactive gas treatment. But more significantly aliovalent ions enhance the diffusion of hydroxide in the crystal and if stored or processed at elevated temperatures they could lead to an unexpectedly rapid deterioration of the crystal's optical properties.

Anion analysis in alkali halide is difficult. Most analyses depend on the observation of known anion bands in the optical spectra and, if the oscillator strength or absorption coefficient is known for these bands for a particular impurity, it is possible to estimate the concentration of that impurity. No absorption band at 215 nm was detected in these KBr crystals. M. P. Klein et al. (7) report  $\Delta\beta(\text{OH}, 215 \text{ nm})$  is  $1 \text{ cm}^{-1}$  per  $2.05 \text{ OH}^-$  ions per million anions (ppm A). A Perkin-Elmer Model 450 spectrophotometer was used to measure absorption and transmission from 205 nm to  $2.1 \mu\text{m}$  ( $4762 \text{ cm}^{-1}$ ). In the

UV region, when flushed with prepurified nitrogen, this instrument can detect an absorbance change of 0.02 A in its normal range and even less on the expanded transmission range. Assuming that Klein et al.'s data is valid at extremely low concentrations, then with no 215 nm band observed in these crystals the upper limit of the hydroxide concentration can be set. The shortest crystal used in these measurements was 8 cm; this gives a conservative estimate of the  $\text{OH}^-$  concentration as  $[\text{OH}^-] < 0.01 \text{ ppm A}$ . A Perkin-Elmer Model 180 spectrophotometer was used to measure absorption and transmission from  $4200 \text{ cm}^{-1}$  to  $500 \text{ cm}^{-1}$ . All spectra were taken at room temperature as no cryostat that will cool crystals 8 to 10 cm long was available. The entire range was devoid of any absorption bands.

Particular attention was paid to the region from  $1800 \text{ cm}^{-1}$  to  $2200 \text{ cm}^{-1}$ ; where P. Klein observed the hot band of  $^{11}\text{BO}_2^-$  in several crystals, no bands were detected. When  $\text{BO}_2^-$  is present in alkali halides, it exists not only as the isolated metaborate ion but also as polymers. The lowest trace in Figure 24 shows the spectra of  $\text{BO}_2^-$  doped KBr crystals. The bands at the extreme left are the usual bands assigned to metaborate ions; those on the right are due to various polymeric species. The spectra shown in Figure 29 were made at  $100^\circ\text{K}$  between 700 and  $1600 \text{ cm}^{-1}$  and at  $300^\circ\text{K}$  from 1930 to  $2080 \text{ cm}^{-1}$ . The spectra designated "a" were made on "as grown" crystals. Spectra "b" were made after quenching from  $605^\circ\text{C}$  to  $0^\circ\text{C}$ . The "c" spectra illustrate the effects of annealing from  $605^\circ\text{C}$  to room temperature on the formation of polymeric species of  $\text{BO}_2^-$ . Note that when KBr is quenched, most of the  $\text{BO}_2^-$  is present as an isolated ion, but when annealed or when "as grown" a large portion of the  $\text{BO}_2^-$  exists in a polymeric form and does not contribute to the 1960 band used to detect metaborate ion (9). Becker showed that in KCl the annealed

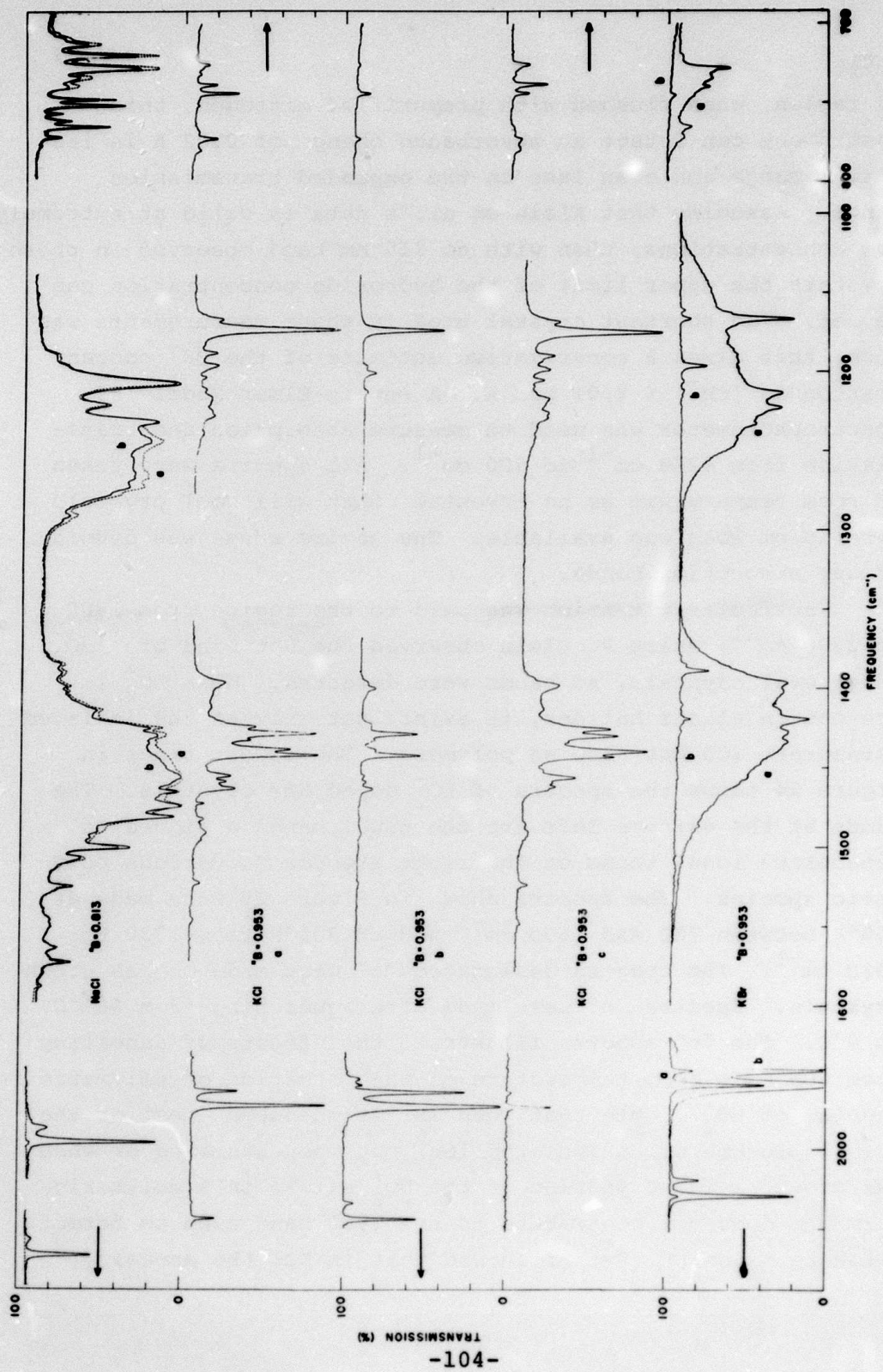


Figure 29. Spectra of Metaborate Ion in Alkali Halides

crystals as much as 100 times the amount of boron present as metaborate ion was present as polymeric species. Because of this complication, portions of the ends of the crystals used for the optical measurements reported here were analyzed colorimetrically for boron using the carmimic acid determination (9). In this method the metaborate reacts with carmimic acid to shift its normal absorption at 520 nm to 585 nm. The method can detect 1 to 10 micrograms of boron. The amount of boron present in the KBr Crystals used in this work was below the detection limits of the carmimic acid method.

Neither carbonate, sulfate, nor nitrate could be detected in the purified salts. None of these species were expected to exist at the melting point of KBr when saturated with HBr. It is most likely that the absorption is due to the species derived from the carbon that was present in all of these salts. HBr does not effectively remove carbon. Oxygen was used to oxidize the carbon to volatile species. This was not as effective as chlorine because pure oxygen is not very soluble in KBr while chlorine is quite soluble; however,  $\text{Cl}_2$  does react with the KBr to displace the bromine. The oxidations used here were carried out below the melting point of the salt. Table 13 illustrates the effectiveness of oxygen in reducing the absorption at 10.6  $\mu\text{m}$ . However, in each case, the absorption at 9.27  $\mu\text{m}$  was increased. It appears that a product of the oxidation of the organic species remains behind which deteriorates the shorter wavelength transparency. Unfortunately, because our 14 meV neutron source was shut down, we could not analyze these crystals for residual oxygen.

At the present time, results from Dr. D. Edwards at Los Alamos have not been reported.

## XII. PURIFICATION OF ALKALINE EARTH FLUORIDES

The purification of alkaline earth fluorides by ion exchange is a very different problem than the purification of alkali halides. Alkaline earth fluorides are too insoluble to use directly in the purification process. There are no ion exchange resins in which the order of selectivity are normally inverted for the alkaline earth ions. Any inversion effects on such resins are primary concentration efforts. A further problem with the purification of the alkaline earths results from the much larger selectivity coefficients of divalent ions than those of the monovalent ions on all resins available. That requires that the process include reactions which allow the separation of the monovalent ions from the divalent ions.

## XIII. CHARACTERISTICS OF ALKALINE EARTH IONS ON ION EXCHANGE RESINS

Polyvalent ions behave differently in their interactions with ion exchange resins than the monovalent ions. These differences are more of extent rather than differences in actual mechanisms of the reaction. Table 16 shows distribution coefficients (10) of some alkaline earth ions on Dowex 50W-X12. Distribution coefficients, as defined by equation XIII-1, are convenient for use with ions that form a series of complexes and, for that reason, are often used in concentrated solutions of polyvalent ions. Here,  $D_{H^+}^{M^{2+}}$

$$D_{H^+}^{M^{2+}} = E_{H^+}^{M^{2+}} / 2 \cdot \frac{[M^{2+}]}{[M^2] + \sum_i [Mx_i]^{2-i}} \cdot \frac{[M^{2+}] \text{ resin}}{[M^{2+}] \text{ solution}} \quad \text{XIII-1}$$

is the distribution coefficient for the species  $M^{2+}$  compared to  $H^+$  on the resin,  $E_{H^+}^{M^{2+}/2}$  is the selectivity coefficient.

Table 16. Distribution Coefficients on Dowex 50W-X12\*

Dilute solutions	$Be^{2+} < Mg^{2+} < Ca^{2+} < Sr^{2+} < Ba^{2+} < Ra^{2+}$
4 M $HCLO_4$	$Ra^{2+} < Ba^{2+} < Sr^{2+} < Ca^{2+}$
6 M HCl	$Ra^{2+} < Ba^{2+} < Sr^{2+} < Ca^{2+}$

\*From reference 10.

The next term is the fraction of the total concentration of  $M$  that occurs as  $M^{2+}$ , and the last fraction is the ratio of  $M^{2+}$  on the resin to  $M^{2+}$  in the solution. The alkaline earths do not usually form strongly bound complex ions with inorganic ligands; however, they do hydrate and form weak complexes with halide ions. Table 16 illustrates the behavior of the ions with regard to hydration and its effect on the exchange of the ion on the resin. The dilute solution order of distribution coefficients is considered the normal order. This order is independent of the anion present in the solution. The dilute solution order  $Be^{2+} < Ca^{2+} < Ba^{2+}$ , occurs because the smallest ion is in the most need of solvation, preferentially going into the aqueous phase. Thus, the smallest ions have the lowest distribution coefficient. However, as the water activity decreases with increasing perchloric acid concentration, anion-cation interactions become more important with the dipositive alkaline earth cations. Perchloric ion is a poor

complexing anion compared with the sulfonate ion of the Dowex 50W-X12. The largest of the three cations, barium, solvates least and does not compete well as the proton for the available means of solvation. As the water activity falls, the protons from the perchloric acid will preferentially move into the resin to replace water molecule interactions with the sulfonate ion and the barium ions tend to remain in the aqueous phase to a greater extent than in dilute solutions. Eventually, the amount of resin invasion by nonexchanged perchloric acid begins to become appreciable. At about 4M perchloric acid the distribution coefficient's order is reversed. If the tendency of the anion of the acid to form complexes is increased, as it is with hydrochloric acid or hydrobromic acid, then concentration at which the order can be reversed is increased. Note that it requires 6M hydrochloric acid to invert the order of the alkaline earths on Dowex 50W-X12. In the very strong hydrobromic acid solutions used in the purification system developed here, the reversal of distribution coefficients occurs at a very high concentration. While it appears that a selective ion filter could be made from Dowex 50W-X12, the range concentration change required is impractical for use here. The behavior of ion exchange resins can be reasonably well understood on the basis of competition for solvation and complex formation, but it is clearly not the full story. The behavior of these resins is sometimes rather unpredictable and oscillations in the distribution coefficient as a function of concentration occurs. Consider Table 17 which illustrates the behavior of the alkaline earth cations on Dowex 50W-X12 in  $\text{HNO}_3$ . At 1M, the order is normal,  $\text{Be} > \text{Ca} > \text{Ba}$ ; that is, small to large. At 3M, the distribution coefficients of the three ions become equal. At 6M, the order has been reversed large to small, but at 10M calcium has the lowest distribution coefficient followed by barium, then

Table 17  
Effect of Nitric Acid on Concentration on  
Distribution Coefficients on Dowex 50W-X12\*

1 M	$\text{Be}^{2+} < \text{Ca}^{2+} < \text{Ba}^{2+}$
3 M	$\text{Be}^{2+} = \text{Ca}^{2+} = \text{Ba}^{2+}$
6 M	$\text{Ba}^{2+} < \text{Ca}^{2+} < \text{Be}^{2+}$
10 M	$\text{Ca}^{2+} < \text{Ba}^{2+} < \text{Be}^{2+}$

\*From reference 10.

beryllium. In nitric acid, the magnitudes of distribution coefficients for all ions are below those found in perchloric acid. The nitrate ion is a poorly complexing ion and these peculiarities of order reversals are very difficult to explain on the basis of charge on the ions, simple solvation, or complex formation.

Measurements of the separation of the alkaline earths and removal of transition metals were made on Chelex 100, AG50W-X8, Bio-Rex 40 and Bio-Rex 70. As a typical transition metal, nickel was chosen as the test ion.

Complete selectivity coefficient surfaces were not required in this design and so were not determined. Because alkaline earth salts are contaminated with large amounts of other alkaline earths, the capacity of the resins required in this purification system must be larger than in potassium bromide system. Chelex 100 has the advantage that its specific volume per mole of exchangeable sites in the strontium or barium form is small. However, separation coefficients are

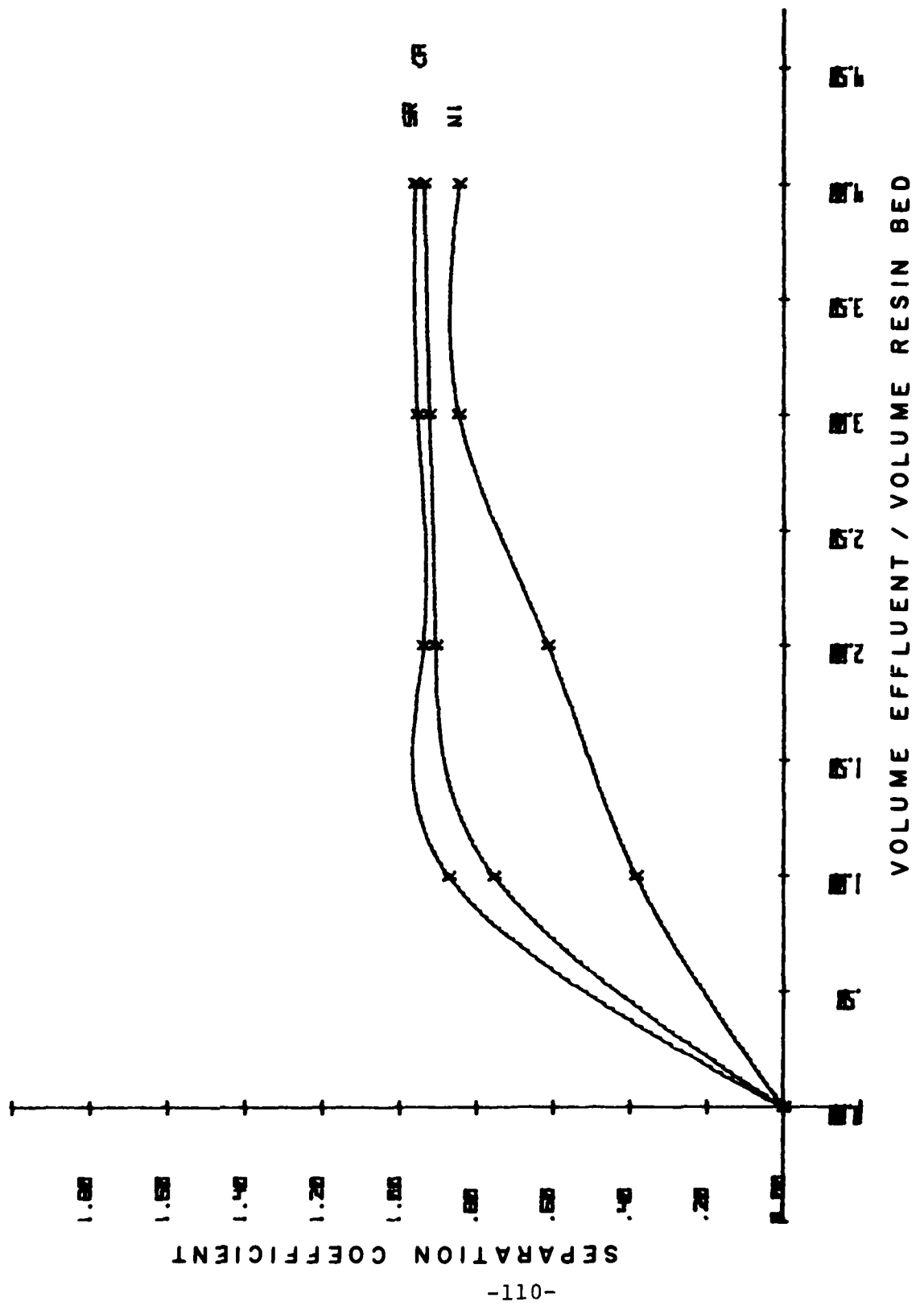


Figure 30. Separation Coefficients for  $\text{Ca}^{2+}$ ,  $\text{Sr}^{2+}$  and  $\text{Ni}^{2+}$  on Chelex 100 in the Barium Form

not as favorable as those of other resins. Figure 30 shows the separation coefficients for strontium, calcium, and nickel on Chelex 100 in the barium form from an 0.996M Ba Br<sub>2</sub> solution. A barium bromide solution on Chelex 100 which had been converted to barium form using barium hydroxide. In the case illustrated, the pH was 4.98. It was essential to maintain the barium solutions at an acid pH because of the tendency of barium carbonate to precipitate. The precipitation of barium carbonate from barium hydroxide solutions was such a troublesome occurrence that it was impossible to use barium hydroxide for conversion of the resin. But the major problem with alkaline earth hydroxides is the magnitude of their contamination with other alkaline earths. Figure 31 shows the separation coefficients for Rio-Rex 70 converted to the strontium form for removal of Ca<sup>24</sup> and Ba<sup>24</sup>. The lines are labelled with the composition of the solution used to convert the resin to the strontium form. The separation coefficient for calcium was excellent when Sr(OH)<sub>2</sub> was used to convert the resin. However, strontium hydroxide contained so much barium that a fraction of the resin was converted to the barium form. When the strontium bromide passed through this resin, the barium was eluted to the solution, and it became more Ba<sup>2+</sup> concentrated than the original solution. After a large amount of strontium bromide had passed through the column, the barium concentration was eventually returned toward the original contamination of barium in the strontium bromide solution. The two curves toward the center of Figure 31 show the behavior of the resin when converted using strontium nitrate. As discussed earlier, that type of conversion depends only on the relative chemical potentials of the strontium in solution and on the resin. It was not particularly an effective conversion for the type of

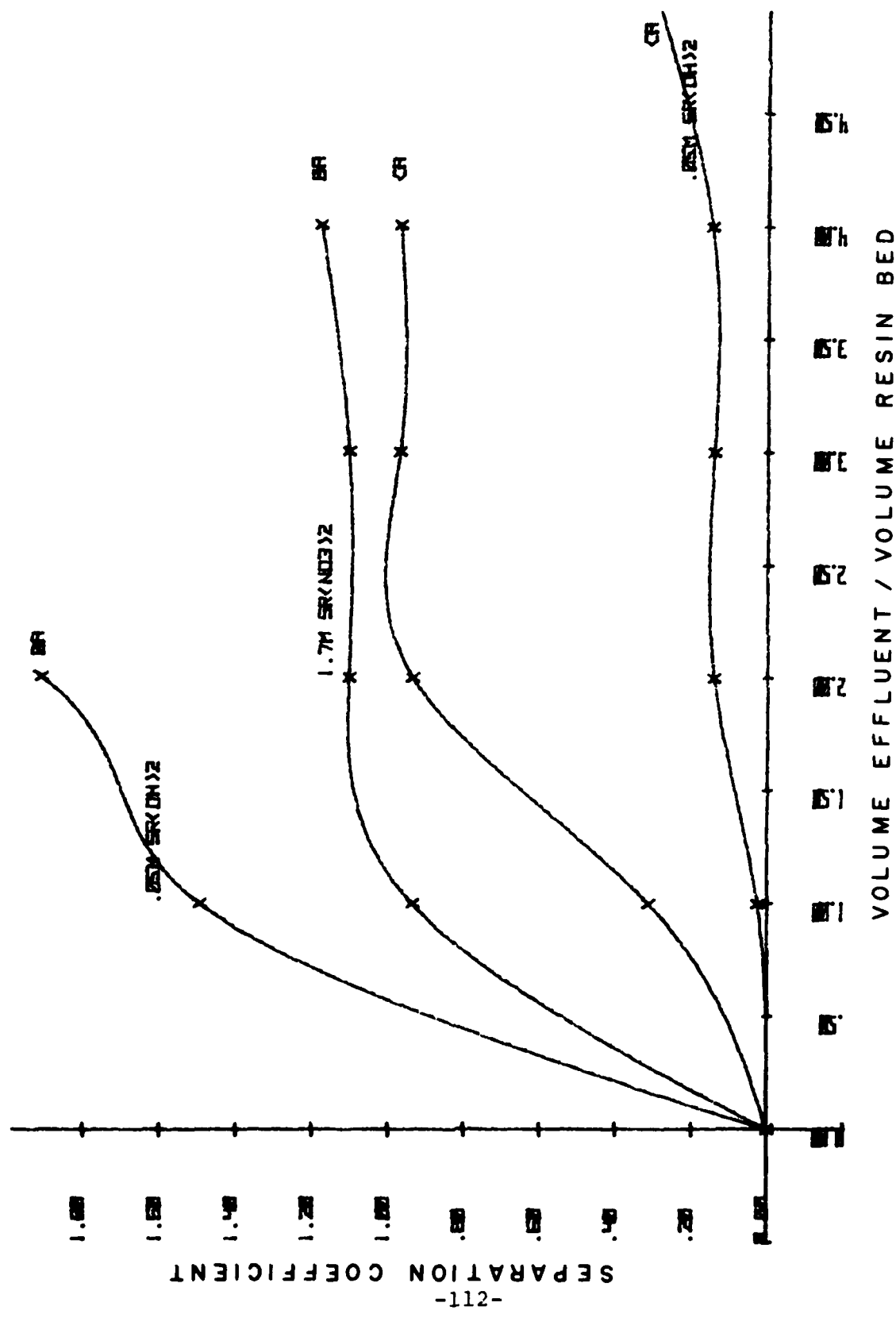


Figure 31. Separation Coefficients for Calcium and Barium on Bio-Rex 70 in the Strontium Form Showing the Affect of Different Conversion Processes

purification used in these processes. The selectivity coefficient for  $\text{Ba}^{2+}$  is greater than 1, showing the  $\text{Sr}(\text{NO}_3)_2$  was contaminated with  $\text{Ba}^{2+}$ .

Because of the problems of carbonate precipitation and the impurity levels present in both strontium and barium hydroxide, the conversions from the hydrogen form to the cationic form of all resins were carried out using barium acetate or strontium acetate. These salts can be recrystallized with ease for initial purification. Figure 32 shows the separation coefficient for calcium on Bio-Rex 70 when the resin has been converted to the barium form using 2M barium acetate. In this case, we were unable to detect nickel in the effluent solution although 100 parts per million had been added to the barium bromide solution passed through the resin. The hydroxide reaction has more favorable thermodynamics for resin conversion than the acetate reaction. But, the inability of recrystallize the hydroxides from solution and the precipitation of carbonates from absorbed  $\text{CO}_2$  made their use in purification of strontium and barium salts undesirable. All resins used in this work were converted to the appropriate cationic form using solutions made from recrystallized acetates. Figure 33 shows the separation coefficients for nickel, calcium, and barium on Bio-Rex 70 in strontium form.

Figures 34 and 35 show the effect of pH on the separation coefficients for barium, nickel, and calcium on AG50W-X8 to the strontium form using the acetate conversion. When the separation coefficients settle to their relative constant values, their order was inverted from  $\text{Ba} > \text{Ni} > \text{Ca}$  at a pH of 5.05 to  $\text{Ni} > \text{Ca} > \text{Ba}$  at a pH of 6.05. At a concentration of 1.5M, a region for effective separation of barium from strontium exists between pH's of 6.05 and 5.06

Figure 36 shows the separation coefficient for Bio-Rex 40 at a pH of 5.06 for the resin in the strontium form. It is not

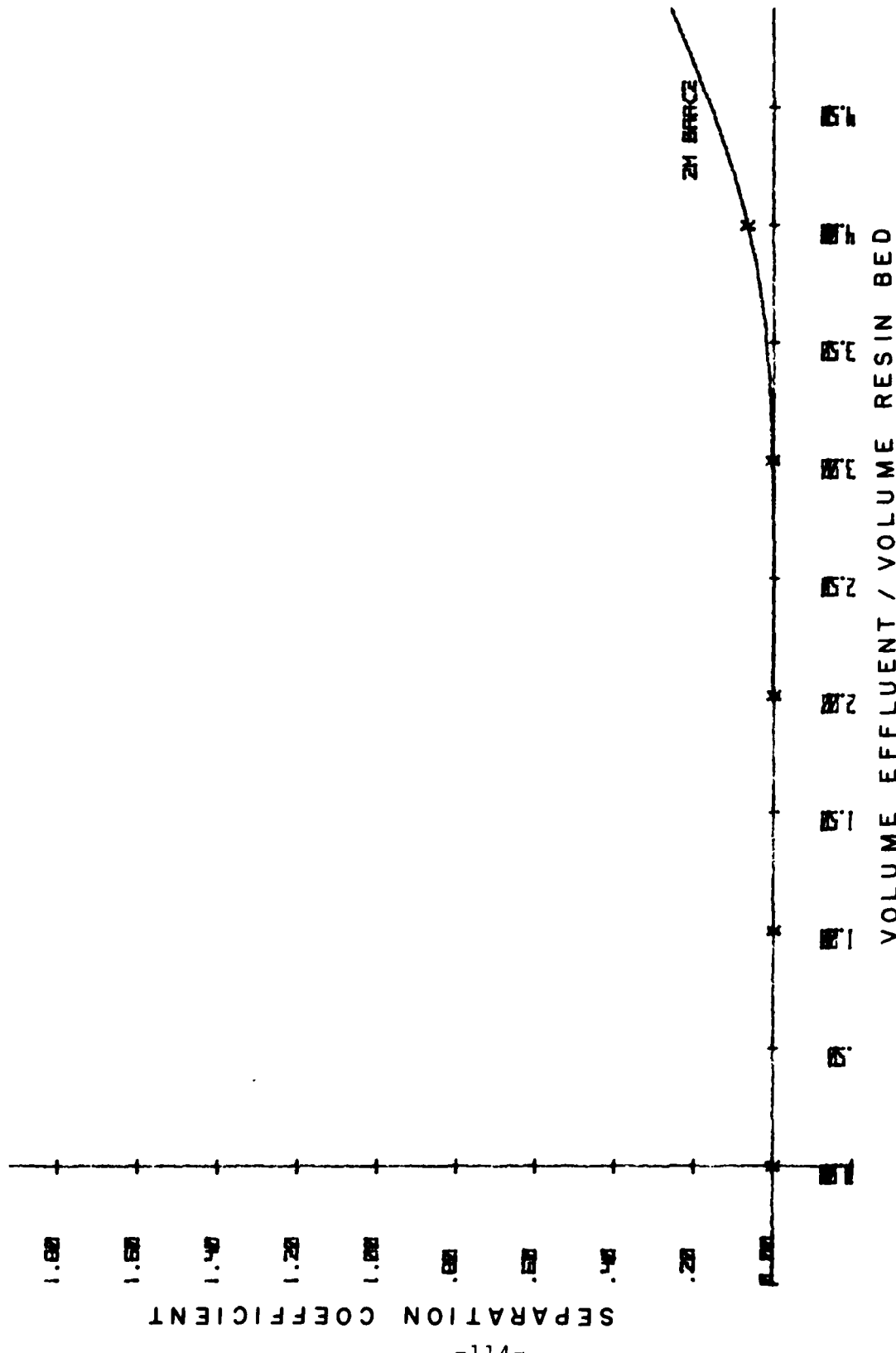


Figure 32. Separation Coefficient for  $\text{Ca}^{2+}$  on Bio-Rex 70 from a 0.99 M  $\text{Ba}(\text{Br})_2$  Solution with a pH of 5.08

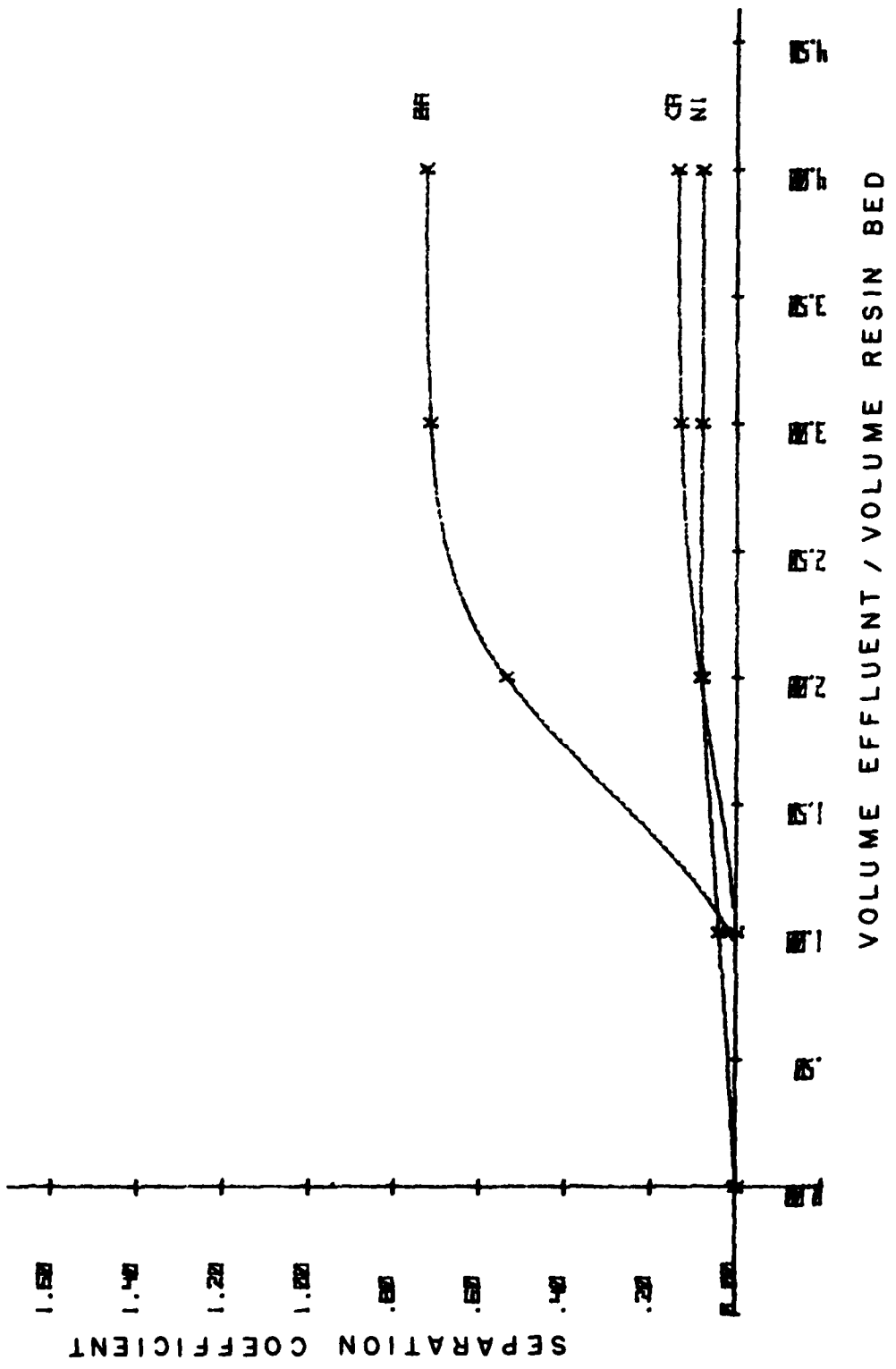


Figure 33. Separation Coefficients for  $\text{Ba}^{2+}$ ,  $\text{Ca}^{2+}$ , and  $\text{Ni}^{2+}$  on Bio-Rex 70 in the strontium form

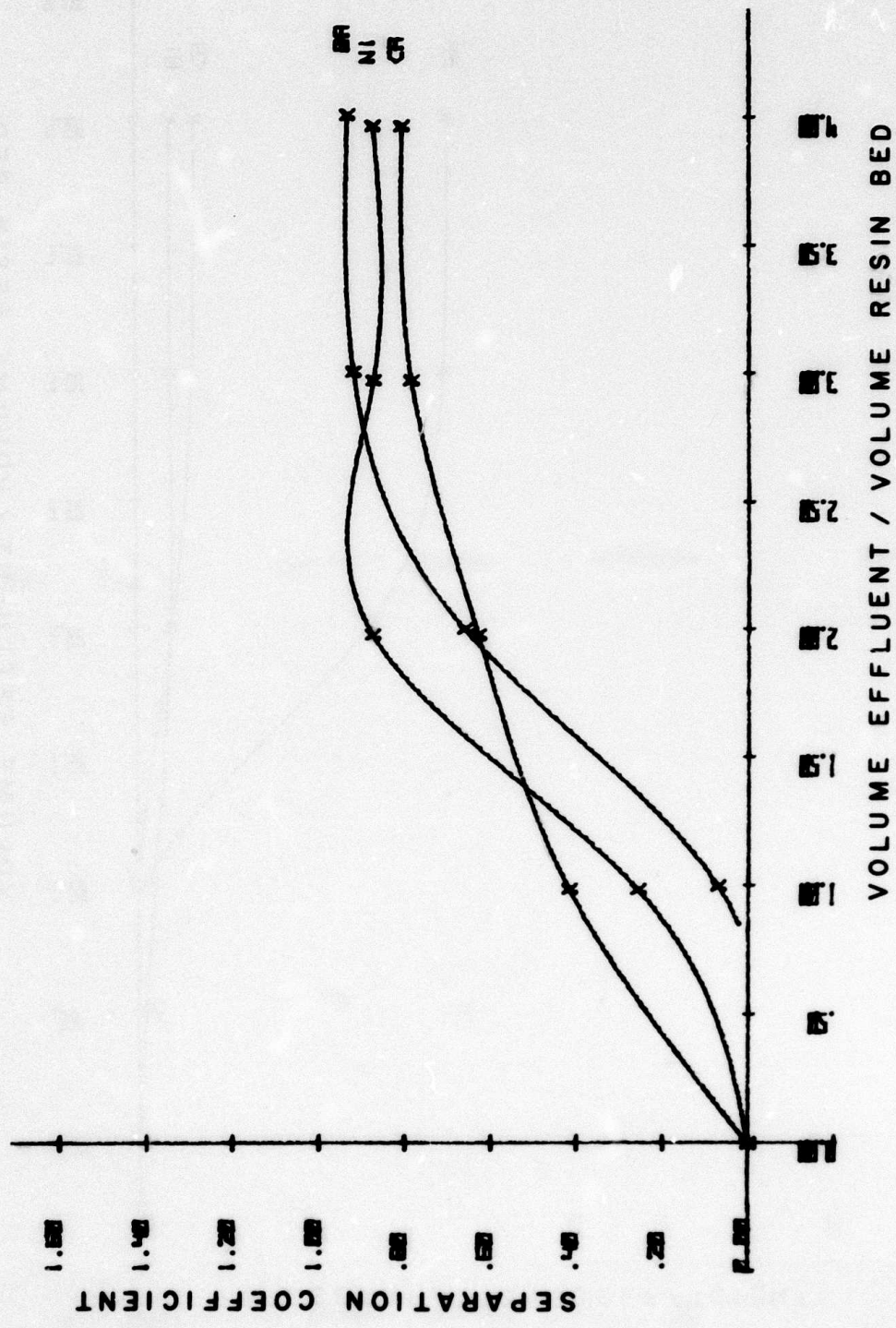


Figure 34. Separation Coefficients for  $\text{Ba}^{2+}$ ,  $\text{Ca}^{2+}$ , and  $\text{Ni}^{2+}$  on AG50W-X8 from 1.05 M  $\text{SrBr}_2$  with a pH of 6.05

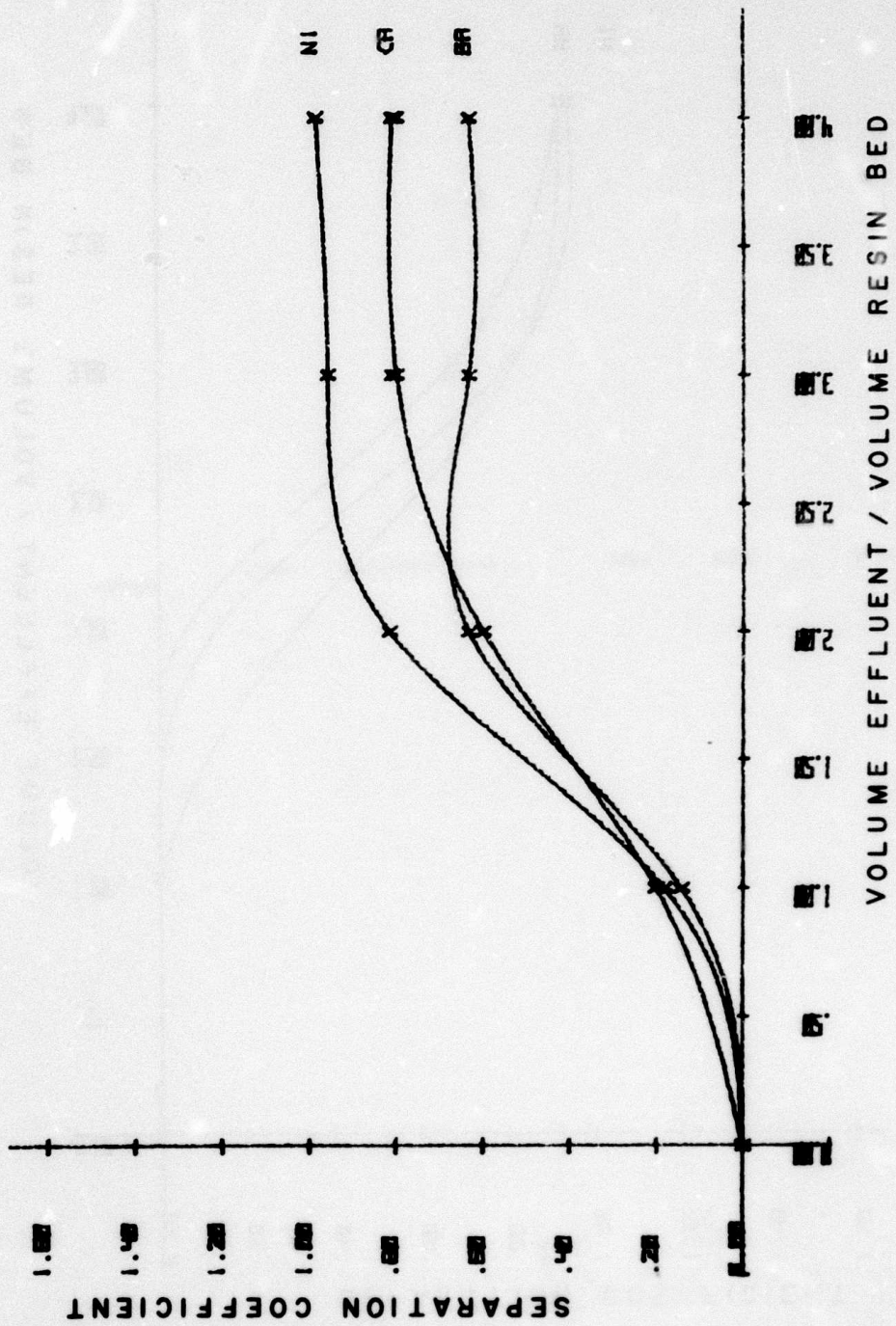


Figure 35. Separation Coefficients for  $\text{Ba}^{2+}$ ,  $\text{Ca}^{2+}$ , and  $\text{Ni}^{2+}$  on AG50W-X8 from a 1.05 M solution of  $\text{SrBr}_2$  at a pH of 5.06

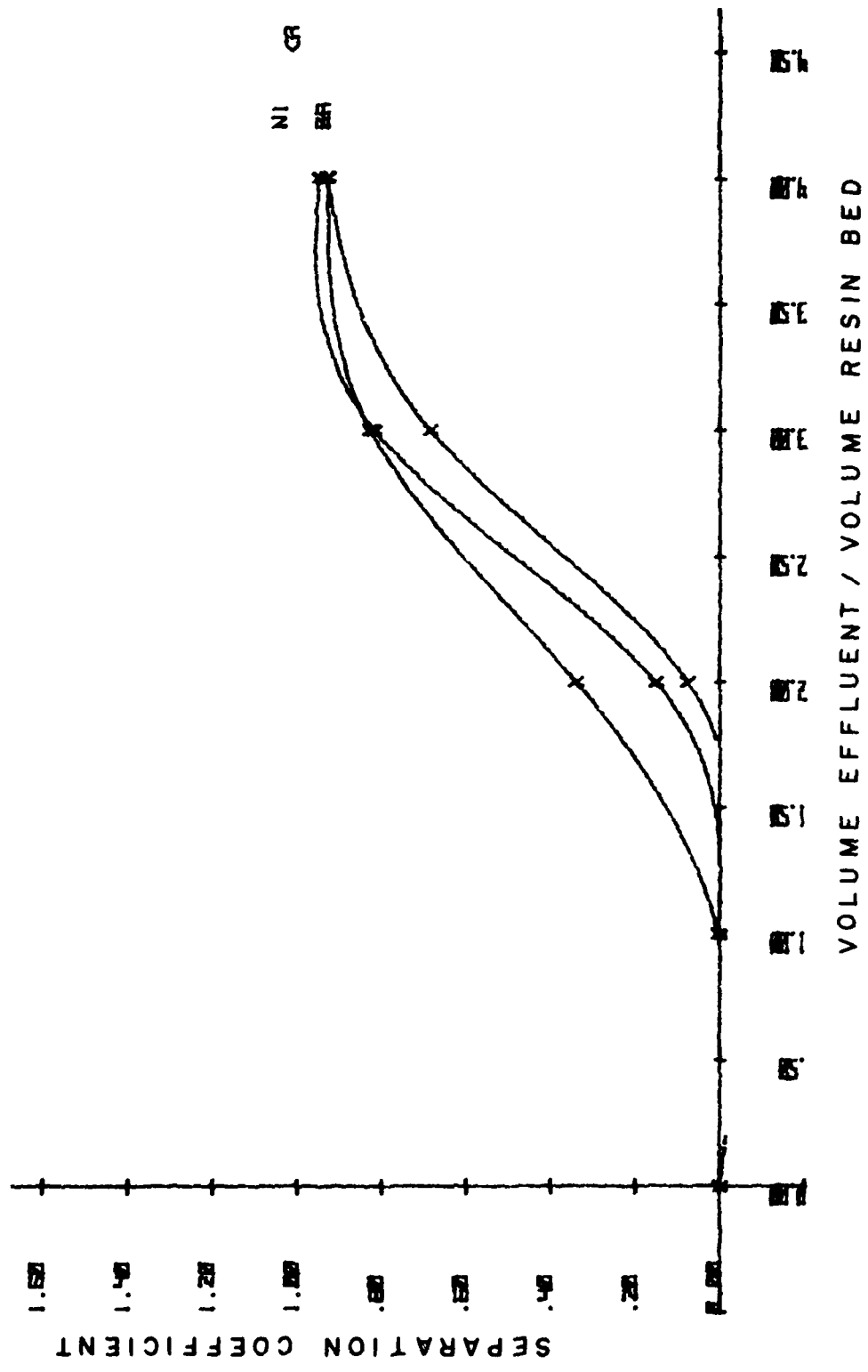


Figure 36. Separation Coefficients for  $\text{Ba}^{2+}$ ,  $\text{Ca}^{2+}$ , and  $\text{Ni}^{2+}$  on Bio-Rex 40 from 0.05M  $\text{SrBr}_2$  at a pH of 5.06

a particularly useful resin for purification of strontium or barium solutions.

Because of the previous work on potassium bromide, the soluble alkali earth solutions chosen for this work were the bromines. This made use of our apparatus to make pure hydrobrominic acid and the knowledge gained in the purification of bromides for the anion purification. The anion purification consisted of AG1-X2 and AG2-X8 operated in a similar fashion to that used for potassium bromide purification.

The properties of these cation exchange resins toward alkaline earth bromide solutions are summarized in Table 18.

Table 18

Properties of Certain Resins for Purification of  
Strontium Bromide and Barium Bromide Solutions

<u>Resin for SrBr<sub>2</sub></u>	<u>pH</u>	<u>Separation Coefficients for 1M Bromide Salt Solutions</u>
AG50W-X8	6.05	Ba(0.93) > Ni(0.86) > Ca(0.80)
AG50W-X8	5.06	Ni(0.95) > Ca(0.80) > Ba(0.60)
Bio-Rex 70	5.06	Ba(0.76) > Ca(0.10) > Ni(0.06)
Chelex 100	4.98	Ba(0.93) > Ca(0.88) > Ni(0.80)
Bio-Rex 40	5.06	Ba ≈ Ca ≈ Ni ≈ (0.95)

<u>Resin for BaBr<sub>2</sub></u>	<u>pH</u>	<u>Separation Coefficients for 1M Bromide Salt Solutions</u>
AG50W-X8	5.08	Ni > Ca > Sr
Bio-Rex 70	5.08	Sr(0.80) > Ca(0.18) > Ni(0.01)
Chelex 100	4.98	Sr(0.92) > Ca(0.90) > Ni(0.80)
Bio-Rex 40	5.08	Sr(0.93) > Ca(0.88) > Ni(0.02)

The values of separation coefficients given in parentheses are the average values in the initial region of the slowly varying part of the separation coefficient versus number of resin bed volume plots. The values for  $\text{Sr}^{2+}$  in  $\text{BaBr}_2$  solutions are not reliable because of interference in the atomic absorption analysis from the  $\text{BaBr}_2$  background

#### XIV. DESIGN OF THE PURIFICATION PROCESS

The major cationic impurities in strontium salts were barium, calcium, and sodium, with lesser amounts of other alkali and divalent metal ions. In barium salts, strontium was the major impurity, then calcium and sodium, followed by lesser amounts of other alkali and divalent metals.

The purification process must be isolated from the laboratory to avoid contamination. This required that all chemical manipulation be performed in a closed system. The separation of the monovalent impurities from the divalent ions could be accomplished in two ways in a closed system: (1) chromatography and (2) precipitation.

Chromatographic separation required that the resin initially in the hydrogen form be converted to the strontium or barium form, then the resin bed washed with a solution that causes each ion to be eluted separately. This method is a standard in analytical separations that involve only a few milliequivalents of ions. Good separation requires about one pound of AG50W-X8 for a 100 grams of  $\text{Sr}^{2+}$ . The resin bed must be sufficiently long that the elution of various ions do not overlap significantly. For preparative work, this technique requires a very large system.

Precipitation requires the reaction  $\text{Sr}^{2+}$  or  $\text{Ba}^{2+}$  with an anion that forms insoluble alkaline earth salts, but whose

monovalent salts are soluble. After precipitation, then the precipitate must be washed free of the monovalent ions, and then converted to a soluble salt for ion exchange separation for the polyvalent impurities. Several suitable anions are available for precipitation separation. Either carbonates, sulfates or sulfides could be used.

The separation of  $\text{Sr}^{2+}$  or  $\text{Ba}^{2+}$  from other polyvalent impurities could be accomplished by: (1) chromatography, or (2) controlled ion exchange.

For effective chromatographic separation, the system must have a large resin capacity, long resin beds with a large number of plates, and a convenient strontium or barium tracer to determine when collection of the eluted solution should be started and stopped. Both ions have convenient isotopes available for this purpose, and this type of system could be used for purification.

A more efficient method for controlled ion exchange is a selective ion filter. Ideally, a selective ion filter should be constructed of resins with reverse orders of selectivity that are stable over a reasonable range of concentration and pH. Previous measurements indicated that reversal of selectivity orders occurred over small pH ranges and only at extremely high hydrogen ion concentrations. The measurements reported in Section XIV show that the order of selectivity of calcium and barium can be reversed using Bio-Rex 70 and AG50W-X8 at a pH around 5.0 for solutions near 1M concentration in either strontium or barium. However, this reversal is dependent on the relative concentration of strontium to the impurities in the resin. Eventually it reverts to its natural order even though the required hydrogen ion concentration is maintained. The separation coefficient for both barium and calcium is less than 1 on both resins.

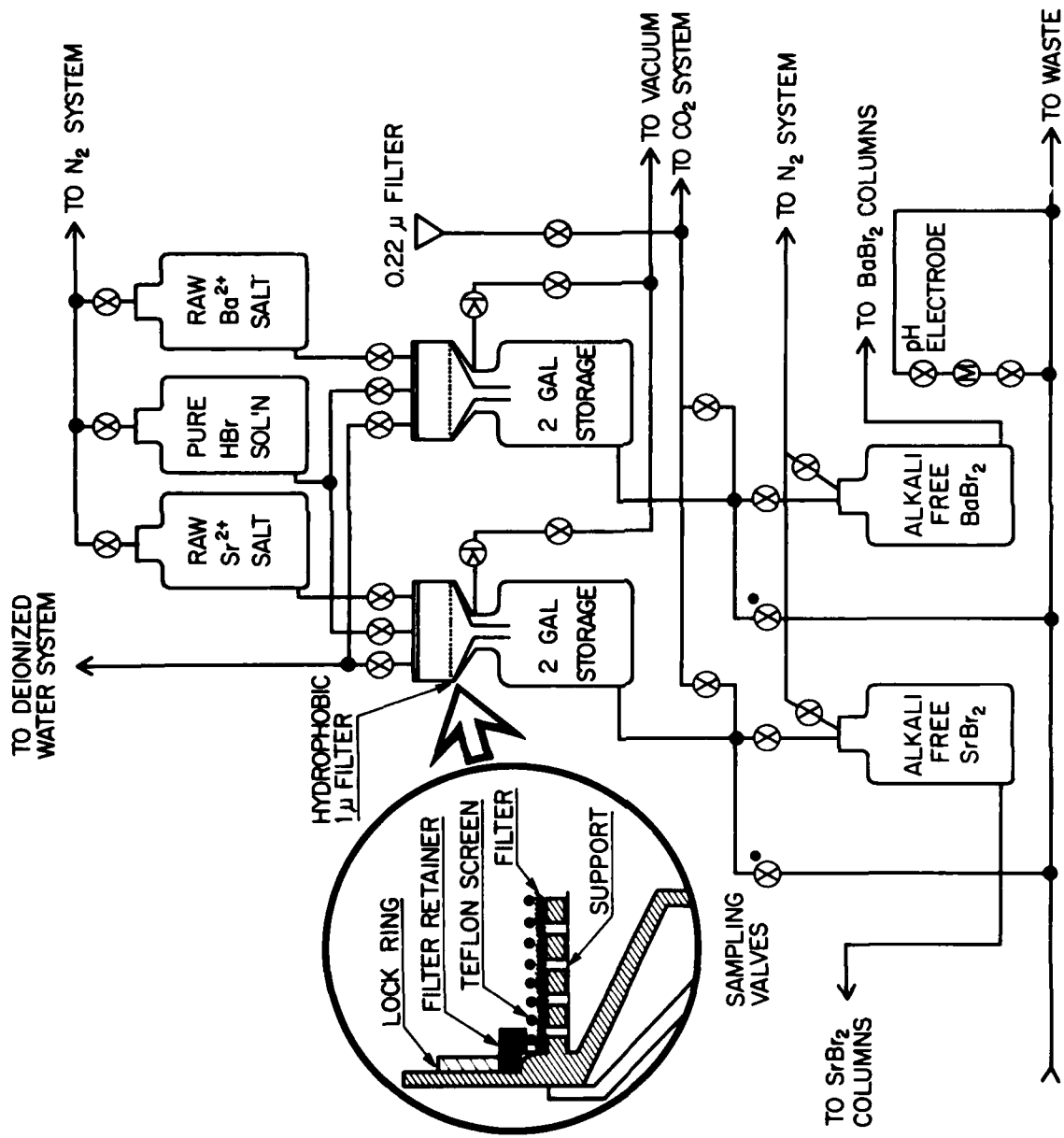


Figure 37. System for Removal of Alkali and Other Monovalent Ions from Sr<sup>2+</sup> or Ba<sup>2+</sup> Salts

This pair of resins can be used as a selective ion filter, but they will pass the less strongly absorbed alkaline earth impurity before the exchange capacity of the resin is exhausted. This characteristic makes it useful to pass the solution to be purified through a less specific resin column with a large capacity to reduce the concentration of major impurities to a level that permits the Bio-Rex 70 and AG50W-X8 to pass a substantial amount of solution before it reverts to its normal separation order. The initial apparatus was designed for both chromatographic and controlled ion exchange modes of operation.

The system for removal of monovalent ions from polyvalent ions by precipitation was designed so that it could be operated as a completely closed system from the beginning of the purification. The initial design of this system is shown in Figure 37. In its operation, the raw salt solution was collected in the top of the filter funnel containing the one micron hydrophobic Mytex filter until the funnel was approximately half full of raw strontium acetate solution. Carbon dioxide was admitted to the two gallon storage container and contacted the solution by diffusing through the filter. When precipitation was complete, the carbon dioxide was removed through the vacuum system and the precipitate washed with deionized water until a sample extracted from the sampling valve in the waste flow line showed no sodium coloration in a flame test. Then the sample was checked for sodium content with an atomic spectrometer. When free of sodium, hydrobromic acid was admitted to the filter region to convert the solid carbonate to a solution of strontium bromide. The alkali free strontium bromide was stored in the reservoir until approximately five gallons of alkali free strontium bromide solution was present. This was then pumped by nitrogen pressure to the reservoir for the ion exchange system. The barium purification system is identical. During operation of this basic

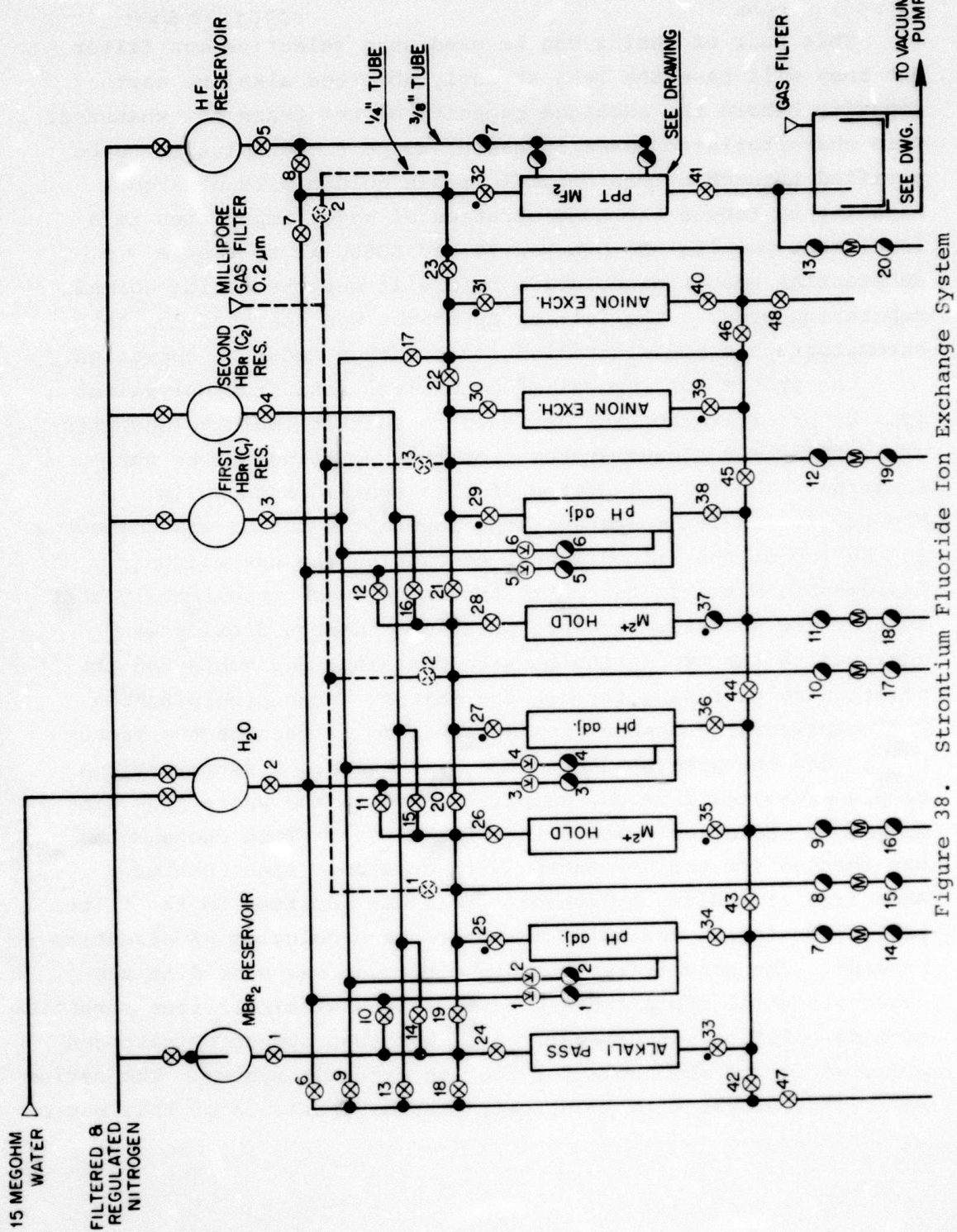


Figure 38. Strontium Fluoride Ion Exchange System

system, several problems arose and the system was modified to correct them. The modifications will be discussed later.

Strontium and barium ion exchange systems are identical. A schematic diagram of the strontium system is shown in Figure 38. It consists of nine columns, each of which are used in purification and the ninth for precipitation of the insoluble fluorides. In Figure 38, the columns are labelled according to their function in a chromatographic system. Before measurements of the characteristics of the resins were completed, it was thought that a series of chromatographic separations would be required to remove impurities. A chromatographic process would be extremely slow. Fortunately, the measurements of separation coefficients of the resins indicated that we need not operate in this fashion. In addition, measurements indicated that the alkali content of the salt could be reduced to an extremely low value by the precipitation scheme described previously.

The system was originally designed to permit several modes of operation without major changes. The column labelled alkali pass was used for the rough separation of major divalent impurities. The resin in the barium or strontium form in the first column was used to remove ions with separation coefficients lower than that of the ion on the resin. Initially almost all ions would have lower separation coefficients because of the high chemical potential of the desired ion on the resin. However, as the concentration of the impurities increased in the resin, the separation coefficients would eventually become unfavorable. A resin with a large specific volume exchange capacity, such as Chelex 100, should be used in the first column. The second column was used for pH adjustment. The third column contained a resin with the most favorable separation coefficients for the larger alkaline earth ion. Based on the measurements shown in section XIV, this was AG50W-X8. The fourth column allowed

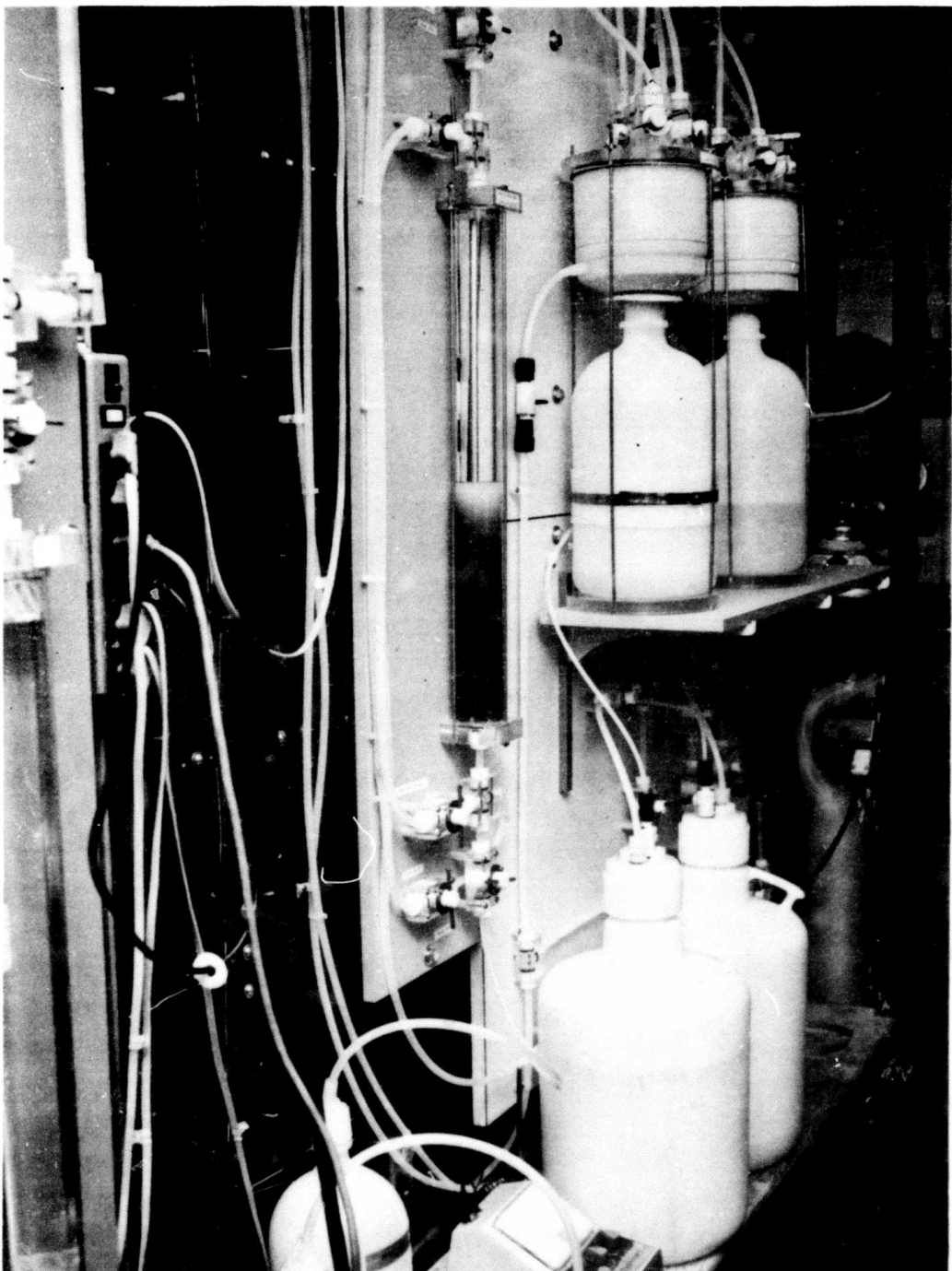


Figure 39. The Monovalent Ion Removal System

for pH and concentration adjustments and the fifth column contained a resin with the most favorable separation coefficients for smaller cations, that was Bio-Rex 70. The sixth column was used to adjust the solution to a low pH and the solution passed through the pair of anion exchange resins, AG1-X2 followed by AG2-X8. The strongly acid effluent from column eight then passed downward into column nine, where hydrofluoric acid was mixed with the strontium or barium bromide. The precipitate formed was washed into the vacuum filter where the alkaline earth fluoride precipitate was collected.

#### XV. CONSTRUCTION OF THE SYSTEM

The materials of construction were discussed in Section VI. The standard fittings, columns, valves, sampling devices, pH electrode chambers and mixing columns were of identical construction to those used in the potassium bromide system. However, two unique closed chemistry systems were developed for purification of strontium and barium fluorides. The first was the monovalent ion removal system that was shown schematically in Figure 37.

The monovalent ion removal system was initially constructed as shown in the schematic. Figure 39 shows the filter units assembled. The funnel is a standard Nalgene Buchner funnel, 17.3 cm in diameter. The two gallon storage reservoir is a two gallon polypropylene aspirator bottle. The one micron hydrophobic Mytex filter was held in place by the lock ring and retainer shown detail drawing in Figure 37. The line and valve shown at the extreme right of Figure 39 is the vacuum line; and, as no solution passed through it, a commercial ball valve could be used in this line. The Mytex filters can be used to separate small traces of water from organic fluids. To get the aqueous solution

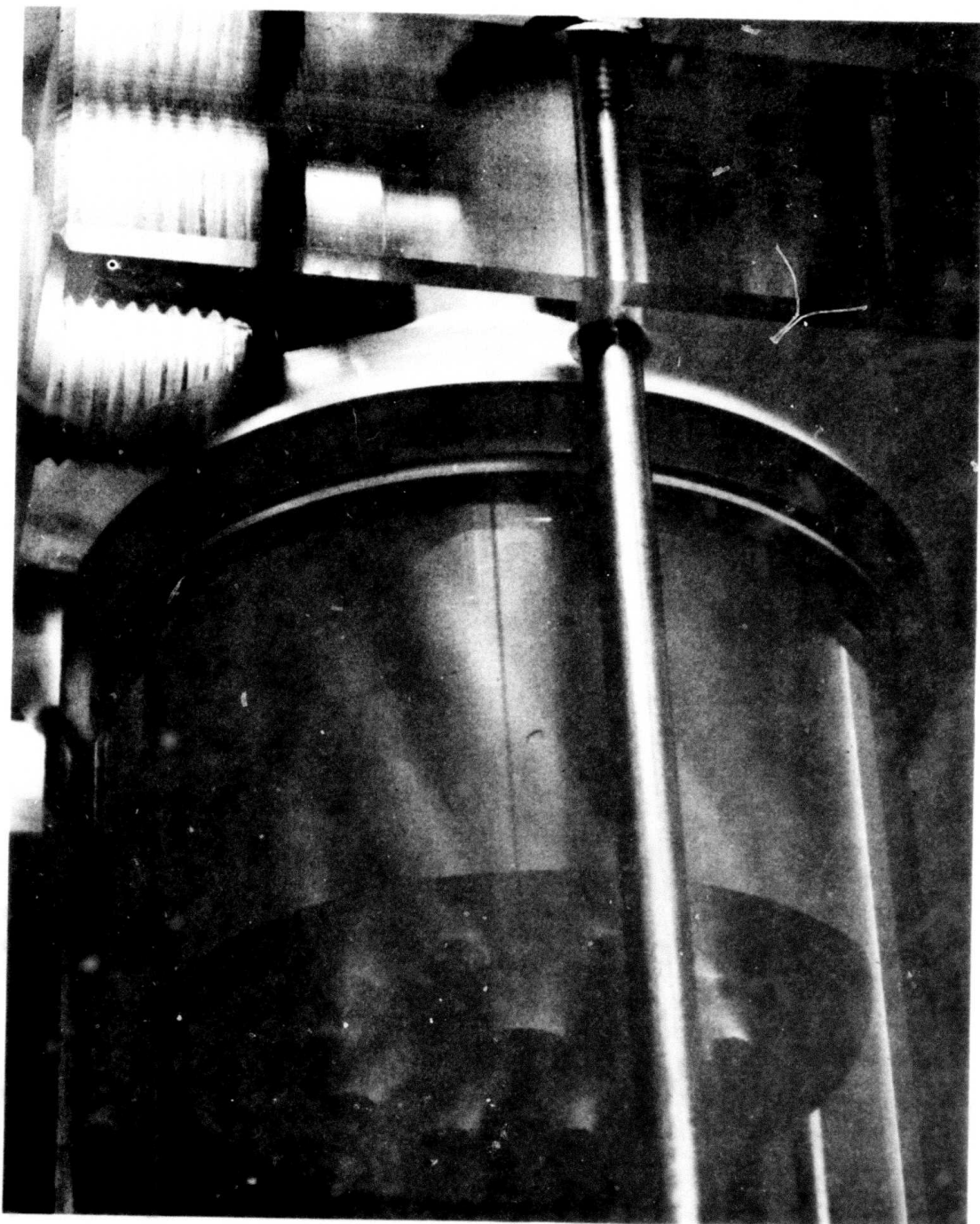


Figure 40. Top Closure for Precipitation Column

to pass through the filter, the filter must initially be treated with a few drops of alcohol. The hydrocarbon portion binds to the filter element leaving the hydroxide end of the alcohol exposed toward the solution. By choice of type of alcohol, the flow rate for aqueous solutions through the filter can be controlled. Without vacuum, the aqueous solution does not pass through the Mytex 1 micron filter and, thus, it acts as a valve for the aqueous solution. Initially  $\text{CO}_2$  was brought into the bottom of the two gallon storage container and diffused through the Mytex filter into the solution for precipitation of strontium or barium carbonate. This method of  $\text{CO}_2$  injection proved faulty, because it was not possible to control the differential pressure sufficiently well to avoid lifting the Mytex filter. To avoid that problem, two additional valves were installed on the methylmethacrylate top closure for the filter and the  $\text{CO}_2$  line was connected to the top of the system as well as the two gallon storage reservoir. A line was brought from the  $\text{CO}_2$  valve into the solution where the  $\text{CO}_2$  was diffused through a porous teflon tube, of the type used in dialysis machines. The second valve in the system connected the top compartment of the filter to the .22 micron filter used to vent excess pressure to the atmosphere. By admitting carbon dioxide to both the upper and lower portions of the filter system simultaneously, efficient precipitation was obtained without disturbing the Mytex filter. Figure 39 shows the overall view of the system modified in this fashion. The two five gallon polypropylene containers on the bottom shelf are the reservoirs for alkali free strontium bromide and alkali free barium bromide. The pH electrode can be seen just above the right hand reservoir and the sampling valves for barium and strontium are just above the electrode. The remainder of the plumbing is immediately below the shelf that contains the two filter systems. The column to the left of this system was used for purification of potassium

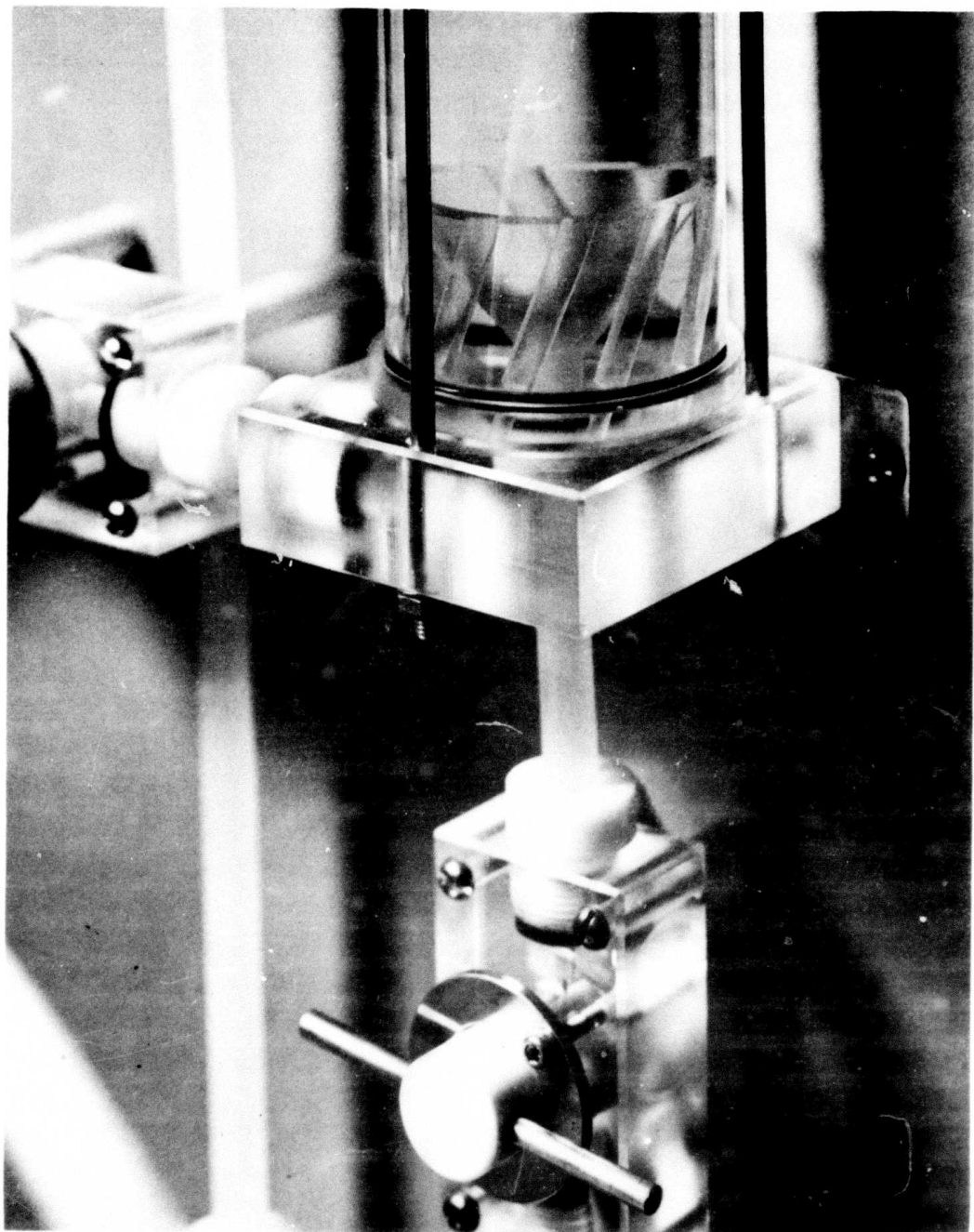


Figure 41. Bottom Closure for the Precipitation Column

hydroxide that was used in conversion of the resins in potassium bromide purification.

The final column in this nine column system was used to precipitate the alkaline earth fluoride. The basic column resembles the standard column for the system. The end plates are similar to the pH adjusting column end plates with the exception that a deflector was built into the top plate that causes the hydrofluoric acid to enter the system with right hand rotation along the axis of the column, while the purified alkaline earth bromide enters through the center port in the column with a directed downward flow. Figure 40 shows the construction of this special top plate. The bottom closure, Figure 41, for the column is a similar plate except here the hydrofluoric acid enters through a series of grooves machined in the outside of a methylmethacrylate plate which give a spiral flow opposite to that of the incoming hydrofluoric acid entering from the top plate. The center of this plug is a funnel to collect the precipitated strontium or barium fluoride. The spiralling upward flow keeps the fine precipitate from collecting in the edges of the funnel. The point at which the two spiralling hydrofluoric acid flows mix is controlled by the relative rate of acid entrance between the upper and lower ends of the column. The total rate of both acid flows plus the purified salt flow is fixed by the rate at which the filter, in Figure 42, can remove solution from the precipitate. The waste solution from the bottom of the two gallon container under the filter is reacted with calcium carbonate to minimize the disposal problem for the excess fluoride present in the solution.

Figure 43 shows the initially assembled board; the precipitation column is on the extreme right and between the left edge of the board and the first column is the constant head device used to keep the electrode chambers full. The cross at the top of the board between the sixth and seventh columns connects to

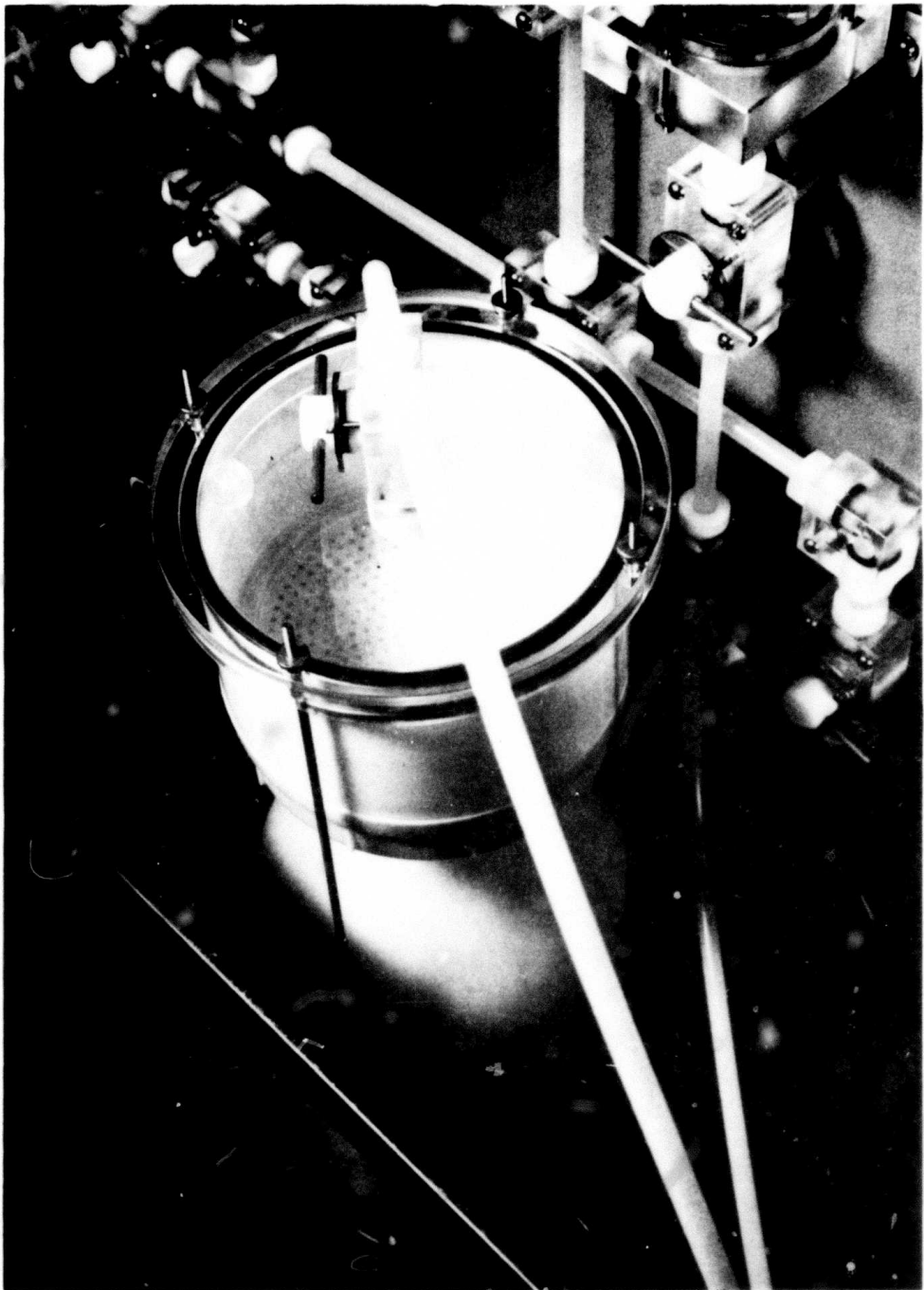
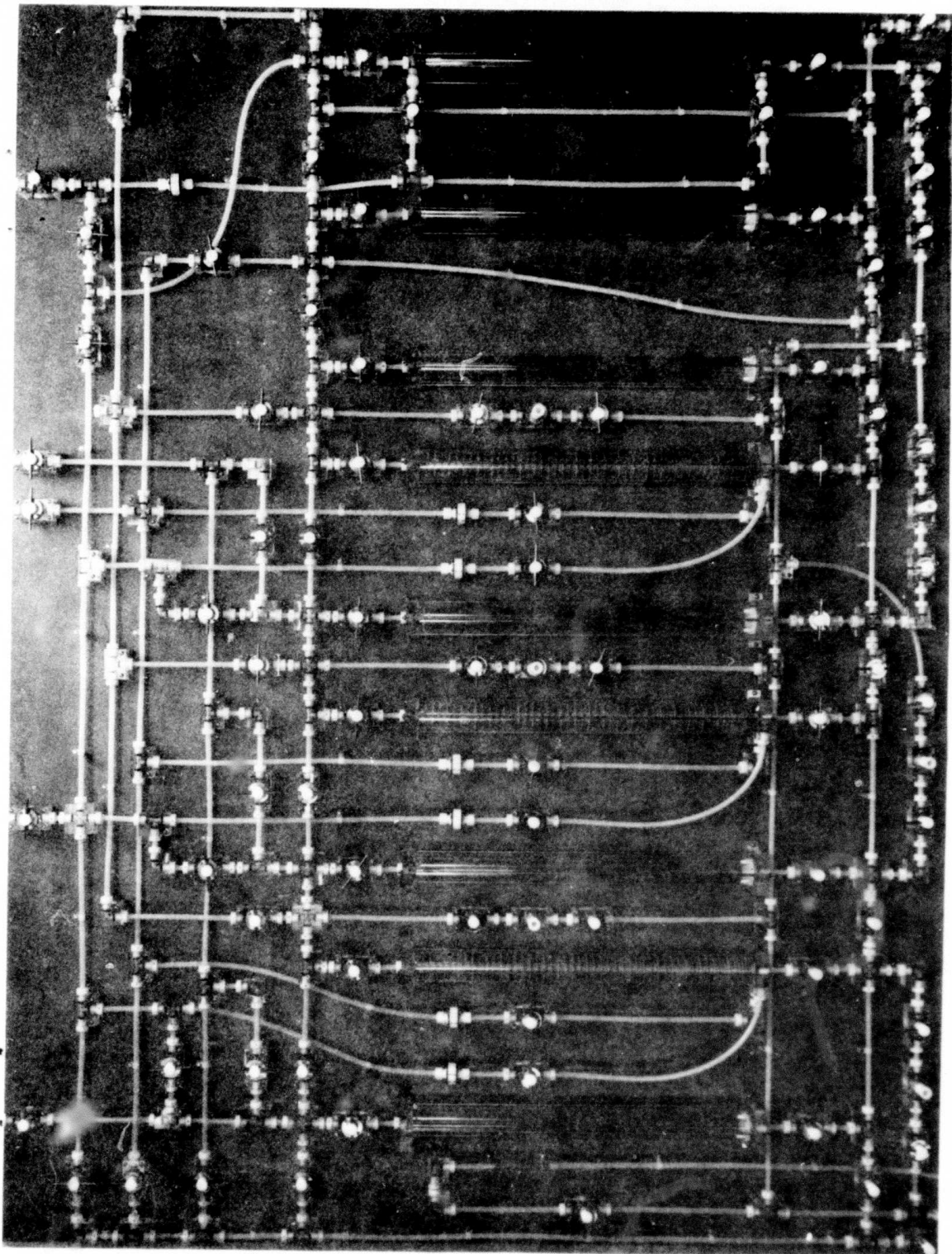


Figure 42. Filter for Fluoride Column

Figure 43. Fluoride Board Assembly



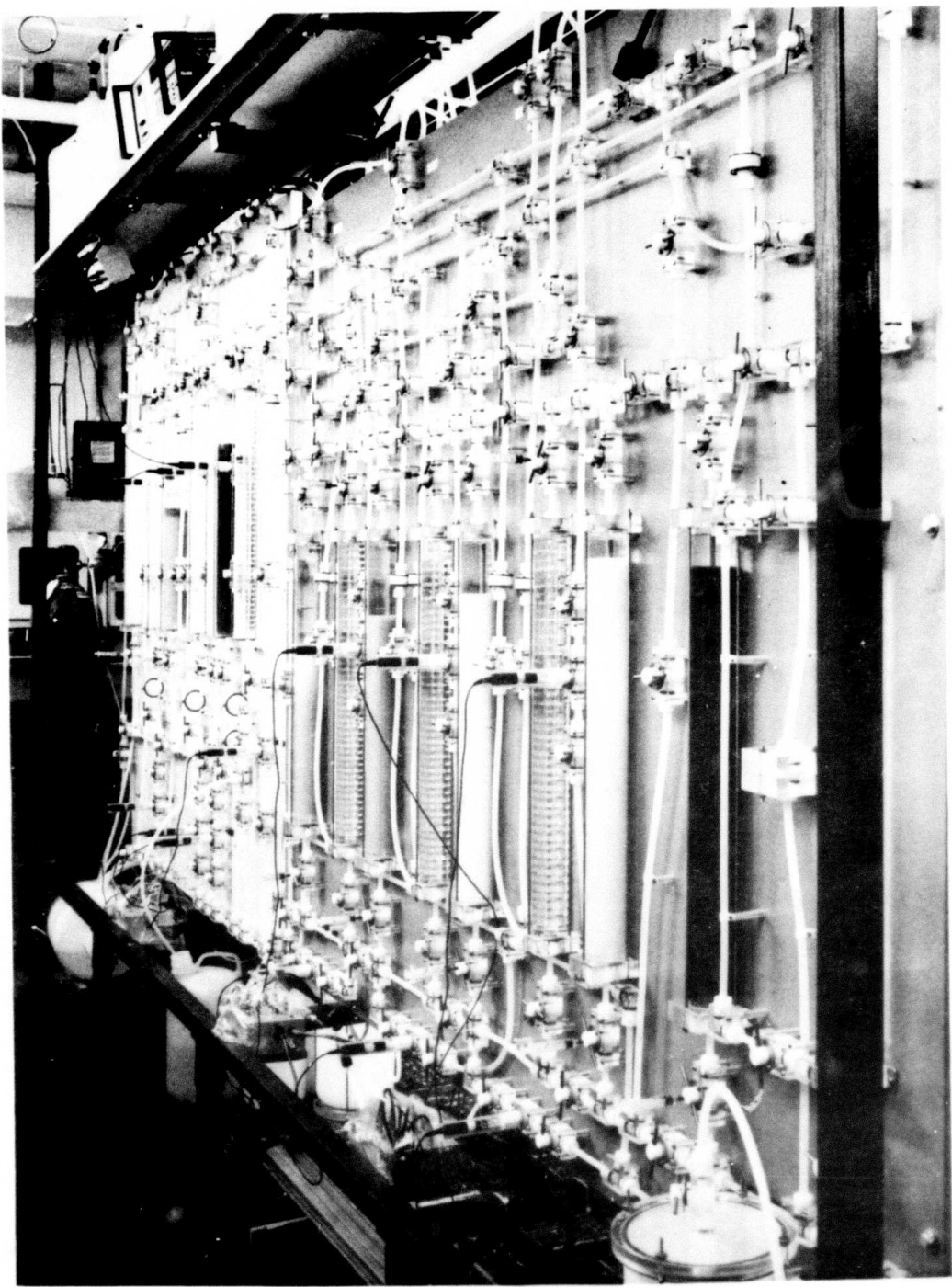


Figure 44. Final Assembly of the Strontium Fluoride System

the .22 micron filter used to exhaust nitrogen from the system when filling. Two modifications of the system were found necessary for operation of this board. A mytex filter was installed before the precipitation column in the line between the bottom of column eight and the top of column nine and a valve was inserted in the line that runs from the horizontal line at the extreme top of the figure to the top of column nine. The final assembly of the strontium fluoride purification system is shown in Figure 44. It is the system in the foreground on the darker of the two backgrounds. The light of the two back-boards is the potassium bromide system. In this figure, the filter and the valve modifications are completed. The ninth column is hidden by the frame post on the extreme right. The 9060 Broadly James calomel reference electrodes have been installed; their location is obvious, and the calibration amplifiers are located on trays at the bottom of the rack. These are covered with plastic to avoid solution falling on the electrical components. The reservoirs are on the shelves on top. They are pressurized with nitrogen as were those used in the potassium bromide system. The barium fluoride system is exactly similar and located on the rack directly behind the strontium fluoride system.

## XVI. MATERIALS

Of the many chemicals analyzed in this laboratory, the most difficult analyses have been those of the alkaline earth salts. The problem occurs because barium salts contain large amounts of strontium, and strontium salts contain a large amount of barium. Table 19 gives an analysis of typical strontium and barium compounds that were considered for use in this work.

Table 19. Analysis of Strontium and Barium Compounds

Salt/Impurity	Source	Na	Mg	Ca	Sr	Ba	Cu	Cr	Mn	Fe	As
SrCl <sub>2</sub> · 6H <sub>2</sub> O	1*	220	24	870	X	540	-	-	0.18	518	-
SrBr <sub>2</sub> · 6H <sub>2</sub> O	2*	300	30	509	X	I	-	-	-	-	-
Sr(NO <sub>3</sub> ) <sub>2</sub> · 4H <sub>2</sub> O	1*	31	< 2	7	X	240	29	< 24	< 0.04	< 0.31	-
Sr(OH) <sub>2</sub> · 3H <sub>2</sub> O	2	--	--	0.05%	X	I	-	-	-	-	-
Sr(C <sub>2</sub> H <sub>3</sub> O <sub>2</sub> ) <sub>2</sub>	3*	30	< 2	6.9	X	193	25	20	-	5.6	-
BaBr <sub>2</sub> · 2H <sub>2</sub> O	2	--	--	0.06%	I	X	-	-	-	-	-
Ba(OH) <sub>2</sub> · 8H <sub>2</sub> O	2	I	--	-	0.7%	X	-	-	-	-	-
Ba(C <sub>2</sub> H <sub>3</sub> O <sub>2</sub> ) <sub>2</sub>	1*	22	1.9	6.9	530	X	19	19	0.011	0.74	0.11
	4*	30	1.9	32	1080	X	25	20	0.007	0.56	-

Reported in ppm except where \* given.

X indicates host ion

- indicates not analyzed

I indicates concentration too large for Atomic Absorption or interference in Induced Neutron Activation Analysis.

\* indicates INAA analysis; if not present, by A.A.

#### Source of Salts:

- 1 J. T. Baker Analytical Reagent
- 2 Alfa Products
- 3 Barium and Chemicals, Inc.
- 4 Mallinckrodt, Reagent Grade

In most cases when an impurity was found in sufficient concentration to require special separation prior to analysis because of analytical interference, the salt was abandoned. The impurities that are reported in the percentage range were measured using dilute solutions of the original salt. The accuracy of those determinations should be considered to be of low accuracy. They are given only to illustrate the extreme impurity ranges found in some of the alkaline earth compounds. Both strontium bromide and barium bromide left a brown muddy appearing material on the filter used for initial filtration of the salt solutions. Even after filtration, the barium bromide was somewhat turbid. This muddy looking residue was not analyzed as the salts were unsatisfactory for purification. The salts selected for purification and use in conversion of the resins were strontium acetate and barium acetate. Both of these contained significant amounts of the adjacent alkaline earth, but they were the best available salts on which to attempt purification. These same salts were used for conversion of resins after the initial filtration through a 1 micron Mytex filter and recrystallization.

The hydrobromic acid used in this work was prepared in this laboratory as described earlier in this report.

The hydrofluoric acid used for precipitation of the fluoride in the final stage was J. T. Baker Chemical Company, low sodium MOS electronic grade hydrofluoric acid. The major impurity in that acid was fluorsilicic acid which occurs at four thousandths of a percent. Its specifications list a large number of other impurities in maximum concentrations of a fraction of a part per million. Barium is specified as 0.2 parts per million, strontium as 0.02 parts per million. An analysis of samples from two separate lots by atomic absorption showed both barium and strontium to be below the specifications listed.

All water used in the purification procedures was obtained from a Milli-Q2 purification system.

## XVII. OPERATION OF ALKALINE EARTH PURIFICATION SYSTEMS

Both the strontium and barium purification systems were operated in the same manner. Therefore, it is only necessary to describe the detailed operation of one of the systems.

The raw 2M strontium acetate solution was filtered to remove minor amounts of insoluble materials, and this solution was transferred to the reservoir for the alkali removal system. Nitrogen was bubbled through the solution to reduce the concentration of dissolved O<sub>2</sub> and CO<sub>2</sub>. Then sufficient ammonium hydroxide was added to make the solution slightly basic and the reservoir sealed and pressurized to five psi nitrogen. The Buchner funnel was filled to about two-thirds of its capacity with this solution and carbon dioxide at three psi was admitted to both the funnel and the two gallon polypropylene bottle used as the intermediate reservoir. The carbon dioxide was left in contact with the solution until the precipitate of strontium carbonate had settled. The CO<sub>2</sub> valve was closed and the valve for the filtered room vent was opened to allow the pressure in the system to drop to one atm of CO<sub>2</sub>. The vent valve was closed and the CO<sub>2</sub> valve again opened. If no additional precipitate formed on the increase in carbon dioxide pressure, the precipitate was considered complete and the CO<sub>2</sub> removed through the vacuum system and the excess solution above the strontium carbonate drawn into the reservoir below. The funnel was filled with deionized water which was then drawn through the precipitate into the intermediate reservoir. The solution in the reservoir was removed through the waste line passing through the sampling valve and the pH electrode on its way to the waste disposal system. Five milliliter samples were drawn from the sampling valve to roughly assay the sodium content of the sample with a simple flame test using a platinum wire and a bunsen burner. The characteristic sodium emission occurred first, followed by

the bright crimson strontium emission. The strontium carbonate was washed until no sodium emission could be observed in the flame test; then the sample was examined for sodium content using an atomic absorption spectrograph. The detection limits for sodium in these strong strontium solutions were about five parts per million. When sodium could not be detected in these samples, washing was considered complete. The precipitate was dissolved in pure hydrobromic acid and transferred through the filter and intermediate reservoir to the alkali free strontium bromide reservoir. This process was repeated until the reservoir was filled.

This system was very successful in removing alkalis from the strontium carbonate. However, it has some disadvantages. It was a very slow process. The washing required several days because of the extreme slowness with water can be brought through the precipitate. The strontium carbonate precipitate formed under these conditions was of such extremely fine grain that a small amount passed through the Mytex filter, but the greatest problem with the fineness of the precipitate was that it clogged the filter membrane which made the flow of wash water through it extremely slow.

When the alkali free strontium bromide reservoir was full, its contents were pumped by nitrogen pressure to the reservoir on the extreme left above the ion exchange system. From that reservoir, the strontium bromide solution passed through the first ion exchange column, which contained 4284 milliequivalents of exchange capacity of Chelex 100 in the strontium form. The effluent from this column was nearly neutral and sufficient acid was mixed with it as it passed through the adjacent mixing column to produce an effluent with a pH of 5.0 or less as measured at the second electrode in the system. The strontium bromide solution next passed through the AG40W-X8 resin column; this column contained 2300 milliequivalents of exchange capacity of

the resin in the strontium form. Normally the effluent from this third column was of approximately the same pH as the solution entering. If the pH drifted above 5, more hydrobromic acid was added to the solution to adjust the pH to 5 or less at the effluent of the fourth column, which was a mixing column. The solution was then passed into the Bio-Rex 70 column which contained 4600 milliequivalents of exchange capacity of Bio-Rex 70 in the strontium form. The effluent from this column was adjusted to a pH of 3 or less in the final pH adjusting column and then passed to the anion exchange resins in columns seven and eight which contained 659 milliequivalents of AG1-X2 and 1369 milliequivalents of AG2-X8, respectively. The cation exchange capacity of this system was far greater than that used in the potassium bromide systems, because of the extremely high and widely variable impurity levels found in these salts. The anion exchange columns were identical to those used in the potassium bromide system.

The solution produced by this ion exchange system was strongly acid when it passed into the fluoride precipitation column. In this column hydrofluoric acid was introduced with a spiralling right hand flow around the central flow of the strontium bromide. A second flow of hydrofluoric acid with a left hand spiralling flow was injected at the bottom of the column. By adjusting the relative velocities of the three streams, the precipitate can be formed as a cloud in a relatively small region of the column. This fine precipitate was carried through the funnel in the bottom of the precipitation column to a filter funnel containing a Mytex filter where it was collected. The solution which passed through the filter into a two gallon polypropylene aspirator bottle below was pumped to a five gallon closed container in which a large amount of calcium carbonate precipitated insoluble calcium fluoride. The excess hydrobromic acid, of course, reacts with the carbonate to form soluble bromides which pass out of the system.

The operation of this ionic exchange system is extremely stable in comparison to the potassium bromide system. The requirements on control of the pH are not particularly rigorous. Any pH lower than 5 was satisfactory for the critical AG40W-X8 and Bio-Rex 70 resins, and a pH less than 4 functioned correctly in the anion exchange resins so that few problems were encountered in the system. The plumbing for the ion exchange system is sufficiently flexible that, if one of the teflon checkvalves stuck, the acid required to adjust pH could be routed through the water addition line while the checkvalve was repaired. None of the oscillations encountered in the early operation in the potassium bromide system occurred in operation of these systems.

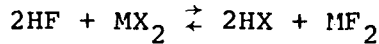
#### XVIII. REACTIVE GAS TREATMENT AND CRYSTAL GROWTH

In the reactive gas treatment, HF was the reactive gas used. The Gibbs free energies of the reaction of HF with various alkaline earth halides are summarized in Table 20.

The desired reactions are less favored at high temperatures, so most conversion of residual bromide in  $\text{SrF}_2$  occurred in the diffusion limited region below its melting point. In both salts, the fluorides are much less soluble than the other halides (12) (Table 21). The salts are precipitated then washed, and so should contain very small quantities of other halides. This proved true for bromide ion which should be the worst case. Therefore, it was better not to risk contamination by other cations carried into the purified salt as fluorides during treatment with a fluorinating agent until the bromide remaining as a trace impurity (< 0.5 ppm in  $\text{SrBr}_2$  and ~ 3 ppm in  $\text{BaBr}_2$ ) proved harmful to optical properties.

Table 20

Gibbs Free Energies (in Kcal) for Alkaline Earth Halides at 1 atm



Salt $\text{MX}_2$	T (°K)	300	500	1000	1500	$T(\Delta G=0)$	T (melt)
$\text{CaCl}_2$	-13.24	-12.46	-9.16	+0.090	1495	1055	
$\text{CaBr}_2$	-15.31	-14.87	-12.00	-2.84	--	1033	
$\text{CaI}_2$	-19.78	-19.47	-16.62	-10.30	--	1013	
$\text{SrCl}_2$	-5.33	-4.84	-1.66	+0.039	1200	1145	
$\text{SrBr}_2$	-4.84	-4.04	-0.300	+10.91	1013	926	
$\text{SrI}_2$	-10.21	-9.35	-1.52	-1.52	1086	788	
$\text{BaCl}_2$	+4.41	+4.90	-1.60	+14.34	1005	1233	
					(second crossing)		
$\text{BaBr}_2$	+6.05	+5.85	+3.10	+14.16		1120	
$\text{BaI}_2$	-0.214	-0.354	-1.62	+13.60	1053	984	

(Calculated using data of references 3 and 11.)

Table 21. Solubilities of Strontium and Barium Halides

Salt	$\text{SrF}_2$	$\text{SrCl}_2$	$\text{SrBr}_2$	$\text{SrI}_2$	$\text{BaF}_2$	$\text{BaCl}_2$	$\text{BaBr}_2$	$\text{BaI}_2$
Units	gm/l	wt %	wt %	wt %	gm/l	wt %	wt %	wt %
$T(^\circ\text{C})$								
0	0.1135	30.3	46.0	62.3		24	49.5	62.5
10		32.3	48.3		1.586	25	50.2	64.8
20	-0.1173	34.6	50.6	64.0	1.607	26.3	51.0	
30	-0.1193	37.0	52.8		1.620	27.7	52.1	
40		39.5	55.2	65.7		28.9	53.2	
50		42.0	57.6			30.4	54.1	
60			60.0	68.5		31.3	55.1	
70			64.5			34.4	57.4	

Hydrogen fluoride was an effective drying agent. At high temperatures, the residual water on the surface and that occluded in the precipitate converts to the alkaline earth oxide. These were reduced to fluorides by HF (Table 22).

Table 22

Gibbs Free Energies (Kcal) for the Reaction of HF  
with Alkaline Earth Oxides

T (°K)	300	500	1000	1500
CaO	-58.52	-52.59	-36.03	-25.54
SrO	-65.97	-59.34	-43.33	-28.10
BaO	-57.29	-54.77	-50.63	-39.95

(Calculated using data from references 3 and 11.)

The HF system used in this work was conventional and constructed of monel from standard Swagelok fittings and Whitney valves. Anhydrous HF was absorbed on NaF in a 5 cm ID monel column 10 cm long. The column had the capacity of 10 moles of HF as  $\text{NaHF}_2$ . The delivered pressure of HF as a function of temperature is given in Table 23. The pressures were measured using a polypropylene bourdon gauge in the delivery line ahead of a final  $\mu\text{m}$  Mytex filter. During use of the system, the gauge was removed and the temperature used to estimate HF pressure.

The system flush gas was dry Argon. The only unusual features of the system was the use of 5  $\mu\text{m}$  Mytex filters at the outlet of the  $\text{NaHF}_2$  cylinder. Because the manifold had to

located in the laboratory, it was constructed on a small 1/4 inch steel plate and the system enclosed in a plexiglass box that was connected to the laboratory hood by a 2-1/2 inch flexible tube. To avoid danger of valve packings, each valve shaft was extended through the plexiglass box by an extension shaft with a disc next to the shaft exit hole to shield the operator's hand. The waste HF was reacted with  $\text{CaCO}_3$  contained in a steel can which could be periodically evacuated with a trapped aspirator.

Table 23

Pressure of HF over  $\text{NaHF}_2$  at Various Temperatures

T ( $^{\circ}\text{C}$ )	HF Pressure (Torr)
200	87
230	208
244	369
250	422
260	496
275	706

The crystal growth apparatus consists of a small platinum furnace mounted on a transport system that moves it along an  $\text{Al}_2\text{O}_3$  atmosphere control tube. The crucible is of graphite similar to the design used by Pastor and Arita (13).

The crucible is 0.5 in diamater and 6 m. long. The apparatus is similar to guggenheim's (14).

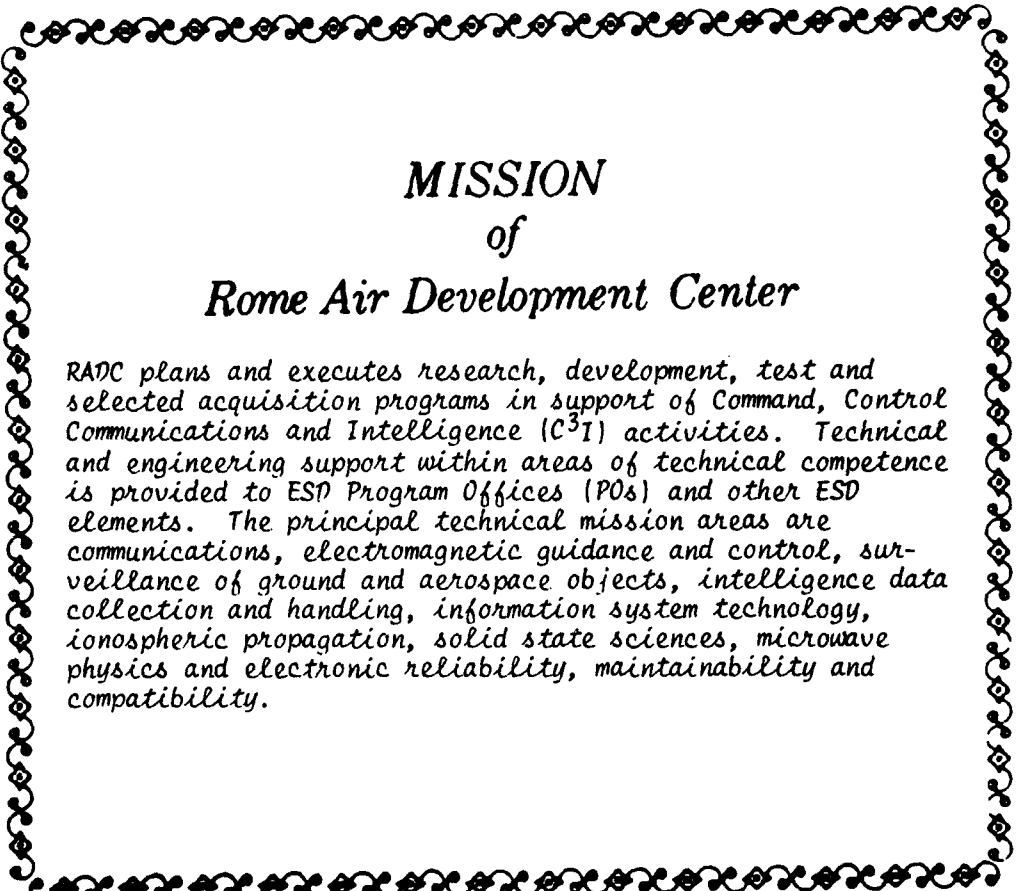
## XIX. RESULTS

Purified  $\text{SrBr}_2$  and  $\text{BaBr}_2$  were not produced until late in the time allotted for this research. Therefore, only preliminary evaluation measurements have been started. There are not yet sufficient data to set confidence limits on the analyses and very low level analyses are not reliable until sufficient data are available for detection of anomalous results.

Preliminary atomic absorption analyses show:  $\text{Na} < 5 \text{ ppm}$ ,  $\text{Ca} \sim 3 \text{ ppm}$ ,  $\text{Mg}$  undetectable,  $\text{Ba} < 12 \text{ ppm}$  in  $\text{SrF}_2$ , and  $\text{Sr} \sim 20 \text{ ppm}$  in  $\text{BaF}_2$ . The atomic absorption analysis of a relatively small amount of impurities in alkaline earth compounds is not very accurate. More accurate INAA results must be available before an accurate estimate on the usefulness of this process can be made.

### References

1. S. Peterson, Ann. N.Y. Acad. Sci., 57, 144 (1954).
2. D. T. Sawyer and J. L. Roberts, Jr. "Experimental Electrochemistry for Chemists." Academic Press, New York. (1974).
3. D. R. Stull, Prophet, H., et al. "JANAF Thermochemical Tables, NSRDS-NBS 37 (1971).
4. Bernard Bendow. Multiphonon Infrared Absorption in the Highly Transparent Frequency Regime of Solids, in "Solid State Physics," 33 (eds. Ehrenreich, H., Seitz, F., Turnbull, D.) Academic Press, New York (1978) p. 308.  
(a) Deutsch, F. F. (b) Harrington, J. A. (c) unidentified.
5. M. Sparks. "Theoretical Studies of Materials for High Power Infrared Coatings." Sixth Technical Report, 31 December 1975. p. 226. (measured on Raytheon CO<sub>3</sub>/CO laser calorimeter)
6. P. M. Klein. Growth of Lowloss KBr in Halide Atmospheres. A Xerox copy. Publication source not known. (a) unidentified  
(b) Harrington, J. A. (University of Alberta calorimeter)
7. M. P. Klein, Kennedy, S. O., Gie, T. I., Wedding, B. Mat. Res. Bull. 3, 677 (1968).
8. C. R. Becker, Thesis, Chemistry Department, Oregon State University (1969).
9. J. T. Hatcher and Wilcox, L. V. Analy. Chem. 22, 567 (1950).
10. D. C. Whitney and R. M. Diamond. J. Inorg. Nucl. Chem. 27, 219 (1965).
11. Quill. "The Chemistry of Metallurgy of Miscellaneous Materials, Thermodynamics." McGraw-Hill, New York (1950) pp. 60-275.
12. Stephen and Stephen. "Solubilities of Inorganic and Organic Compounds." Vol. I, part 1, MacMillan, New York (1963).
13. R. C. Pastor and K. Arita, Mat. Res. Bull. 10, 493 (1975).
14. J. Guggenheim, ibid., 32, 1337 (1961); ibid., 34, 2482 (1962).



## *MISSION of Rome Air Development Center*

RADC plans and executes research, development, test and selected acquisition programs in support of Command, Control Communications and Intelligence (C<sup>3</sup>I) activities. Technical and engineering support within areas of technical competence is provided to ESD Program Offices (POs) and other ESD elements. The principal technical mission areas are communications, electromagnetic guidance and control, surveillance of ground and aerospace objects, intelligence data collection and handling, information system technology, ionospheric propagation, solid state sciences, microwave physics and electronic reliability, maintainability and compatibility.